Modeling and Optimization of Crude Oil Desalting

By

Shahrokh Ilkhaani

A thesis

presented to the University of Waterloo

in fulfillment of the

thesis requirement for the degree of

Master of Applied Science

in

Chemical Engineering

Waterloo, Ontario, Canada, 2009

I hereby declare that I am the sole author of this thesis. This is a true copy of the thesis, including any required final revisions, as accepted by my examiners. I understand that my thesis may be made electronically available to the public.

Abstract

When first received by a refinery, the crude oil usually contains some water, mineral salts, and sediments. The salt appears in different forms, most often times it is dissolved in the formation water that comes with the crude i.e. in brine form, but it could also be present as solid crystals, water-insoluble particles of corrosion products or scale and metal-organic compounds such as prophyrins and naphthenates. The amount of salt in the crude can vary typically between 5 to 200 PTB depending on the crude source, API, viscosity and other properties of the crude.

For the following reasons, it is of utmost importance to reduce the amount of salt in the crude before processing the crude in the Crude Distillation Unit and consequently downstream processing units of a refinery.

1. Salt causes corrosion in the equipment.
2. Salt fouls inside the equipment. The fouling problem not only negatively impacts the heat transfer rates in the exchangers and furnace tubes but also affects the hydraulics of the system by increasing the pressure drops and hence requiring more pumping power to the system. Salt also plugs the fractionator trays and causes reduced mass transfer i.e. reduced separation efficiency and therefore need for increased re-boiler/condenser duties.
3. The salt in the crude usually has a source of metallic compounds, which could cause poisoning of catalyst in hydrotreating and other refinery units.

Until a few years ago, salt concentrations as high as 10 PTB (1 PTB = 1 lb salt per 1000 bbl crude) was acceptable for desalted crude; However, most of the refineries have adopted more stringent measures for salt content and recent specs only allow 1 PTB in the desalted crude. This would require many existing refineries to improve their desalting units to achieve the tighter salt spec.

This study will focus on optimizing the salt removal efficiency of a desalting unit which currently has an existing single-stage desalter. By adding a second stage desalter, the required salt spec in the desalted crude will be met. Also, focus will be on improving the heat integration of the desalting process, and optimization of the desalting temperature to achieve the best operating conditions in the plant after revamp.

Acknowledgments

First and foremost, I would like to thank my advisors and supervisors, Prof. Ali Elkamel, Prof. Mazda Biglari, Prof. Ting Tsui, and Prof. Ali Lohi, who have assisted me patiently and generously to achieve another milestone in my life. They have been exceptionally understanding and helpful through the course of preparation of this thesis workbook. It has been an honour, an enriching experience and such superb personal development for me to work with Dr. Elkamel, and other world-class professors and students at the University of Waterloo.

I am also grateful to fellow researchers and potentially life-long friends and collaborators in the Process Systems Engineering group and in the Department of Chemical Engineering in the University of Waterloo.

Last but definitely not least, I would like to extend my most heartfelt gratitude to my parents, my beloved mother, Noor Afagh Arabi and father, Shahpour Ilkhaani, for sacrificing a great part of their lives through unconditional love to ensure that I will receive the best of care, attention and education. I would also like to thank and recognize truly my best friend, my brother Shaahin, who has played a significant role in my achievements and personal development.

I wish I could hereby name each and everyone who has touched my life in so many meaningful ways. I shall not forget your kind deeds and presence in my mind and my heart. Indeed, I salute and thank you all with the utmost sincerity and appreciation.

To my beloved mother, father and brother, and all my respected teachers, past and present

Table of Contents

List of Figures

List of Tables

Chapter 1: Introduction to Crude Oil Desalting

1.1. Introduction

As oil production is often accompanied by significant amounts of water, it is necessary to provide desalting and dehydration systems to separate the oil and water before the oil can be sold. Oil desalting and dehydration process is the process of removing the water-soluble salts from the crude oil.

In view of the expected oil shortage worldwide and the fact that most crude oil is produced with some entrained water, the ability to describe the relationship of crude to water percentage with all the various factors that affect the desalting process has become increasingly important. Therefore all oil industries like petroleum technology, production operations and oil refining will greatly benefit from such correlations, in a direct approach for the study of water-in-oil emulsion formation in petroleum fluids as well as for understanding the behavior of interfacial tension.

With the increasing regulations on effluent water purity and the ever-increasing cost of producing a barrel of oil, the use of emulsion-treatment plants have become an important aspect in crude oil processing. Treating of emulsions has always ranged from the simple ways of gravity settlement to the highly sophisticated ways of electrostatic desalting and dehydration systems. The development of desalting systems has always been evaluated in terms of quantities of salt and water being removed. When crude oil is heated in various refining processes, the water could be driven off as steam. The salt in the water, however, wouldn't leave with the steam and could crystallize and either remains suspended in oil or could form scale within heat-exchangers and other equipments. Entrained salt crystals could deactivate catalyst beds and plug processing equipment. Therefore, desalting and dehydration facilities are often installed in crude oil production units in order to minimize the occurrence of water-in-oil emulsions.

Because of these potential problems, refineries usually reduce crude oil salt contents to very low levels prior to processing. To reduce the amount of desalting required at the refinery some oil purchasing contracts specify a maximum salt content as well as maximum water content.

Due to the fact that processes are becoming more complex, more dependent on catalyst, less tolerant for downtime of equipment, and more intense operating conditions are deployed, the level of salt in the crude for refineries is a lot more stringent than before, specs of 1 PTB or less are defined by refiners at present. To satisfy such tight specifications producers are usually required to perform extensive crude oil desalting.

The desalting process involves six major steps including separation by gravity settling, chemical injection, heating, addition of fresh (less salty) water, mixing, and electrical coalescing. These steps are further explained in Chapter 2.

1.2. History of Desalting and Dehydration

In the mid 1800's, there was increasing demand on salt production industries in the United States, based on evaporation of underground brines to recover salt. At that time, crude oil was a contaminant that would often accompany the produced brine. It was skimmed off and then discarded. The first analysis of crude oil at Yale University revealed the origin and organic nature of oil and its valuable properties and enterprising petroleum producers were intrigued by this new product, the rock oil. The search technique for salt was slowed down and the race for oil production started. Thus, the roles of contaminant and product have been reversed in the case of brine and oil, which since the beginning have been associated in the underground and offshore reservoirs. Since then, all phases of petroleum technology have kept pace with the ever-lasting industrial thirst for more oil production and the never-ending search for better and more efficient methods. Oil production techniques have advanced from the very crude wooden troughs and pipes used in the early development of the industry to the modern complex gathering systems, staged separation, and treating plants.

In the early days water-in-oil emulsions were treated by allowing time for water to settle out and later be drained off. Settling time and draining are accomplished in various mechanical devices such as wash tanks. However, this mechanism was time taking and resulted in a crude oil with a high salt content because of the inefficient separation process. Therefore, to speed up settling time, and in order to increase the efficiency of the process, other factors were to be found and applied.

Heating was later found to be an efficient means of reducing oil viscosity, allowing water droplets to settle out faster. At best, however, the heating factor was also unreliable because crude oil, in which the water remains emulsified, would not separate with moderate temperatures or time. The demand for efficient methods of desalting and dehydration continued. The advent of two techniques in 1910 changed our perception of emulsion treatment. One of these techniques was the introduction of a proper chemical that causes water droplets to fall out more easily and faster by breaking up the emulsion film around the water droplets in oil and hence speeding up the separation process. The other technique was introduction of a high voltage field to water-in-oil emulsions through which the small droplets are forced to coalesce. Coalescing would increase the separation efficiency by increasing the gravity.

Many commercial installations nowadays are employing chemically aided electrical dehydration, which is a complex employing chemical demulsifiers, heat, dilution water, mixing and electrostatic field to dehydrate and desalt the crude.

1.3. Global Trends in Crude Oil Quality

Conventional crude oil composition and properties could range broadly from heavy and sour to light and sweet crude. Heavy (low API) and sour (high sulphur content) crude oil is more difficult and more expensive to refine compared to light and sweet crude. Global production of light sweet crude peaked in the year 2000, and has been declining since. The diminishing supply of light sweet crude oil will also contribute to its price volatility.[2] As the world supplies of light sweet crude dry up, increasing attention is being turned to the heavier sour crudes. More than half of the global oil production is currently heavy and sour, and is expected to increase in the future.[3] This includes oil produced by OPEC member nations, Venezuela and Saudi Arabia in particular, as well as non-OPEC members such as Russia. Figure 1.3.1 shows a plot of the average API gravity of crude oils entering U.S. refineries.[4]

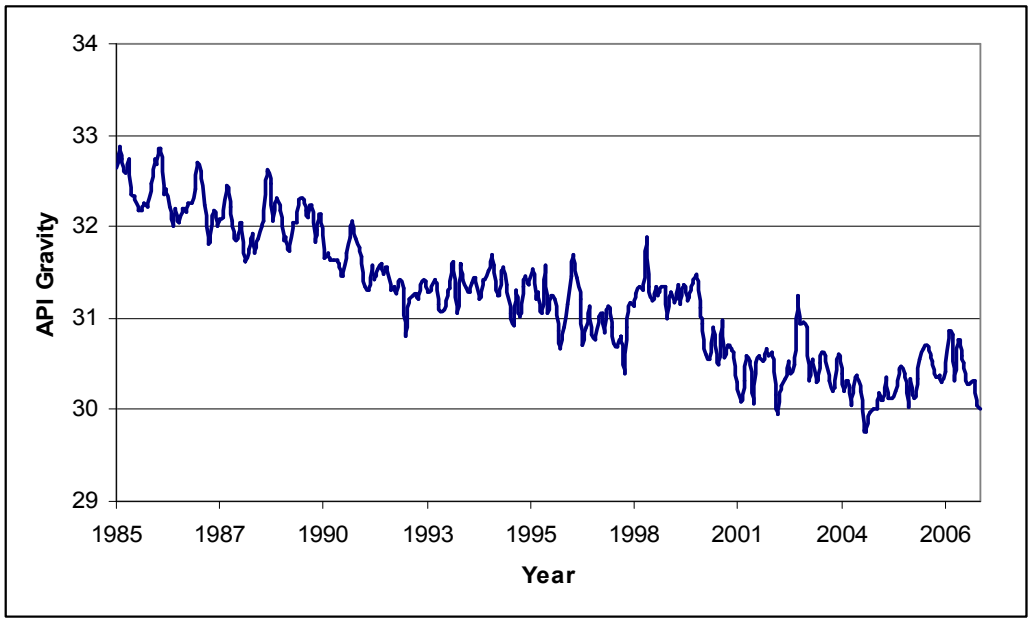

Figure 1.3.1 - Average API Gravity of U.S. Refinery Input Crude Oil

The higher demand for light sweet crude reduces supplies and drives up the selling cost.[5] This is illustrated in Figure 1.3.2, which charts the price differential between Brent Crude, a light and sweet crude, and Maya Crude, a heavy and sour crude.[6]

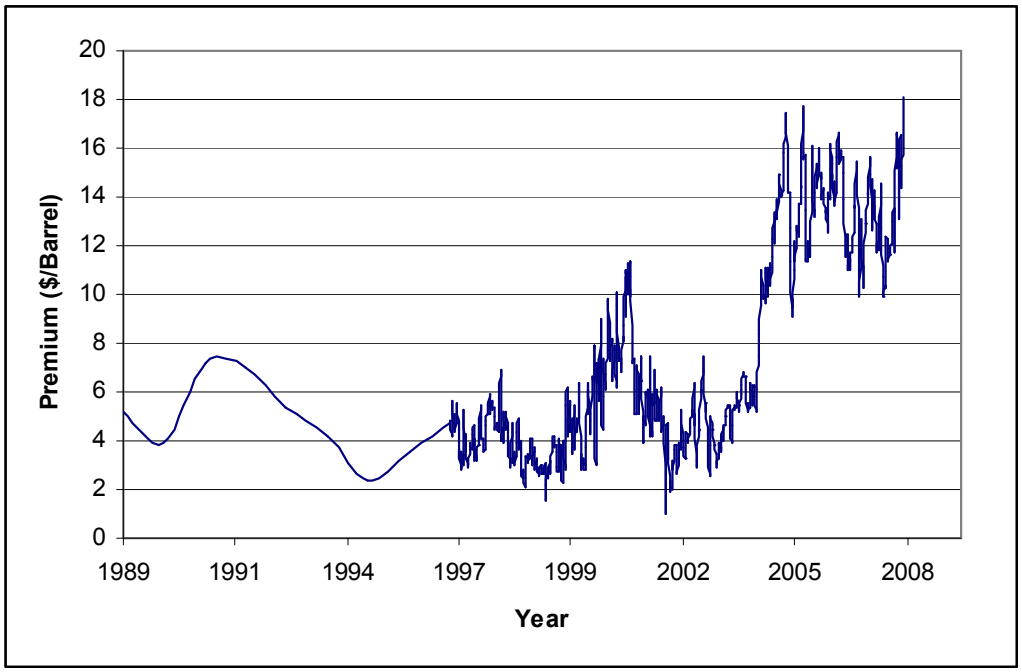

Figure 1.3.2 - Price Differential between Brent and Maya Crudes

This increasing reliance on cheaper, lower quality crudes underlies the impact of increasingly stringent legislation on sulphur-content in gasoline,[5] which may increase reliance on low-sulphur crudes.[2] Figure 1.3.3 displays the history of world oil production, and the predicted trends for the future.[7]

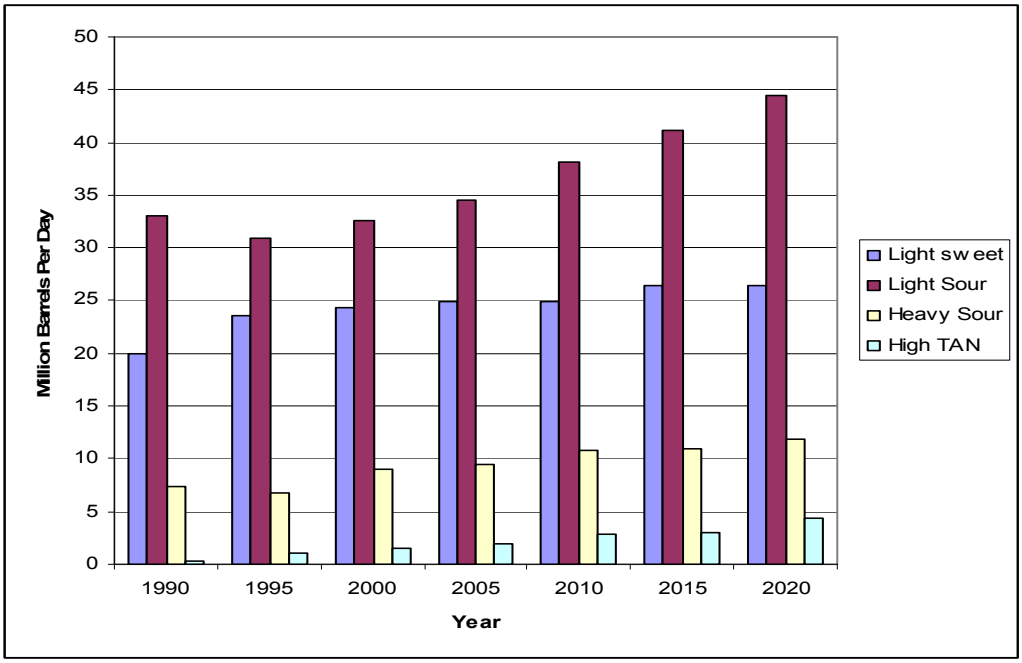

Figure 1.3.3 - Past and Predicted Trends for World Oil Production

*TAN = Total Acid Number

Much of the world-wide refining infrastructure is not equipped to refine the lower-quality crudes. As it stands, the upgrading process is a multi-billion dollar, multi-year process. However, due to the scarcity of light crude and the fact that as a well starts to deplete the remaining crude oil in that well will be heavier in composition compared with its early days of production, the trend of the crude oil production is towards heavier and more difficult crudes.

1.4. Sources of Wet Oil

Water-contaminated oil reservoirs are subject to water influx. Water is often present at the bottom of reservoirs and exerts pressure on the oil accumulations. As the oil is produced and withdrawn up to the surface, the water advances into the void spaces replacing the oil. Emulsions generally occur as a result of flowing crude oil streams and shaking (agitation) of water along the flowing streams. However, when discussing the main sources of wet oil production, there are three main causes encountered in both theory and practice i.e. the so called primary, secondary and tertiary causes.

1.4.1 Primary Causes

At some time in the production history of almost every oil well, more water is withdrawn with oil than is acceptable to the buyer. Some wells produce water from the beginning of production and others come much later in the life of the field. Figure 1.4.1a shows a very simplified form of three wells, A, B and C drilled at a distance from one another, on the same reservoir.

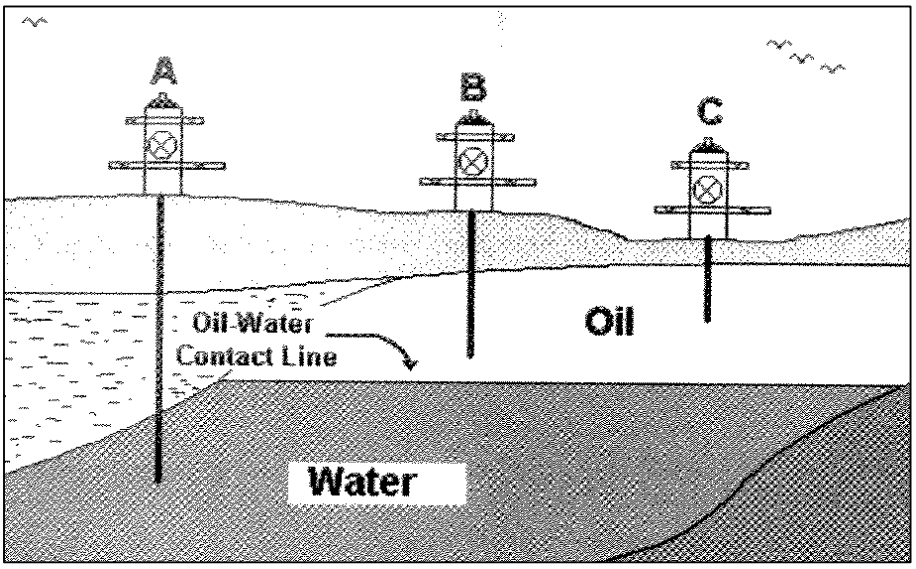

Figure 1.4.1a - Early Life of a Field; Wells B and C Produce Dry Oil

The reservoir contains oil and water. In this case, a large quantity of water lies under the oil and acts as the driving force from the bottom. Early in the life of the field, well A, drilled deep near the point of oil-water contact interface or at the edge of the reservoir, produces too much water. The other wells B and C drilled higher up on the reservoir structure produce dry oil at the beginning.

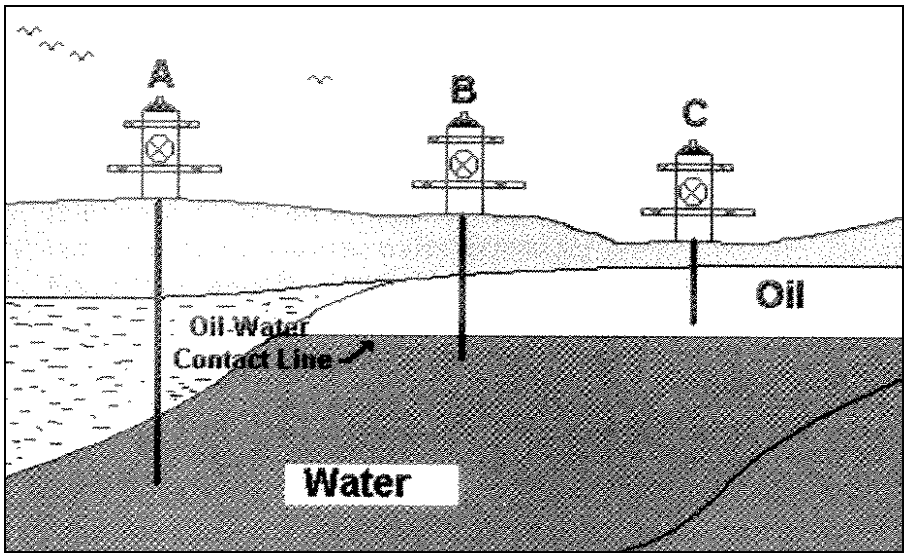

Figure 1.4.1b - Aquifer Level Moving up With Time; Well B Produces Wet Crude

Figure 1.4.1b shows the same reservoir later in the life of the field. At this later phase, well A is completely watered out. Well B produces some percentage of water associated with oil and well C continues to produce dry oil.

Other primary causes could be one or a combination of the incidents such as water coning, water fingering or an early water breakthrough shown in Figures 1.4.1c, 1.4.1.d and 1.4.1.e.

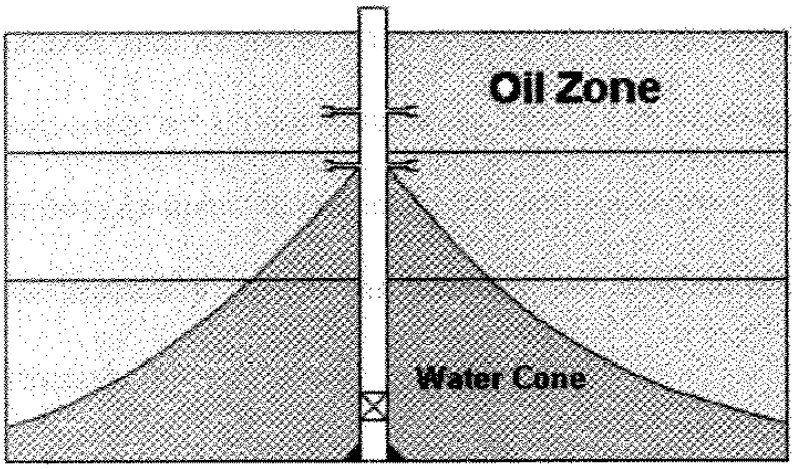

Figure 1.4.1c - Water Coning Phenomenon

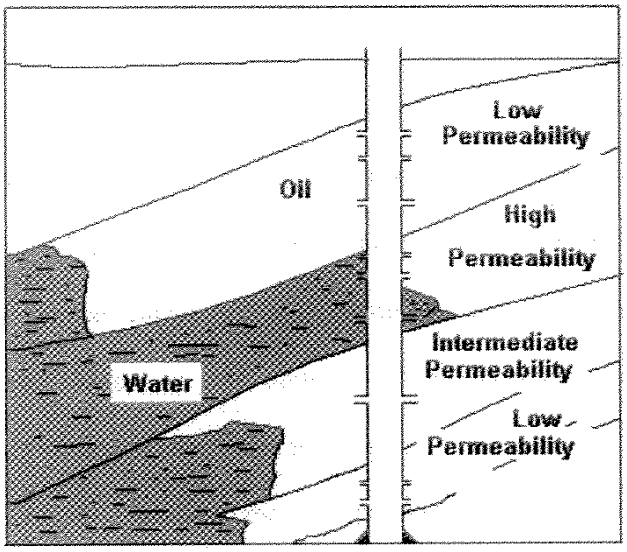

Figure 1.4.1d - Water Encroachment/ Early Water Breakthrough

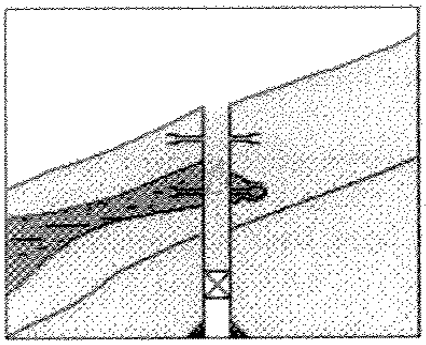

Figure 1.4.1e - Water Fingering Phenomenon

1.4.2 Secondary Causes

Other possible causes of oil wells producing salty water are those of sudden irregular water intrusion such as following.

- Inter-communication between tubing and casing strings.
- A hole in the casing near water formation.
- Fracture or crack between oil and water formations.
- Casing failure due to corrosion or,
- Channeling caused by a poor cementing job.

Figure 1.4.2 shows one of those possible causes, casing failure. The casing failure caused by either corrosion or poor cementing job at a point above the producing zone, which allows water from an upper zone to enter the well and contaminate the oil production. However, the above secondary causes can possibly be rectified in practice and therefore prevent water intrusion.

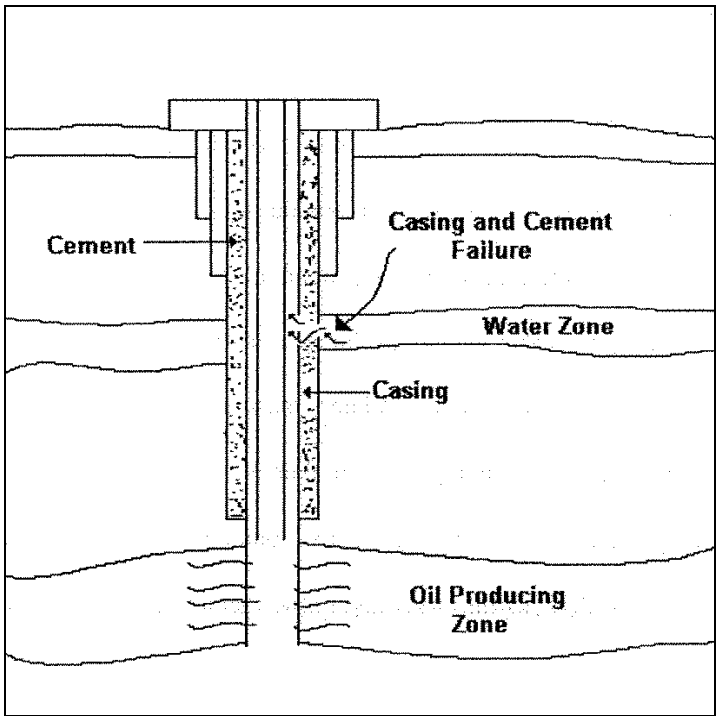

Figure 1.4.2 - An Example of a Casing Failure

1.4.3 Tertiary Causes

There are still other causes of water intrusion that are induced as a result of later technology in stimulating or enhancing the production of oil. Among these technologies are steam or water injections into the oil reservoir. These injection methods are used to help or increase the amount of oil recovered from depleted pressure reservoirs. The injection of water or steam, of course, causes water to be mixed and produced with oil. These causes usually come into the picture at later steps in oil recovery. Sea water or steam injection plants are implemented mainly to boost oil recoveries.

The aforementioned causes are the main producers of wet crude. Nevertheless, water-in-oil emulsions reaching desalting and dehydration plants are also caused by mixing-intensifiers like moving and agitation of formation brine with crude oil. The agitation normally takes place when producing a well via subsurface pumps or gas lift methods. The agitation influence is also intensified when flowing through casing perforations, production tubing, subsurface safety valves, bottom and well head chokes, or in the flow lines and pipeline restrictions.

1.5. Importance of Desalting in Refineries

The removal of formation water from wet oil streams has long been an essential part in the crude oil processing. Amongst many reasons why desalting and dehydration units are installed is avoiding transportation of high viscosity liquid, as well as water-in-oil emulsions, which require more pumping energy. Nevertheless, crude oil desalting and dehydration has become a necessity because of the salts carried to refineries and the problems caused as a result.

In most oil refineries, salts and water are removed in day to day operation because of three major reasons: corrosion, scale accumulation and catalyst poisoning.

1.5.1 Corrosion

The most frequent problem that salts and water cause is corrosion in pipelines, vessels, valves and instrument parts in the processing plants. Chloride salts melt in heaters, where the temperature could reach as high as 300°C. As a result, and in the presence of water, HCl forms, which could cause serious corrosion problems with equipment and instrumentation that are made of iron.

1.5.2 Scale Accumulation

Calcium sulfides come also into the picture of precipitation and development of scale in heating tubes. Scaling or precipitation causes the following problems.

- Reducing heat transfer in heaters, causing more fuel consumption and higher cost.
- Creating Hot Spots in heating tubes, which reduces their operational expected life.
- Increasing flow rates excessively, which overloads pumping units making them less efficient.
- Causing blockage in tubes and thus lowering their capacities and efficiencies.

1.5.3 Catalyst Activity

Salts have negative effects on catalysts, which are used in cracking plants and hydrogen processing units for heavy oil products. As the processing temperatures are high in these units, salt could deposit on catalysts in high concentrations and therefore could lower catalyst activity or could cause poisoning of the catalyst and thus could reduce the life cycle of the processing unit.

1.6. Research Objectives

This piece of work will focus on the development of desalting operation in an old refinery. The current capacity of the refinery is 60,000 BPSD and the refinery is planning to increase the capacity to 70,000 BPSD. The refinery currently uses different crude blends from different sources. Design conditions will be based on 80 vol% Maya and 20 vol% Brent crudes. In addition to increasing the capacity and changing the crude slate, based on the economic studies done by the refinery, it is advantageous to further process the bottom of the barrel and turn the low value Vacuum Tower Bottoms (VTB) product to more valuable products such as Naphtha, Kerosene and Diesel by building a grass-root Delayed Coking Unit (DCU) in the plant. This addition to the refinery, requires the VTB to have a low salt content as salt can accumulate in the furnace tubes of the DCU feed heater and cause operational problems.

Due to the above modifications in the refinery there is a need for full revamp of the Crude Distillation Unit (CDU) as well as the desalting unit, which is an integrated part of the CDU. Currently there is only one single desalter in the unit. The salt concentration in the desalted crude stream should be 1 PTB. The current operation allows up to 10 PTB salt in the crude stream. A second stage desalter is needed to achieve this design spec on the desalted crude.

Following are the main objectives of this study and will form chapters of this thesis:

1. Investigate the effect of different variables on the desalting process.
2. Compare different industrial technologies for desalting operation.
3. Understand and develop a model to predict the optimum operating temperature of the Maya crude.
4. Develop heat integration scheme to achieve the required temperature in the desalter.
5. Develop HYSYS simulation for the two stage desalting process.
6. Develop Process Flow Diagrams for the desalting process.

Chapter 2: Process Design Parameters

2.1. Introduction and Background

Emulsions play a great role in our daily life. They are of great practical interest because of their widespread occurrence in most aspects of our daily usage and consumption. Some familiar emulsions include those found in foods (mayonnaise, milk, etc.), cosmetics (lotions and creams), pharmaceuticals (hormone products and soluble vitamins), and agricultural products (herbicide emulsion formulations). However, petroleum and water emulsions are one of many problems directly associated with the oil industry, during both field production and in the refinery environment. Whether these emulsions are created along the process or are unavoidable, as in the oil-field production area, or are deliberately induced, as in refinery desalting operations, the economic necessity to eliminate emulsions or maximize oil-water separation is always present.

2.2. Nature of Petroleum Emulsions

Oil production is associated with the simultaneous production of formation water from petroleum reservoirs. In its early life, a production well produces water at rates normally relatively low, whereas towards the end of the well's lifetime the produced water may be as high as 90% or more of the total liquid production. From a geological point of view, formation water resides in crude oil principally because salt water generally underlies the crude oil in the formation from which it is produced. As the producing life of a field is extended, however, increasing proportions of formation water are produced with the oil. Eventually, most producing wells, at some point in their life spans, will produce water and oil simultaneously, either as a result of natural formation conditions or as an effect of secondary or tertiary production methods. Emulsification of the water and oil, by intimate mixing, may occur in the formations themselves, or in mechanical equipment, such as chokes, pipeline network, separators, and feed pumps.

Water intrusion normally starts at the edge of an oil field and progresses until the production is predominantly water. Oil field waters vary widely in composition and quantity of salt, which is usually dissolved in water, but their salinity is generally greater than that of seawater. Generally, the concentrations of solids in oilfield waters are much higher than in seawater. The total solid concentrations in formation waters range from as little as 200 PPM to saturation i.e. approximately 250,000 PPM. Most sea waters contain approximately 35,000 PPM total solids. The important point is that the water contained in a producing formation has different composition compared with any other brine, even those in the immediate vicinity of that formation.

Emulsions vary from one oil field to another simply because crude oil differs according to its geological age, chemical composition, and associated impurities. Furthermore, the produced water's chemical and physical properties, which also are specific to individual reservoirs, will affect emulsion characteristics. It should be emphasized that formation waters from two different fields are never similar and they vary widely in characteristics. Some have relative densities greater than 1.2, whereas others are essentially non-saline. Ions presents usually include Na^{+}, Ca^{2+}, Mg^{2+}, Cl^{-}, HCO^{3-}, SO_4^{2-}, and sometimes Ba^{2+}.

An emulsion can be defined as a system consisting of a mixture of two immiscible liquids, one of which is dispersed as fine droplets in the other and is stabilized by an emulsifying agent. The dispersed droplets are known as the internal phase. The liquid surrounding the dispersed droplets is the external or continuous phase. The emulsifying agent separates the dispersed droplets from the continuous phase. For an oil field, the two basic types of emulsions encountered are water-in-oil and oil-in-water. Oil-in-water emulsions are often termed reverse emulsions. More than 95% of the crude oil emulsions formed in the oil field are the water-in-oil type. Ideally, there are three components in a water-in-oil emulsion:

(1) Water being the dispersed phase.
(2) Oil being the continuous phase.
(3) Emulsifying agent to stabilize the dispersion.

Besides these three components, certain conditions must also be met before an emulsion could form. Two conditions necessary to form stable emulsions are a) the two liquids must be immiscible, and b) there must be sufficient agitation to disperse the water as droplets in the oil. These emulsions may comprise varying proportions of oil and water. Purchasing oil is always dependant on water content, which must be reduced to as little as 2%, varying with specifications prevalent for the geological area or dictated by the purchaser.

In oil field operations, two types of emulsions are now readily distinguished in principle, depending on which kind of liquid forms the continuous phase.

(i) Oil-in-water (O/W) for oil droplets dispersed in water.
(ii) Water-in-oil (W/O) for water droplets dispersed in oil.

The emulsified water exists predominantly in the form of dispersed particles that vary in size from large drops down to small drops of about 1 μm (0.0004 in.) in diameter. The size distribution and stability of emulsions are usually determined by two factors a) character of water and oil (gravity, surface tension, chemical constituents, etc.) and b) production methods.

In field operations, oil and water are encountered as two phases. They generally form a water-in-oil (W/O) emulsion, although as the water cut increases and secondary recovery methods are employed, reverse or oil-in-water (O/W) emulsions are increasing.

Further reference to emulsion in this research implies water-in-oil type emulsions, which is the predominant type in crude oil production.

2.2.1 Role of Emulsifying Agents

Water-in-oil emulsions contain complex mixtures of organic and inorganic materials. The compounds that are found along with water and oil are called emulsifying agents. Those agents are surface-active materials that tend to stabilize emulsions to an even greater degree. These include asphaltenes (Sulfur, Nitrogen, and Oxygen), resins, phenols, organic acids, metallic salts, silt, clays, wax, and many others.

Emulsifying agents have surface-active preferences. Some have preference to oil, and other are more attracted to water droplets. Ideally, an emulsifying agent has a head and a tail. The head is hydrophilic, attracted to water droplets, and the tail is Lipophilic, which attracts oil.

Some emulsifying agents may form a complex at the surface of droplets and thus yield low interfacial tension and a strong interfacial film. Nevertheless, emulsifying agents either tend toward insolubility in either liquid phase or have an approach mechanism for both phases, but always found concentrated at the surface. In general, the action of emulsifying agents can be visualized as one or more of the following:

(a) Reducing the interfacial tension of water droplets, thus causing smaller droplets to form. Smaller droplets are difficult to coalesce into larger droplets, which can settle quickly.

(b) Forming a viscous coating, physical barrier, on droplets that keeps them from coalescing into larger droplets.
(c) Suspending water droplets. Some emulsifiers might be polar molecules creating an electrical charge on the surface of the droplets causing like electrical charges to repel and preventing them from colliding.

The type and amount of emulsifying agent would affect emulsion's stability. Temperature history of the emulsion is also an important effect on the formation of some of the emulsifying agents, paraffin and asphaltene type. The strength of the interface bond and the speed of migration of the emulsifying agents are important factors.

2.2.2 Stability of Emulsions

The stability of emulsions and the contributing factors are of great importance to production of oil from underground reservoirs. Although extensive studies have been conducted in investigation of the destabilization of W/O emulsions, the actual mechanisms are still not well understood.

Emulsions may be stabilized by the presence of a protective film around water droplets. Protective films, created by emulsifying agents, act as structural barrier to coalescence of water droplets. Nevertheless, the factors favoring emulsion's stability can be summarized as follows.

2.2.2.1 Type of emulsifying agent

When water and oil first mix, the emulsion may be relatively unstable. As time goes by, emulsifying agents migrate to the interface of water-in-oil due to their surface-active characteristics. Emulsifying agents' activity is generally related to two function-performance at the interface, and the speed of migration.

2.2.2.2 Droplet size

The more shearing action that is applied to an emulsion the more the water will be divided into smaller drops, and the more stable the emulsion becomes.

2.2.2.3 Water content

As the percentage of water increases, the stability of the emulsion decreases. Experience has shown that the lower the water percentage, the more difficult it is to treat the emulsion. Generally, a water percentage above 60% increases the chance of forming water as an external phase. Thus, when diluted with fresh water, the emulsion may invert to O/W type. The amount of emulsifying agents, which are mostly present at the water-oil interface, is concentrated if water percentage is small.

The stability of an emulsion may also be subject to the following.

- Viscosity of the oil (high viscosity oils have high resistance to flow and thus retarding water droplet movement to coalesce)

- Age of emulsion (in general, as oil and water are mixed the emulsifying agents tend to go toward the interface).

This kind of action causes emulsions to age and become more difficult to treat, as well as causing film strength (foreign materials present in emulsions tend to increase the strength of the film surrounding a drop of water).

To break or rupture the film that surrounds a water drop, it is necessary to introduce chemical action and, in many desalting plants, apply heat. The chemical used to break the film is widely known as demulsifier, the subject of the next section.

2.2.3 Emulsion Breaking or Demulsification

The treatment of emulsions has been approached in a number of ways over the years. Today, however, injecting chemicals (demulsifiers) is by far the most widely used in the oil industry.

Demulsifiers are similar to emulsifying agents. Their action is always at the water-oil interface and, therefore the faster the demulsifier gets there the best job can be done. Demulsifiers reach the interface and then work on three steps a) flocculation b) coalescence and c) solid wetting. Flocculation is joining together of the small water drops, rupturing of the thin film and then uniting the water drops. As coalescence takes place, the water drops grow large enough to settle down and be easily separated. The solid wetting takes its course with solid emulsifying agents as iron sulfide, silt, clay, drilling mud solids, paraffin, etc.

Generally, demulsifiers act to neutralize the effect of emulsifying agents. The cost-effectiveness of a demulsifier program depends on proper chemical selection and application.

2.3. Factors Affecting Desalting Performance

Treatment of emulsions involves allowing time for water drops to settle out and be drained off. Settling time and draining are accomplished in wash tanks, separators, and desalting vessels. However, settling and draining can be speeded up using one or more of the following actions.

- Injecting chemicals (demulsifier)
- Application of heat
- Addition of diluents (fresh water)
- Application of electricity

The main objective of a desalting plant is to break the films surrounding the small water droplets, coalescing droplets to form larger drops, and then allowing water drops to settle out during or after coalescing.

The most important variables affecting desalting performance that have been identified and studied include (1) settling time, (2) demulsifier injection, (3) heat, (4) addition of fresh water, (5) effective mixing of oil and water as well as chemicals for breaking the emulsion and (6) electricity.

2.3.1 Settling Time

The desalting process uses one or more of the above mentioned procedures so as to increase the water weight making it faster to settle and be drained off. Thus, gravity differential is the scientific principle that forms the basis for all emulsion treatment plants.

Formation water could flow with crude in two forms: free and emulsified. The free water is not intimately mixed in the crude and found in larger drops scattered throughout the oil phase. This kind of water is easy to remove simply by gravity-oil-water separators, surge tanks (wet tanks), and desalting vessels. On the other hand, emulsified waters are intimately mixed and found scattered in tiny drops in the oil phase. This kind is hard to remove by simple settling devices, so, further treatment such as chemical injection, fresh water dilution, mixing, heating, and electricity.

The desalting process relies heavily on gravity to separate water droplets from the oil continuous phase. However, a drag force caused by the downward movement of water droplets through the oil always resists gravity. Adequate provision has then to be built into the desalting and dehydration system to ensure better gravitational separation. Gravitational residence time is based on Stokes' equation as follows:

$$\nu = 2\pi r^2 (\Delta\rho)g / 9\eta \qquad (2.3.1)$$

Where ν is the downward velocity of the water droplet of radius r, $\Delta\rho$ is the difference in density between the two phases, and η is the viscosity of the oil phase. This equation implies that gravitational separation can be intensified based on:

(i) Maximizing the size of the coalesced water drops.

(ii) Maximizing the density difference between water drops and the oil phase.
(iii) Minimizing the viscosity of the oil phase.

Heating and addition of diluent (fresh water) can best achieve factors (ii) and (iii), whereas applying electric field will enhance factor (i).

2.3.2 Chemical or Demulsifier Injection

Emulsions can be further treated by addition of chemical destabilizers. These surface-active chemicals adsorb to the water-oil interface, rupturing the film surrounding water drops and displacing the emulsifying agents back into the oil. Breaking the film allows water drops to collide by natural force of molecular attraction. Basically for effective chemical injection, the chemical must be able to dissolve in the surface film surrounding the water drops and it must be made of polar molecules, attracted to acidic or organic skins surrounding water drops, which are also of polar materials.

Emulsifying agents envelop water drops with thin films preventing them from colliding. The films are polar molecules, and the attraction between two water drops become much like two bar magnets being drawn to each other. A demulsifier contacts the emulsifying agent or the film, reacts with it and causes it to weaken or break. Time and turbulence aid diffusion of demulsifiers through the oil to the interface. The demulsifier, having caused the natural skin or film to recede from the entire water-oil interface, exposes a thin film susceptible to rupture by the water-to-water attraction forces at very close distances.

Chemical/demulsifier calculations are based on the following three assumptions:

- The continuous phase is oil.
- The chemical/demulsifier acts and travels in the continuous phase.
- The chemical/demulsifier is water insoluble but oil soluble.

The lower the water percentage in an emulsion the more difficult it is to treat. Reasons for such a rule are as follows.

- The distribution of water drops in the continuous phase depends on the water percentage. As the water percentage increases, the closer the water drops become to each other.
- Emulsifying agents are more concentrated at the water-oil interface if the water percentage is small.
- Dispersed drops are difficult to coalesce compared to the ones close-by. In addition, the rate at which water drops will coalesce is a function of the droplet radius.

2.3.3 Heating

Heat decreases the viscosity, thickness, and cohesion of the film surrounding water drops. Heat also reduces the continuous phase (oil) viscosity helping water drops to move freely and faster for coalescing. Heat is applied so as to accomplish the following functions.

- Dissolve the skin surrounding the water drops.
- Spread demulsifier throughout the continuous phase reacting with films.
- Create thermal current to collide water drops.
- Melt the emulsifying agents.

Controlling the temperature during operations is a very delicate job. Any excessive heat might lead to evaporation, which would result not only in loss of oil volume, but also reduction in price because of decrease in the API gravity. Furthermore, fuel gas is a valuable product that should not be inefficiently wasted.

Heating depends on the amount of water in the oil, temperature rise, and flow rate. The water percentage plays a great role in fuel consumption. It requires about half as much energy to heat oil as it does to heat water. For that reason, it is essential to remove as much water as it is permissible prior to heating. In general, as the water content of the emulsion increases the temperature difference between the inlet, to a heater, and the outlet streams decreases.

Excessive heating might also result in many operational problems. Such problems include:

- Increase in fuel cost.
- Maintenance problems and cost.
- Scale development.
- Increase in oil volume loss and API decrease.

2.3.4 Dilution with Fresh Water

Salts in emulsion could come in solid crystalline form. So, the need for fresh water to dissolve these crystal salts arises and so the dilution with fresh water has become a necessity in desalting/dehydration processes. Fresh water is usually injected before heat exchangers, so as to increase the mixing efficiency and prevent scaling inside pipes and heating tubes.

Fresh water is injected so that water drops in emulsions can be washed out and then be drained off, hence the term “wash water” is used. The quantity or ratio of fresh water injected depends on the API gravity of the crude. Generally the injection rate is 3-10% of the total crude flow.

2.3.5 Mixing

As discussed earlier, high shear actions form emulsions. Similarly, when dilution water or fresh water is added to an emulsion, one needs to mix them so as to dissolve the salt crystalline and to aid in coalescing finely distributed droplets. Mixing takes place in a mixing valve designed to provide a high shear force in the range of 10-25 psi differential pressure. Mixing aids in the following steps:

- Smaller drops join together more easily.
- Chemical or demulsifier mixes with the emulsion.

- Free injected volume of wash water is broken into emulsion sized drops for even distribution.

2.3.6 Electrostatic Field

The applied electrical voltage gradient has a large affect on desalting efficiency. However, this is set at the design stage, since the transformer sends a constant voltage to the electrical grid, and the separation of the electrical grids inside the desalter vessel is not easily changed.

Inside the desalter vessel, the water droplets in the emulsion have positively and negatively charged ends. The electrical grid distorts the originally spherical droplets to more elliptical shapes. Droplets will be attracted by the positive and negative electrodes, based on their internal charges and their position in the desalter. The positive end of one droplet will be close to the negative end of another droplet, thus providing an electrostatic attraction.[17] This is illustrated in Figure 2.3.6.

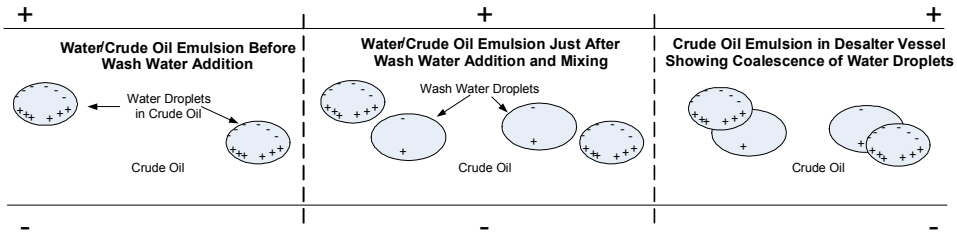

Figure 2.3.6 - Microscopic Representation of Attraction and Coalescence of Water Droplets

The electrostatic attraction between droplets can be represented by the following equation[17]:

$$F = \frac{KE^2d^6}{S^4} \tag{2.3.6a}$$

F Electrostatic force between two adjacent droplets (N)
E Voltage gradient (V/m)
K Dielectric constant for crude oil-water system
D Diameter of water droplets
S Centre to centre distance between two adjacent droplets

As can be seen in Equation 2.3.6a(2.3.6a) if the voltage gradient is increased, the electrostatic force between two adjacent water droplets will increase. However, there are a number of limitations on the voltage gradient. First, transformers can only supply a certain amount of voltage to the electrical grids. Multiple transformers could be installed to supply voltage to the grids, but the initial capital cost of these transformers may outweigh the economic benefit achieved by a higher separation efficiency. Secondly, at a certain voltage, water droplets will begin to rupture, forming smaller water droplets.[17] These droplets will have a higher interfacial tension, thus causing a more stable emulsion. This occurs at the critical voltage gradient defined by Equation 2.3.6b.[17]

$$E_c = k\sqrt{\frac{T}{d}} \qquad (2.3.6b)$$

E_c Critical voltage gradient (V/m)
K Dielectric constant for crude oil-water system
T Surface tension
d Diameter of droplet

As can be seen in equation 2.3.6b the critical voltage gradient decreases as the droplet diameter increases. Thus, the critical voltage gradient must be based on the expected droplet diameter when enough water droplets have coalesced together to settle out of the oil phase.

2.3.7 pH

Crude oil contains a number of organic acids and bases which act as emulsifiers by modifying surface charges at the oil/water interface.[22] The ionizability of these components is controlled by the emulsion pH, which can have a large effect on the physical structure of the emulsion and hence the emulsion stability. Fortunately, the addition of a demulsifier can greatly broaden the range of pH over which successful separation can be achieved.[19]

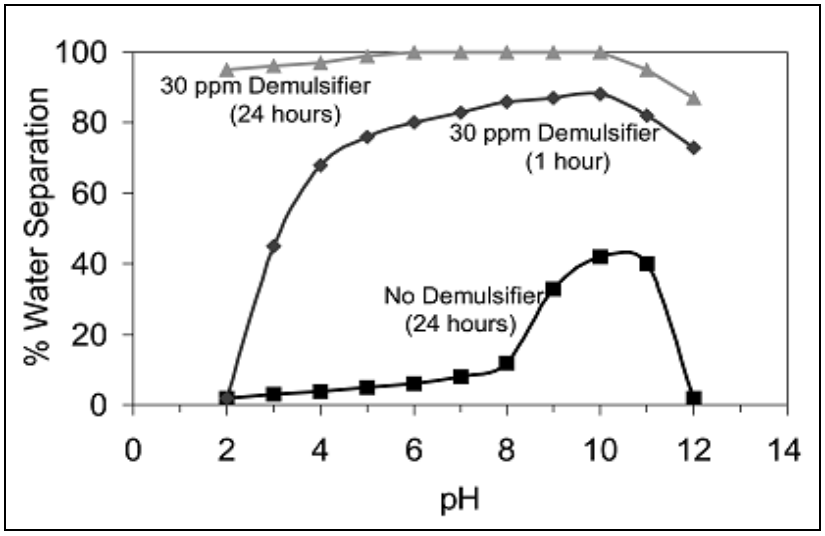

Figure 2.3.7a - Effect of pH and Demulsifier Concentration on Emulsion Stability

The composition of the water phase can also have a large effect on emulsion stability. Due to ionic interactions between salts and the acids and bases at the oil-water interface, higher concentrations of brine in the water phase reduces the optimum pH at which separation occurs, as well as broadens the overall peak as Figure 2.3.7a exhibits.[19]

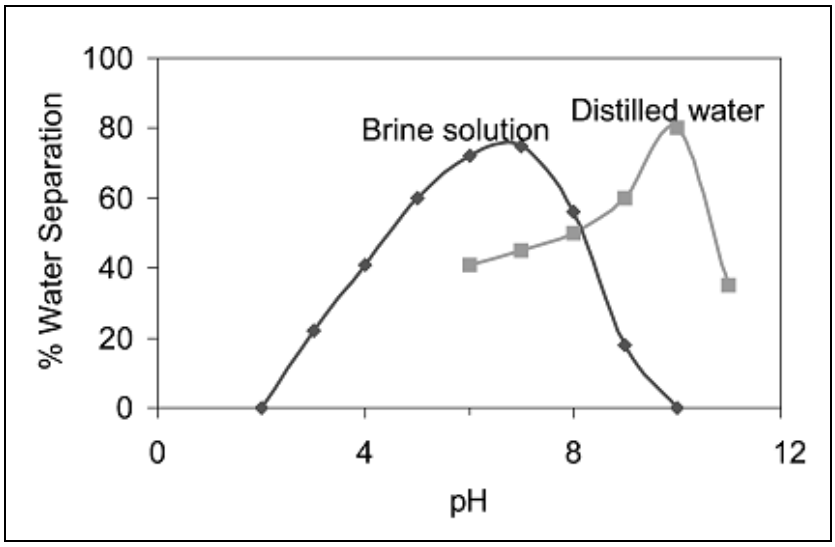

Figure 2.3.7b - Effect of Brine and pH on Emulsion Stability

The industry standard for measuring the acid content of crude oils is the Total Acid Number (TAN) as defined in Equation 2.3.7 below:

$$TAN = \frac{\text{mg KOH}}{\text{g Crude}} \text{ required to neutralize all free acids} \qquad (2.3.7)$$

Crude oils with TANs higher than 1.0 are called high TAN crudes. The total base number (TBN) is correspondingly defined as the amount of perchloric acid required to neutralize all of the bases in the crude.

2.4. Comparison between Desalting Technologies

During this study, two desalter vendors, Cameron and NATCO, were contacted to understand their concepts for designing desalters. The two vendors provide different technologies for desalting operation. Cameron Petreco provides Bilectric Desalter technology whereas NATCO uses the Dual Polarity technology for their desalters. Each technology has its strengths and special considerations. Below are some characteristics of the two technologies.

2.4.1 Cameron's Bilectric Technology

The Bilectric design[47] uses Alternating Current to polarize the water molecules, which promotes coalescence of the water droplets. Figure 2.4.1, shows Cameron's Bilectric desalter design. The Bilectric design utilizes a three-grid electrode system and horizontal emulsion distribution for superior oil/water separation performance.

These units have proven reliable for many years in the refinery application. Since the existing desalter uses the Bilectric desalting technology, it may be an advantage to use the same technology for the second stage desalter.

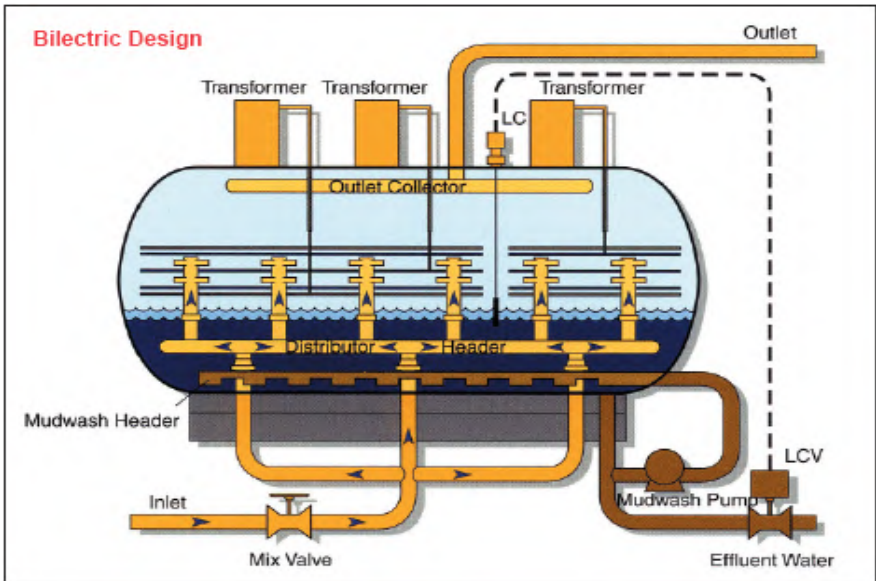

Figure 2.4.1 - Cameron Bilectric® Dehydrator/Desalter

2.4.2 NATCO's Dual Polarity Technology

In place of the AC current electrical system, the Dual Polarity technology[48] uses a system with both AC and DC fields. The crude oil emulsion enters the Dual Polarity equipment and flows upward through the AC field. Free water separates immediately and falls to the water section of the vessel. Larger water droplets coalesce due to the AC field and separate, while smaller water droplets continue with the oil as it flows into the DC section. These remaining water droplets are subjected to the DC electrostatic field, which causes them to coalesce and settle in the bottom of the vessel.

Using the same dependable AC power supply as a conventional electrostatic desalter, the Dual Polarity technology splits the high voltage, with rectifiers, into positive and negative components. Pairs of electrode plates are charged in opposition. Water droplets entering the field are elongated and attracted to one of the plates, accepting the charge of the electrode plate they are approaching.

The dual polarity electrostatics provide for more complete dehydration.[48] Consequently, it can process at higher viscosities, which means less heat is required to lower the viscosity of the oil at processing conditions. In Figures 2.4.2a and 2.4.2b NATCO provides performance comparison between utilizing the AC field only as opposed to combination of AC and DC for desalters.

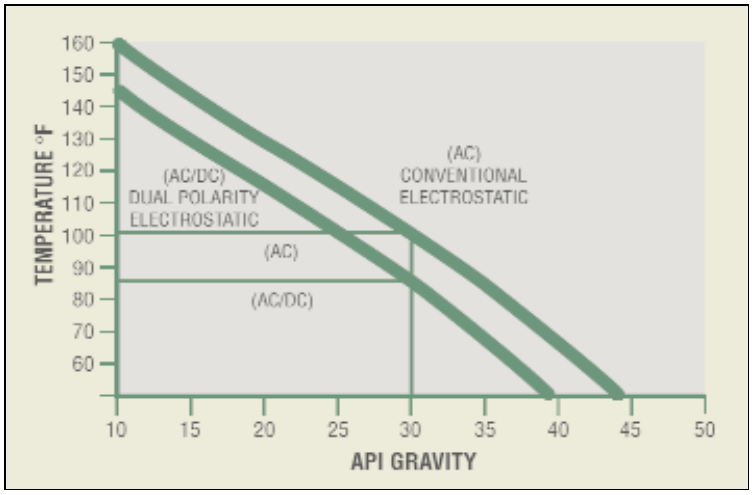

Figure 2.4.2a - Temperature Requirement vs. API Gravity

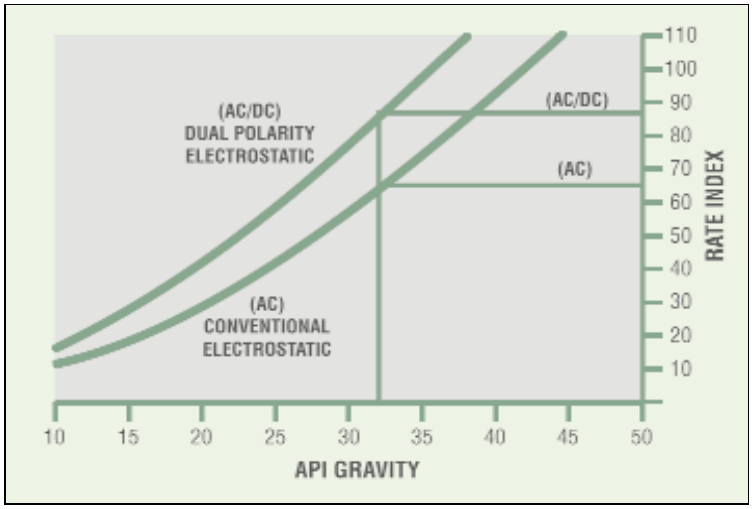

Figure 2.4.2b - Throughput vs. API Gravity

As per NATCO, the Dual Polarity electrostatic desalter requires less space because the vessel can handle much higher flow rates than conventional desalters. The AC/DC process creates larger droplets than conventional AC units, which makes it easier for

these droplets to fall through the opposing emulsion flow, so more oil can be processed in a given size vessel.

2.5. Electrical System for Desalters

As mentioned earlier two desalter vendors, Cameron and NATCO, have been consulted for desalter technology in order to choose a new desalter for revamp of the crude distillation unit. Each vendor is applying different technologies to achieve the required desalting. The brief overview of each vendor electrical system is outlined below.

2.5.1 Cameron's Bilectric System

As explained earlier, the Bilectric system is based on a technology using AC field for removal of particulates. In an AC field, the rapid reversal of the current causes the chemical reaction to be reversed before the corrosion products can be removed from the reaction site by diffusion. Therefore, no net corrosion is observed.

The Bilectric design utilizes a three-grid electrode system and horizontal emulsion distribution.[47] The basic configuration of this process is shown in Figure 2.5.1.

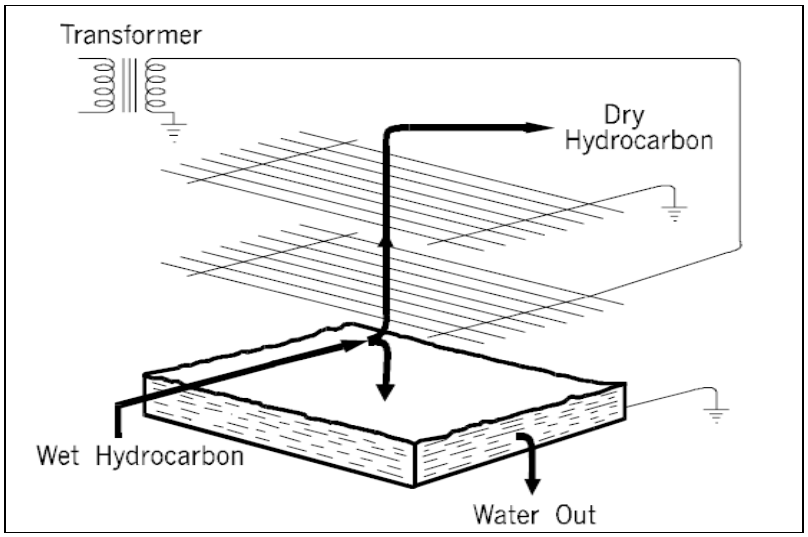

Figure 2.5.1 - AC Electrostatic Coalescer

As per Cameron, the electrical portion of Bilectric system will consist of three 100 KVA, 60 Hz, single phase power units (transformers), level indicator, switchboard panel with three AC voltmeters/ammeters, start/stop pushbutton in explosion proof housing, three voltage/current transmitters (4-20 mA) in explosion proof housing and a junction box for customer interface.

Similar to most conventional electrostatic oil dehydration systems, Bilectric system employs reactance transformers to achieve protection of the electrical power supply. An internal reactor produces a voltage drop in series with the primary winding of the transformer which limits the power to the transformer windings. The demand load for Cameron's Bilectric system is 300 KVA and expected load is 60KW for 2nd stage desalter.

2.5.2 NATCO's Dual Polarity System

NATCO's Dual Polarity system utilizes a combination of AC and DC fields to gain the benefits of both while avoiding the corrosion problems that are associated with just DC field. The basic configuration of this process is shown in Figure 2.5.2.

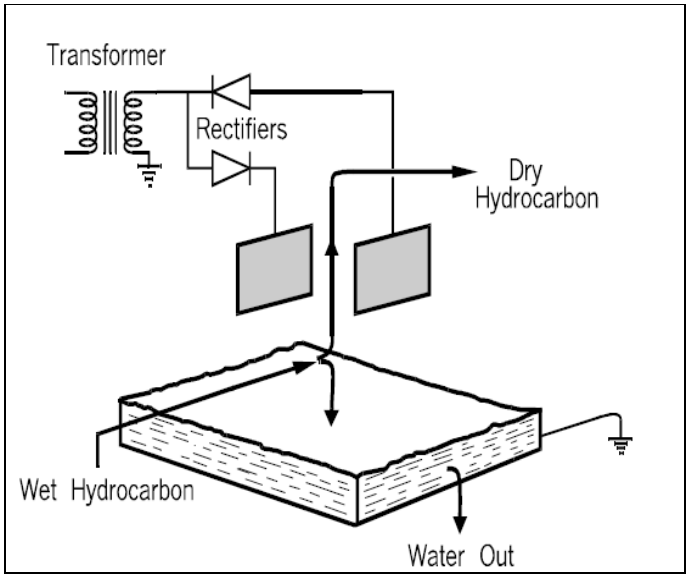

Figure 2.5.2 - Dual Polarity AC/DC Field

By using rectifiers, Dual Polarity system splits the high voltage into positive and negative components. Pairs of electrode plates are charged in opposition. Water droplets entering the field are elongated and attracted to one of the plates, accepting the charge of the electrode plate they are approaching.

As per NATCO the electrical portion of Dual Polarity system will consist of one 100 KVA, 60 Hz, single phase transformer with built-in firing board SCR and rectifiers, circuit breaker, level switches, primary circuit voltmeters, and PC-Load Responsive Controllers (PC-LRC). Built-in firing board SCR and PC-LRC are optional and according to the vendor will provide tuning capabilities of power supply properties and higher tolerance for conductive crude.

Similar to most conventional electrostatic oil dehydration systems, Dual Polarity system employs reactance transformer to achieve protection of the electrical power supply. An internal reactor produces a voltage drop in series with the primary winding of the transformer, which limits the power to the transformer windings. As per the above mentioned, the demand load for Dual Polarity system is 100 KVA and expected load typically is around 30% of demand load.

2.6. Interface Level Control

The second important control function for a desalter is the interface level control. The current trend to operate on heavy crudes can lead to heavier rag layers in desalters, which makes it difficult to control the interface level.

Measurement of the water/oil interface position has commonly been attempted with analog type capacitance level transmitters.[46] However, the measuring probe of this type of device could become coated with carbon, water emulsions, and other material. This coating and buildup creates interface position errors and eventually renders the output signal meaningless. As can be seen in Figure 2.6a the probe cannot measure oil in a water continuous mixture, and a high water cut near the top of the tank causes capacitance probes to read full scale.

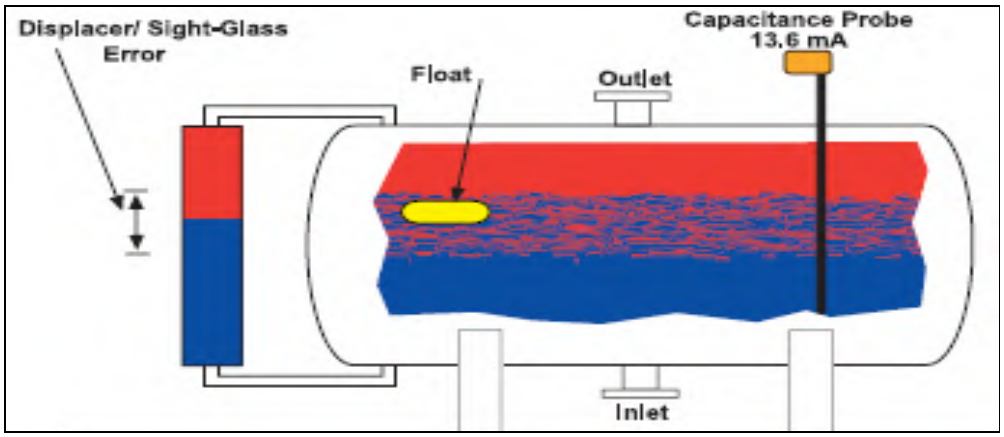

Figure 2.6a - Level Control in the Desalter Using Capacitance Probe

Another more advanced method for controlling the level is AGAR Interface Control. A better control system not only helps in the effective control of the equipment but also helps prevent any oil carryover to the brine system, which goes to effluent treatment. Figure 2.6b depicts a typical AGAR level control system.

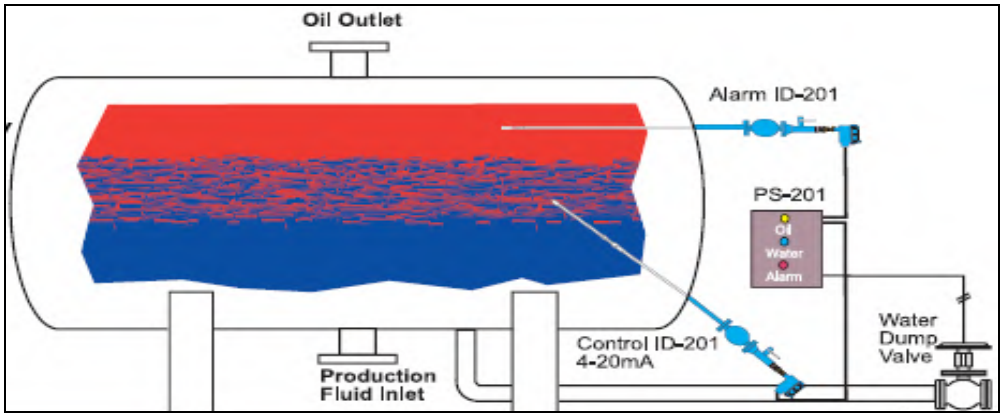

Figure 2.6b - Level Control in the Desalter Using AGAR System

The AGAR Concentration Control gives a current output proportional to water content over the full scale of 0 -100%. This tells the operators about the width of the emulsion pad and also in which direction the rag is growing. It also enables operators to control the level accurately, in the desired direction.

Chapter 3: Determination of Optimum Temperature for Desalting Operation

3.1. Introduction

With the decreasing light crude resources and advancements in the delayed coking technology the heavier crude types are becoming more important options in terms of crude oil refining. The objective of this section is to determine the optimum temperature of the Maya crude, which is to be used in the plant for which this study is being done.

A detailed understanding of the properties of Maya crude is essential in order to determine the optimum temperature required for desalting of this type of crude. The main concern is determination of the dependence of Maya crude oil properties on temperature. The knowledge of this dependence, in addition to providing valuable information about Maya crude, can be used to explore the effect of temperature in the desalting process.

3.2. Analysis of Effect of Temperature on Desalting Process

Based on Stokes' Law, Equation 3.2, settling rate depends highly on temperature.

$$V_s = 2\ gr^2(d_w - d_o) / 9\ \mu^2 \qquad (3.2)$$

Where:

V_s = settling rate, $m.s^{-1}$
g = gravity, $m.s^{-2}$
r = radius of droplet, m
d_W = density of water, $kg.m^{-3}$
d_o = density of oil, $kg.m^{-3}$
μ_o = dynamic viscosity of oil, $kg.m^{-1}.s^{-1}$

Liquid density and viscosity usually decrease with temperature. The effect is even greater regarding viscosity as the dependence is exponential. This means that increasing operation temperature will raise settling rate and therefore, improve separation. In a given desalter, separation improvement means that a larger quantity of oil can be desalted in the same time.

This would suggest that a higher temperature is more convenient. However, crude oil conductivity increases with temperature and so does the power requirement of the process. Additionally, higher temperatures imply an increase of heating costs.

Given these opposing facts, it is expected that there is an optimum temperature. In the case of Maya feedstock it is necessary to know the dependence of density, viscosity and conductivity on temperature in order to determine the optimum temperature.

3.2.1 Density as a Function of Temperature

The dependence of Maya crude density on temperature is given in Figure 3.2.1. Based on the lab data provided, the correlation that best fits the data behavior is given below.

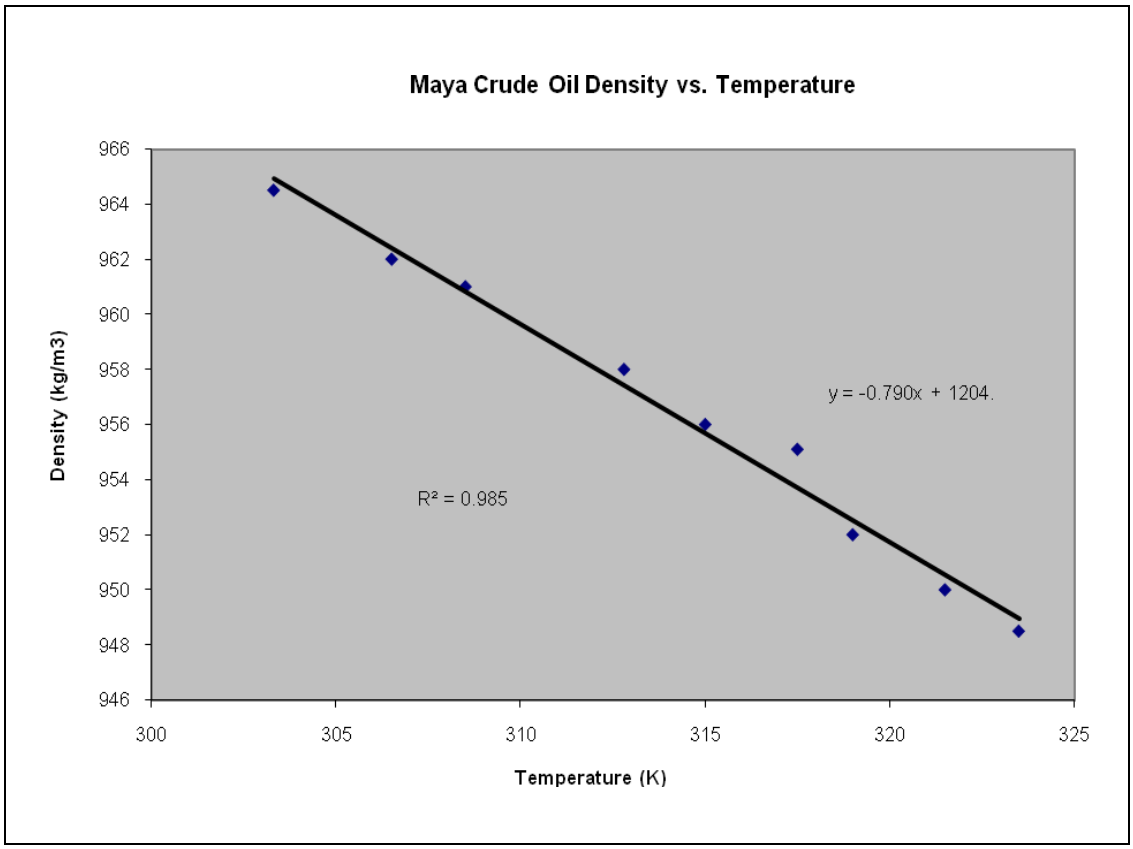

Figure 3.2.1 - Maya Density vs. Temperature

$$d_0 = -0.7902\ T + 1204.6 \qquad (3.2.1)$$

Where:

T is temperature in Kelvin.

3.2.2 Viscosity as a Function of Temperature

Based on the available data for the viscosity of Maya crude at few different temperatures a curve was plotted based on the best fit for the points given. Figure 3.2.2 shows the resulting equation for dependence of viscosity on temperature for a sample Maya crude.

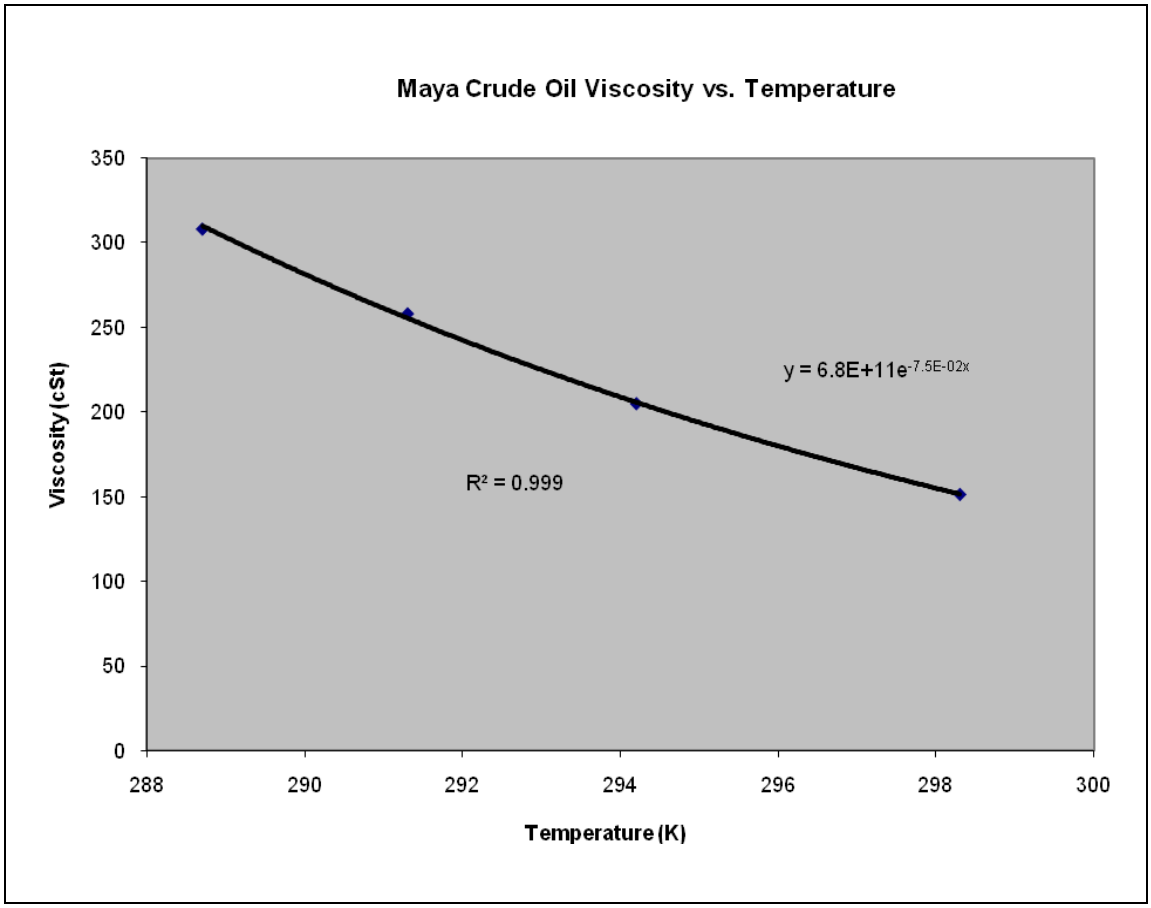

Figure 3.2.2 - Maya Viscosity vs. Temperature

$$\nu = 6.8 \times 10^{11}\, e^{(-0.075T)} \qquad (3.2.2)$$

Where:

ν is Kinematic viscosity in cSt.

3.2.3 Electrical Conductivity as a Function of Temperature

Based on the available data for electrical conductivity of the Maya crude at a few different temperatures a curve was plotted based on the best fit for the points given. Figure 3.2.3 shows the resulting equation for dependence of electrical conductivity on temperature for a sample Maya crude.

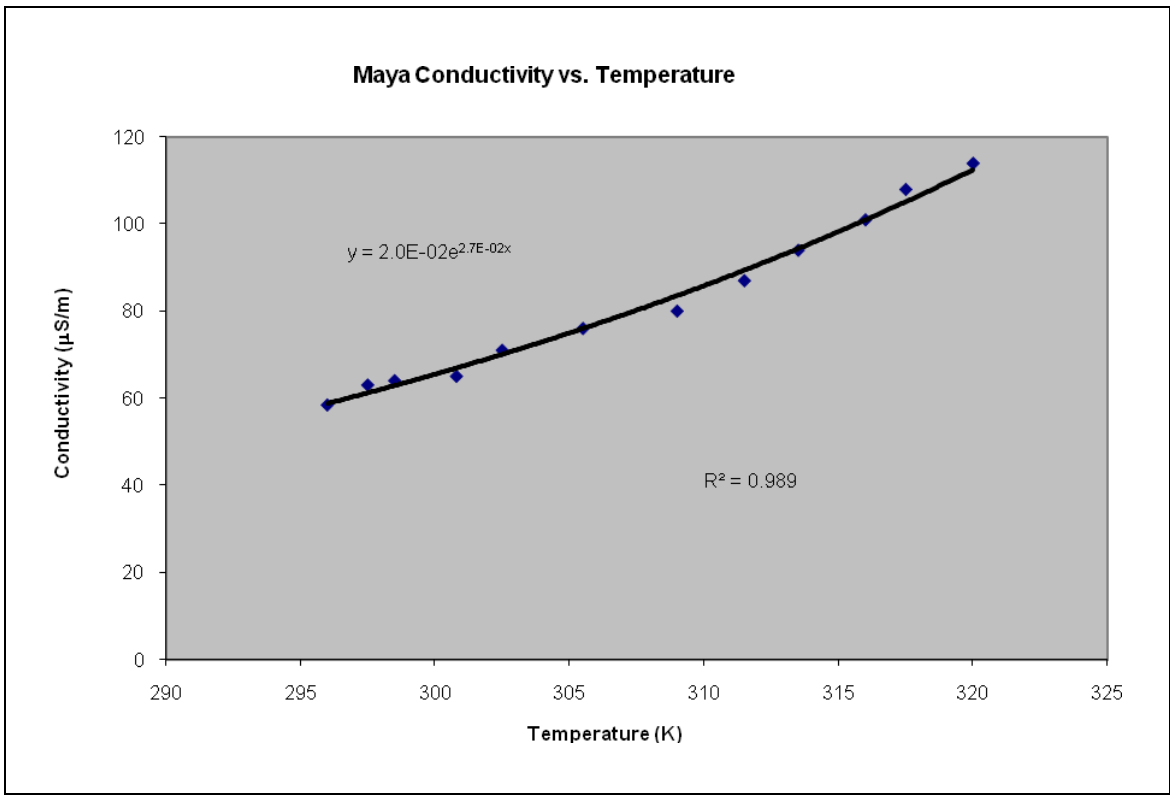

Figure 3.2.3 - Maya Electrical Conductivity vs. Temperature

$$\kappa = 0.02\, e^{(0.0269T)} \qquad (3.2.3)$$

Where:

κ is electrical conductivity in $\mu S.m^{-1}$

Results from these tests show that the properties of Maya are highly dependent on temperature. These equations where used to estimate input data for the mathematical model that determines optimum temperature.

3.3. Mathematical Modeling of Optimum Temperature

The model designed to study the effect of temperature on process economics was developed considering a change in current desalting operating temperature. In order to calculate changes in process economics, the model should include a way of estimating oil inflow based on temperature. The equations presented in the previous sections allow for calculation of the water droplets settling rate from temperature. It is assumed that at a given or fixed operating voltage the droplets population and average size are fixed. Hence, the amount of water separated from oil is distributed in an equal number of equally-sized drops, at any given temperature. An increase in temperature will only cause the drops to move faster across the water-oil interface, increasing the desalter water outflow. From equations 3.2.1 and 3.2.2 equation 3.2 can be transformed into a temperature-dependant equation. Hence, it is possible to know the drop's settling rate by fixing the temperature. For calculation purposes, the drop's residence time within the desalter is defined as the time it takes for a single drop to fall a given distance from the oil phase into the water phase. This is shown in equation 3.3a.

$$\theta_d = h / V_s \qquad (3.3a)$$

Where:

θ_d = Drop's residence time, s
h = Distance covered by the drop

Also drop flow was defined as the volume of water contained in a drop, which flows within the desalter while falling into the water phase. Mathematically, drop flow is defined in equation 3.3b.

$$F_d = V_d / \theta_d \qquad (3.3b)$$

Where:

F_d = Drop flow, $m^3 s^{-1}$
V_d = Volume of water in drop, m^3

Because drop flow is the amount of water moved through the desalter by a single drop, the total water flow through the desalter can be calculated by knowing the number of drops. In order to do this, drop flow is estimated for the current operating temperature, at which the total water flow out of the desalter is known. As mentioned before, water size and number are considered to be constant at any give temperature, so the following relation can be assumed.

$$F_{w\,(out)} / F_d = F_{w\,(out)}^* / F_d^* \qquad (3.3c)$$

Where:

$F_{w\,(out)}$ = Water outflow, $m^3 year^{-1}$

F_d^* = Drop flow at current operating temperature, $m^3 s^{-1}$
$F_{w\,(out)}^*$ = Water outflow at current operating temperature, $m^3 year^{-1}$

Finally, equations 3.3a and 3.3b can be substituted in equation 3.3c to obtain the following linear relation between settling rate and water outflow.

$$F_{w\,(out)} = [V_s / V_s^*] \,.\, F_{w\,(out)}^* \qquad (3.3d)$$

It is to be noted that knowledge regarding the size and number of drops, as well as the distance covered by them while settling is not required to estimate water outflow at a given temperature. The water outflow can then be readily related to oil inflow by considering the desalter dehydration efficiency and the water/oil feed ratio, as shown by the following equations 3.3e and 3.3f.

$$F_{w\,(in)} = F_{w\,(out)} / \varepsilon \qquad (3.3e)$$

Where:

$F_{w\,(in)}$ = Water inflow, $m^3 year^{-1}$
ε = dehydration efficiency

And

$$F_{o\,(in)} = F_{w\,(in)} / R_{wo} \qquad (3.3f)$$

Where:

$F_{o\,(in)}$ = Oil inflow, $m^3 year^{-1}$
R_{wo} = Water/oil feed ratio

Once the oil inflow has been established for a certain temperature, the changes in costs and benefits can be computed. The main elements considered in the model are given in the following sections.

3.3.1 Benefit Due to Flow Increase (BFI)

As increase in temperature increases the settling rate of water, a larger amount of crude oil can be treated and produced by increasing the desalter temperature. To this end BFI is defined for economic evaluation of desalting.

$$BFI = [F_{o\,(in)} - F_{o\,(in)}^{*}] \,.\, [\sum_{i}^{n} x_i P_i - P_{IM}] \qquad (3.3.1)$$

Where:

BFI = Benefit due to flow increase, USD $year^{-1}$
$F_{o\,(in)}^{*}$ = Oil reference inflow, $m^3 year^{-1}$
x_i = Fraction of oil that corresponds to product *i*
P_i = Market price of product *i*, USD m^{-3}
P_{IM} = Price of crude oil in international market, USD m^{-3}
n = Number of distillation fractions considered in the evaluation

The information used to compute BFI is presented in Table 3.3.1.

Table 3.3.1 - December 2003 Price of Crude Products

Product	Vol. Fraction (x_i)	Price (P_i), USDm^{-3}
Gasoline	0.156	485.45
Kerosene	0.020	236.28
Gas Oil	0.161	154.54
Lubricants	0.130	1136.36
Residue	0.505	64.82
Losses	0.028	0.00

*Note: 142.15 USD m^{-3} was used for the international market price (PIM) for Maya crude in 2003.

3.3.2 Costs Due to Power Requirements (CP)

An increase in crude oil conductivity implies that more electric current is used, maintaining voltage constant. This means that, while coalescence does not increase, the power consumption does. CP was estimated as follows:

$$CP = (P - P^*).t.C_{kwh} \quad (3.3.2)$$

Where:

CP = Power Costs, USD $year^{-1}$
P = Power at operating temperature, kW
P* = Power at operating reference temperature, kW
t = Desalter operating time, hours $year^{-1}$
C_{kwh} = Cost of Power, USD kWh^{-1}

3.3.3 Pumping Costs (CB)

A larger flow requires additional pumping, both for oil and for water. This cost is estimated according to the following expression.

$$CB = \{[F_{o\,(in)} - F_{o\,(in)}^*] + [F_{w\,(in)} - F_{w\,(in)}^*]\}\ .Cp \quad (3.3.3)$$

Where:

CB = Pumping costs USD $year^{-1}$
$F_{w\,(in)}^*$ = Water reference inflow, m^3 $year^{-1}$
Cp = Unit pumping cost, USD m^{-3}

3.3.4 Preheating Costs (CC)

Increasing temperature generates extra cost due to preheating either oil or water. These costs are calculated as follows:

$$CC = Q.C_j \quad (3.3.4)$$

Where:

CC = Preheating costs, USD $year^{-1}$
Q = Quantity of heat required, J $year^{-1}$
C_j = Unitary cost of heating energy, USD J^{-1}

3.4. Results and Conclusions

The functions described above can be combined into a single Profit Function, which was used to determine the optimum temperature.

$$P = BFI - (CP + CB + CC) \quad (3.4)$$

The results obtained from the mathematical model show that there is a temperature where the difference between total costs and total income is maximum and hence the profit is maximized. This is shown graphically in Figure 3.4a and the maximum difference is observed at 408.15 K (135°C or 275°F), which is the optimum temperature for desalting operation of a typical Maya crude.[43]

Since Maya crude forms the major part of the blend for the refinery and there may be periods that the refinery under study would use Maya crude only, the optimum temperature of the desalter is determined based on the optimum temperature for desalting of Maya only and not that of blends.

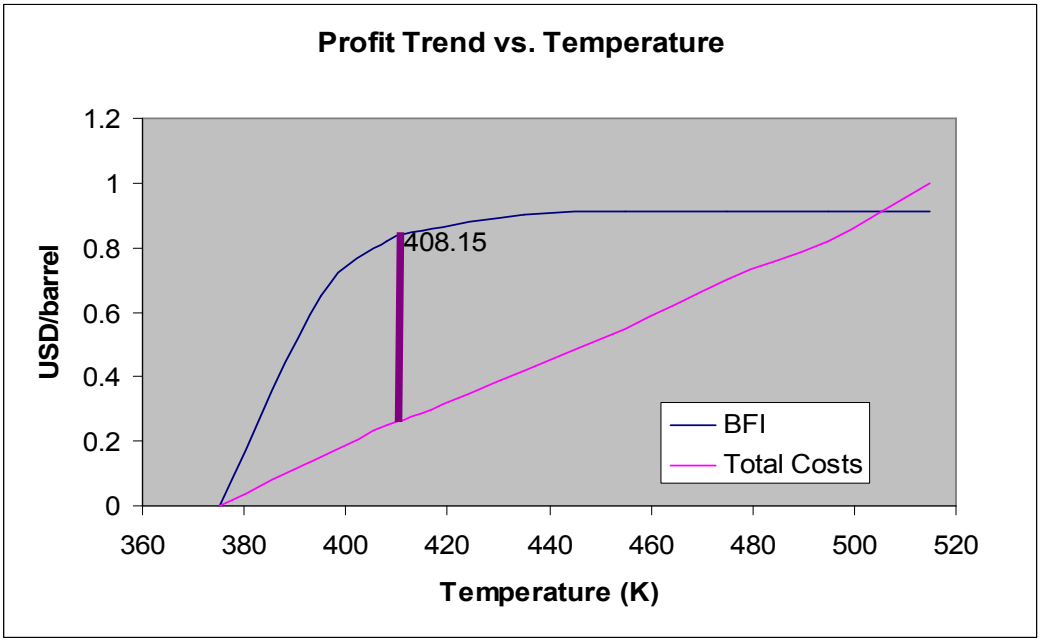

Figure 3.4a - Costs and benefit trends

Figure 3.4b shows the profit curve vs. the temperature, which is another representation for the maximum profit point.[43] Any other operating temperature in the desalter would not produce the most economic results.

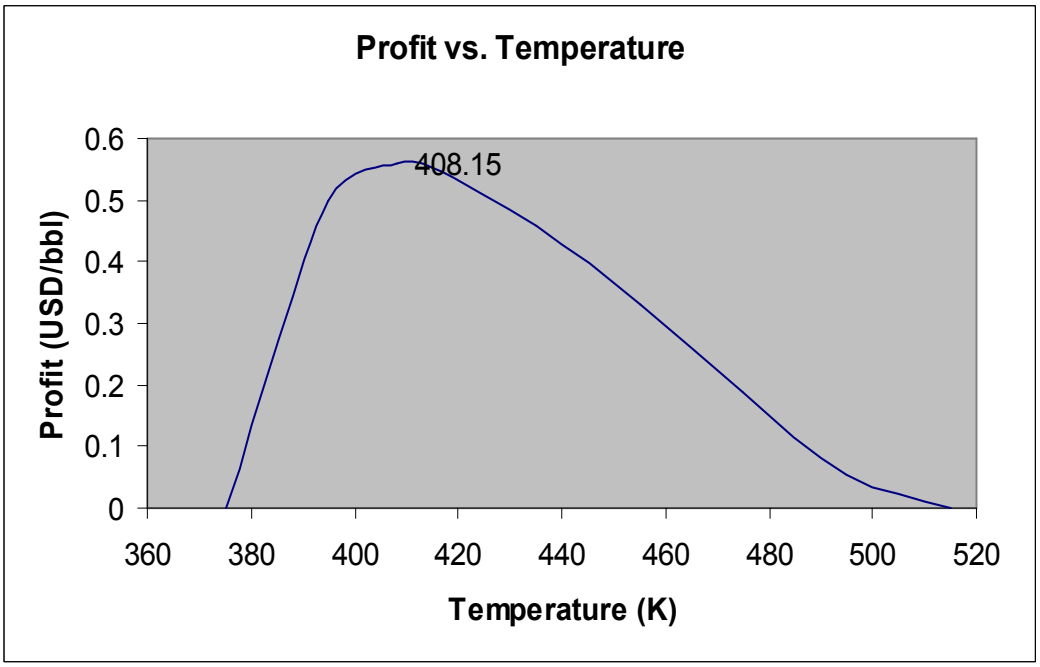

Figure 3.4b - Profit trend vs. Temperature

In view of the achieved result and the fact that current operation temperature is lower than the optimum temperature it is advised to increase the temperature of the desalter to 135ºC or 275 ºF, which is the optimum temperature. This modification will result in maximum profit from the operation. Such a change can be achieved in several different ways. In order to achieve the optimum temperature of 275ºF, a detailed study needs to be done with regards to heat sources available and the limitations thereof. To this end a full fletch simulation of the CDU has been prepared to study the unit operation. The simulation and heat integration options are presented in Chapter 4.

Chapter 4: Process Design, Simulation, and Integration of the Desalter in the Crude Distillation Unit of a Refinery

4.1. Introduction to Modeling the Process in HYSYS

Simulations are needed for generation of Heat and Material Balances (H&MB), design of equipment and in order to predict and plan the operations. So, it is needless to say how important simulations are and what the consequences could be if the simulation results are incorrect. The errors in simulations could come from many different sources including wrong initial assumptions, wrong or insufficient data input, use of inappropriate thermodynamic package, inconsistencies in the model, non-convergence of numerical solution, and other reasons.

A mathematical model or a simulation can be only used for a certain range of operating conditions and may not cover all operating conditions in a processing unit or plant, as there may be so many conflicting constraints and variables. This is also the situation with the crude distillation unit and hence the crude desalting operation. The heat and material balance for the crude distillation unit under study in this thesis is developed in HYSYS. Two thermodynamic packages have been used to simulate the crude distillation unit, BK-10 package to model the vacuum section and Peng-Robinson package to simulate the rest of the unit; however, none of these two packages and no other thermodynamic package built-in HYSYS has the capability to predict the salt balance for the desalting operation. Therefore, assumption has been made that the water in the crude as well as brine leaving the desalter is pure water and heat and material balances for the desalting unit are based on pure water. Salt balance has been done in Excel based on initial salt content reported in the crude, the desalter vessel efficiency and specification required for the desalted crude.

As the desalting process has been simulated in HYSYS, from here on, modeling or simulation refers to HYSYS simulation. In order to model the process, the very first step is to define the composition of the feed to the unit. To this end there is a very comprehensive built-in databank in HYSYS, from which the chemical components can be picked to build up the feed components. Usually, for natural gas and very light hydrocarbon feeds, it is easy to select the constituents as they are readily available from the HYSYS component databank. However, in most often cases, for crude and other complex chemical compounds where it is hard to identify all the components, the feedstock needs to be prepared based on pseudo-components, which are not readily available in the databank. In order to accurately prepare the pseudo-components for the crude slate, detailed lab data and analysis is needed. Once the data is made available for different cuts in the crude, the pseudo-components can be formed and named. The detailed data analysis is referred to as the Crude Assay. The more accurately the crude assay is prepared, the more accurately the crude can be simulated and hence the more reliable the results from the simulation are. Preparation of the crude composition and its properties is also called Crude Characterization, which will be discussed in detail in later sections of this chapter.

If there is more than one crude type in the feed, which is the case in this study, each crude needs to be separately characterized and then the blend feature in HYSYS will be used to make the required feedstock to the unit.

Once the crude characterization and blending process is done the next step would be to select a proper thermodynamic package. As explained earlier, two thermodynamic packages have been used for the crude distillation unit to predict the process more

accurately. BK-10 is selected to model the vacuum tower and equipment in that unit as this thermodynamic package predicts low pressure hydrocarbon processes accurately. Peng-Robinson is used to model the other parts of the CDU and is a more generalized model, covering a wide range of temperatures and pressures for hydrocarbon processes.

After crude characterization and selection of thermodynamic packages are complete, Unit Operation in HYSYS should be set up in the flowsheeter, where different equipments are connected through streams. To complete this part of the simulation a comprehensive Front-End knowledge of the plant is needed. The simulation for this study is a revamp simulation and therefore, UAs (total energy transferred) for heat exchangers, number of trays, height of packed beds, internals and other information for distillation columns, capacities for pumps, compressor curves, and other equipment information are available. Therefore the performance of the plant can be simulated under different operating conditions as the equipments are fixed. The simulation for revamp projects is benchmarked against actual plant data so that different operating envelopes could be covered and predicted, as done in this case. The new equipments are specified based on the spec requirements for the new operation in the plant.

Specifying and rating the equipments, needs a lot of time and attention as at this stage all the parameters for the equipments are inputted, controls and recycle streams are put in place and details of simulation are completed. Once all the equipment information and spec required are inputted, the Unit Operation data entry is complete and the flowsheeter can be run to achieve the results required.

Before starting the simulation work it is absolutely crucial to understand the process scope, the feed composition and the operating conditions and constraints. These topics are covered in the next section before starting the actual modeling process.

4.2. Overview of Crude Distillation Unit (CDU)

The major components of the CDU under study include the preheat train, desalter, flash column, crude tower and the vacuum tower. As far as the scope of this thesis, only the operation around the desalter will be considered as highlighted in the following Block Flow Diagram (BFD). However, in order to properly design and simulate the desalting process, the whole crude distillation unit should be simulated as the desalting process is an integrated part of the CDU and hence the operating conditions in the CDU will affect the desalter performance, specially the temperature in the desalter, which is one of the key parameters for this study.

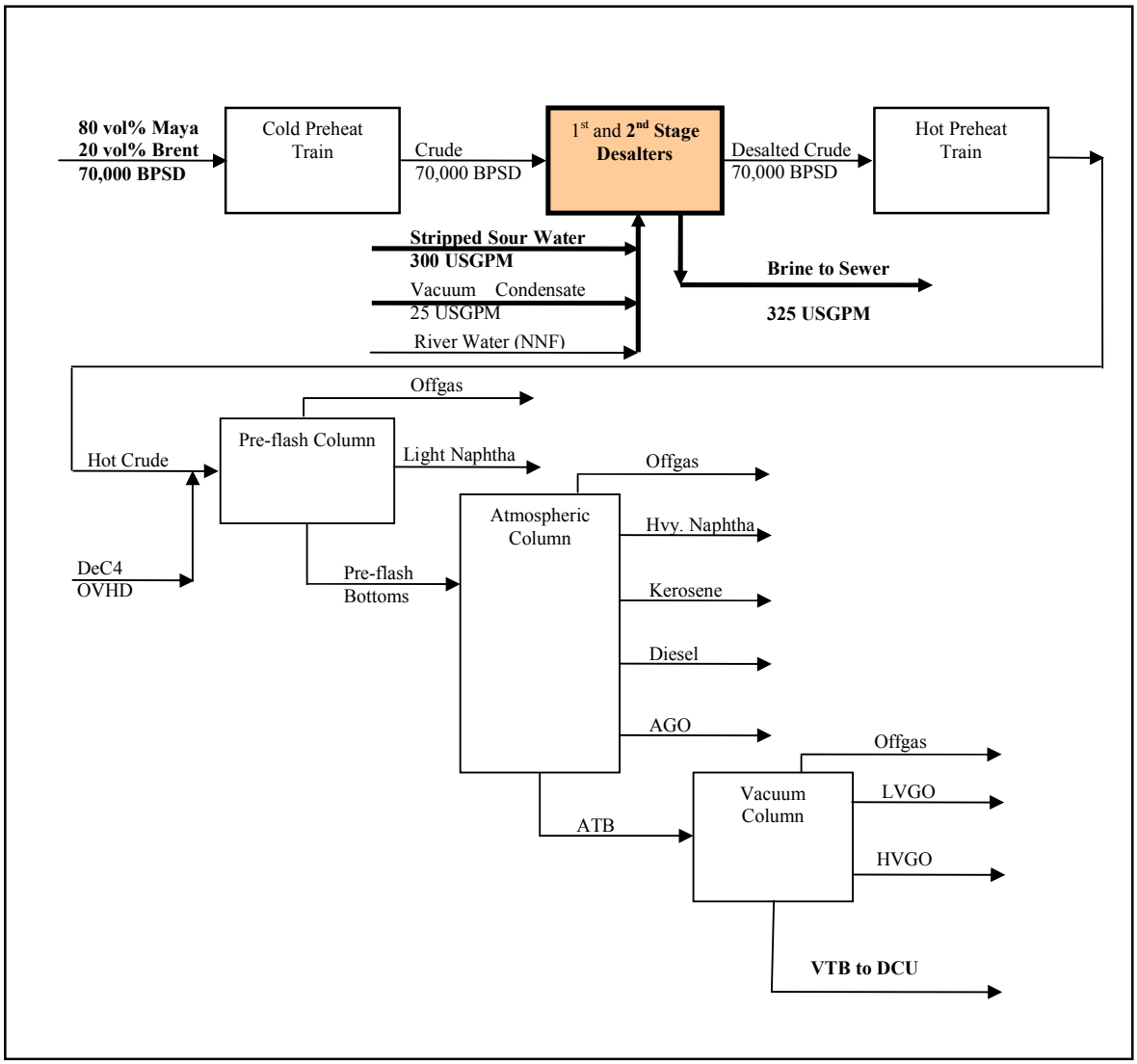

Figure 4.2 - Block Flow Diagram for Crude Distillation Unit

4.3. Overall Project Scope

A North American refinery is going to revamp some of its processing units, including the crude distillation unit. The existing capacity of the existing refinery is 60,000 BPSD and after revamp the refinery will be able to process 70,000 BPSD of crude. In addition to increasing the capacity, the crude type will change from an average API crude to a low API crude. As a result, the crude distillation unit will have to process a higher capacity and a heavier crude blend. Therefore the crude distillation unit will be revamped based on 70,000 BPSD of 80 vol% Maya and 20 vol% Brent. Maya crude is a heavy crude and could contain significant salt in it. For revamp of the crude and distillation unit, it is assumed that the Maya crude received by the refinery could contain as high as 100 PTB of salt in current and future operation during the life cycle of the plant. The revamp spec on salt is 1 PTB in the desalted crude stream, in order to meet the requirement for the Vacuum Tower Bottoms (VTB) salt concentration. Obviously with this spec on salt, other revamp criteria for desalting operation, including protection of downstream equipment against corrosion and fouling as well as protecting the reactor catalysts against poisoning, are satisfied.

The existing refinery configuration is based on a single stage electrostatic desalter, which provides approximately 90% salt removal efficiency on medium crudes and 85% salt removal efficiency on heavy crudes such as Maya. To design equipments for revamp of the desalting unit, it is assumed that the salt concentration in the crude, received by the refinery, is 100 PTB. Therefore, given the best performance of the existing single stage desalter, the desalted crude from 1st stage desalter would still contain some 10 PTB salt, if only one stage of desalting is used. When Maya crude is used in the refinery, after a single stage desalting operation, some 15 PTB of salt will still remain in the desalted crude. Assuming a salt removal efficiency of 85% for the 1st stage desalter, the second stage desalter needs to be 92.5% or more efficient in order to meet spec of 1 PTB, given there is 100 PTB of salt in the crude into the first stage desalter. New electrostatic desalters can provide efficiencies as high as 99% guaranteed by the vendor. Therefore, by installing a second stage desalter in the crude distillation unit, the desalted crude spec of 1 PTB will be met. More details on salt balance calculation is given further in this chapter.

In addition to installation of a new desalter in the crude distillation unit, it is required to increase the desalter operating temperature to reach the optimum temperature for desalting of Maya crude as discussed in chapter 3. These changes will conclude the scope of revamp for crude distillation unit.

4.3.1 Process Design Criteria for Desalting Operation

The objective of crude desalting is removal of salts and solids and the formation water from unrefined crude oil before the crude is introduced to the downstream equipment in the refinery. The followings are the design parameters for revamp of the desalter:

- As per the results of the model in chapter 3, the temperature in the desalter should be kept around 275ºF for optimum desalting operation of the Maya crude.

- It is necessary to adjust the pH of the brine and keep it between 6 and 7 as this range of pH will give the best results for breaking up the emulsions and hence better efficiency in the desalter.
- The source of wash water for desalting is stripped sour water and as such it may contain phenols in it. In order to minimize carryover of phenols, wash water injection to the desalter should be maximized to reabsorb the phenols into the crude streams.
- Desalting efficiency of 93.3% or more should be achieved through the 2nd stage desalter to reduce the salt content of desalted crude stream to 1 PTB.
- Maximum of 0.5 vol% insoluble water content in the oil stream leaving the desalter.
- Maximum of 200 ppmwt insoluble oil content in the effluent water stream leaving the desalter system.
- The new desalter vessel should be designed for 100% unit capacity of 70,000 BPSD for the identified crude oil blend.

4.3.2 Feedstock

The following table shows the feedstock properties for Maya and Brent crudes.

Table 4.3.2: Feedstock properties for Crude Distillation Unit

Feed Properties	Units Of Measure	Maya	Brent	80/20 Blend (HYSYS Sim.)
Unit Throughput	BPSD	56,000	14,000	70,000
Volumetric Flow Rate	VOL%	80	20	100
Specific Gravity @ 60ºF	SG	0.93	0.84	0.88
API Gravity	°API	21.3	38.0	24.1
TAN	Mg KOH/g	0.3	0.05	-
Sulfur Content	wt%	3.42	0.44	2.8
Nitrogen Content	ppmwt	3600	1033	4633
Nickel	ppmwt	55	2	57
Vanadium	ppmwt	280	7	287
Salt Content	lb/1000 bbl	30-80	22	125
Base Sediment and Water (BS&W)	LV%	5	0.1	1.0
Viscosity @ 104ºF(40ºC):	cSt	96	3.54	-
Viscosity @ 122ºF(50ºC):	cSt	60	2.94	-

4.4. Crude Characterization

The crude for which the simulation has been prepared is a blend of 20 vol% Brent and 80 vol% Maya. As seen from the feedstock properties Table 4.3.2, Brent is a relatively light and sweet crude from the North Sea and Maya is a heavy and sour crude from Mexico. In order to blend the crudes in HYSYS, the assay for each crude needs to be separately prepared. Then the two crudes are blended through the Basis Environment Oil Manager in HYSYS. However, before this could be done in HYSYS, the lab data on crude properties such as density, viscosity, etc. need to be analyzed and prepared for use in HYSYS. Data analysis and preparation as well as lab test results for properties of Brent and Maya crudes are presented in the following sections.

4.4.1 Brent crude

Crude assay data was provided in two forms; vendor lab data and calculated data, CAL II, used for LP analysis. Since the vendor data provided complete set of data for analysis, this information was used to develop the Brent crude characterization.

The True Boiling Point (TBP) data for the crude assay is shown in Figure A1.0.

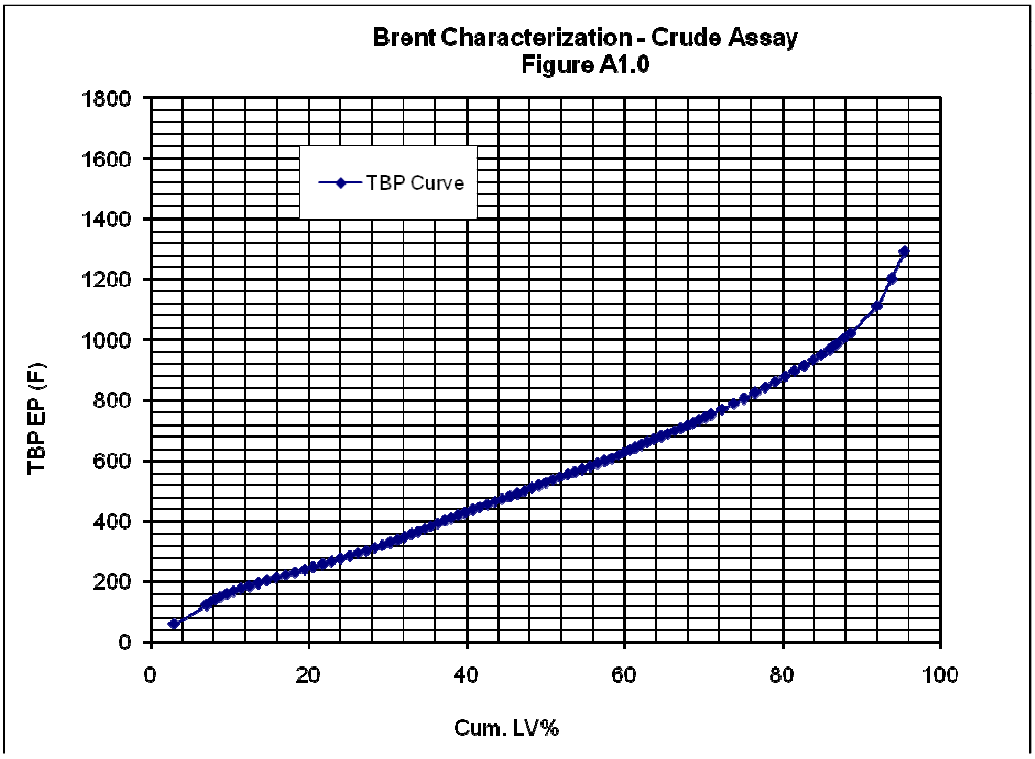

Figure A1.0 – Brent Characterization – Crude Assay – TBP EP vs. Cumulative LV%

This curve was also plotted on logarithmic coordinates, as shown in Figures A1.1 and A1.2, to identify any irregularities. As shown by these curves, the data follows a smooth distribution across each fraction and requires no adjustment.

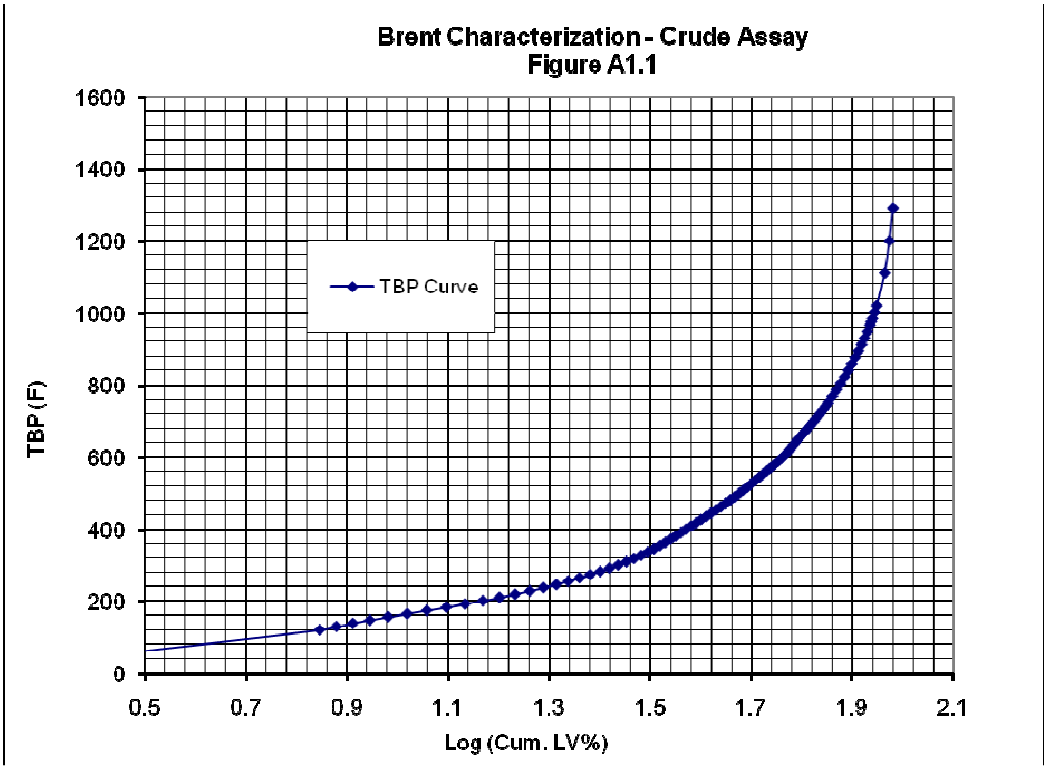

Figure A1.1 – Brent Characterization – Crude Assay – TBP vs. Log Cumulative LV%

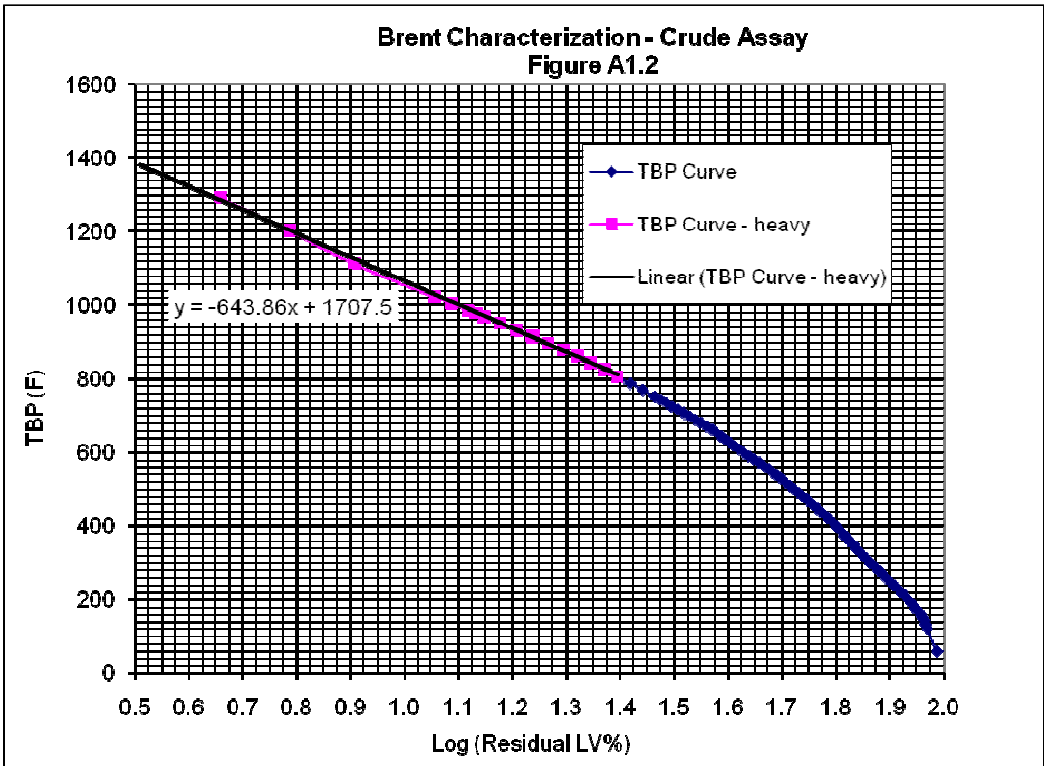

Figure A1.2 – Brent Characterization – Crude Assay – TBP vs. Log Residual LV%

Standard curve fitting procedures available in Excel were used to obtain a curve of best fit through the data points. Due to the nature of the distribution, it was not possible to adequately represent the whole crude with a single equation. Two separate equations were required and the resulting curve is shown in Figure A1.3.

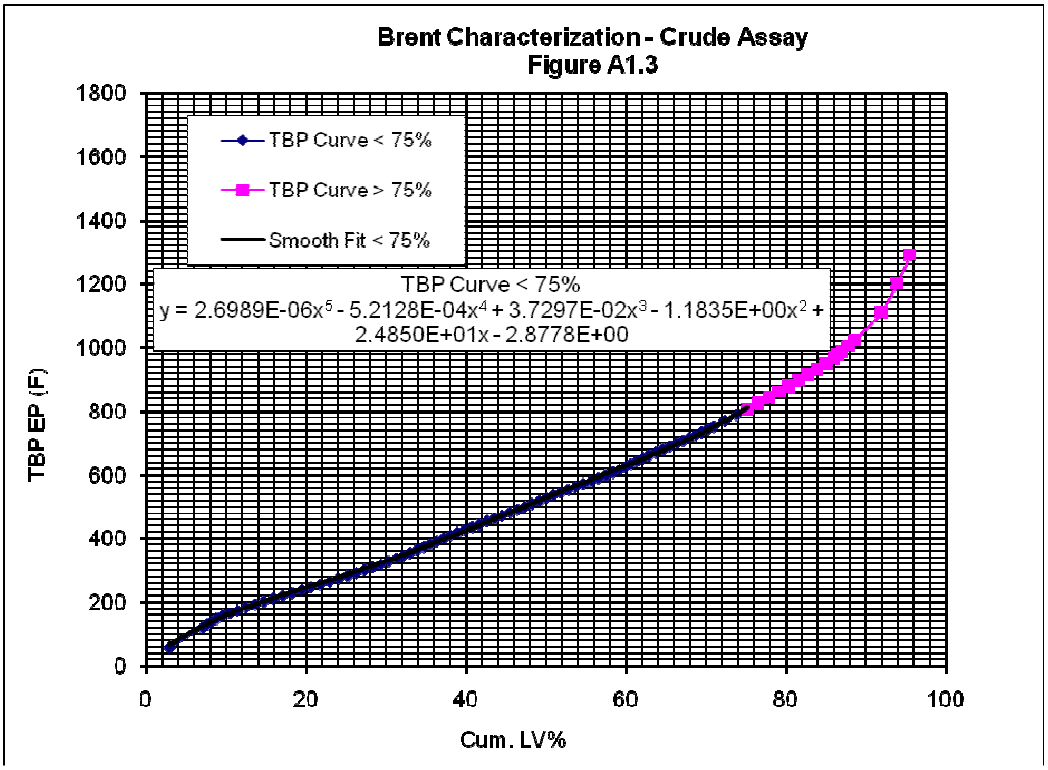

Figure A1.3 – Brent Characterization – Crude Assay – TBP EP vs. Cumulative LV%

The predicted crude curve was input to HYSYS. As shown in Figure B1.0, the crude curve of Figure A1.3 matches the curve generated by HYSYS, which would ensure that HYSYS simulation will behave as per this crude characterization.

The provided gravity data was plotted against the volume average true boiling point as shown in Figure A2.0. The same data was plotted on logarithmic coordinates in Figure A2.2, which shows that the provided gravity data is well behaved and follows nearly a straight line. Next, the gravity curve was extrapolated linearly to find the best fit through the raw data to cover the full range of the crude as shown in Figures A2.4 and A2.5. The curved portion of the gravity distribution was obtained by trial and error, using the n-paraffin line (from the API Technical Database) as reference, to converge with the n-paraffin line as shown in Figure A2.3. These steps were repeated until reasonable weight balance on the whole crude was obtained. Figures A2.0, A2.1, A2.2, A2.3, A2.4 and A2.5 are given below.

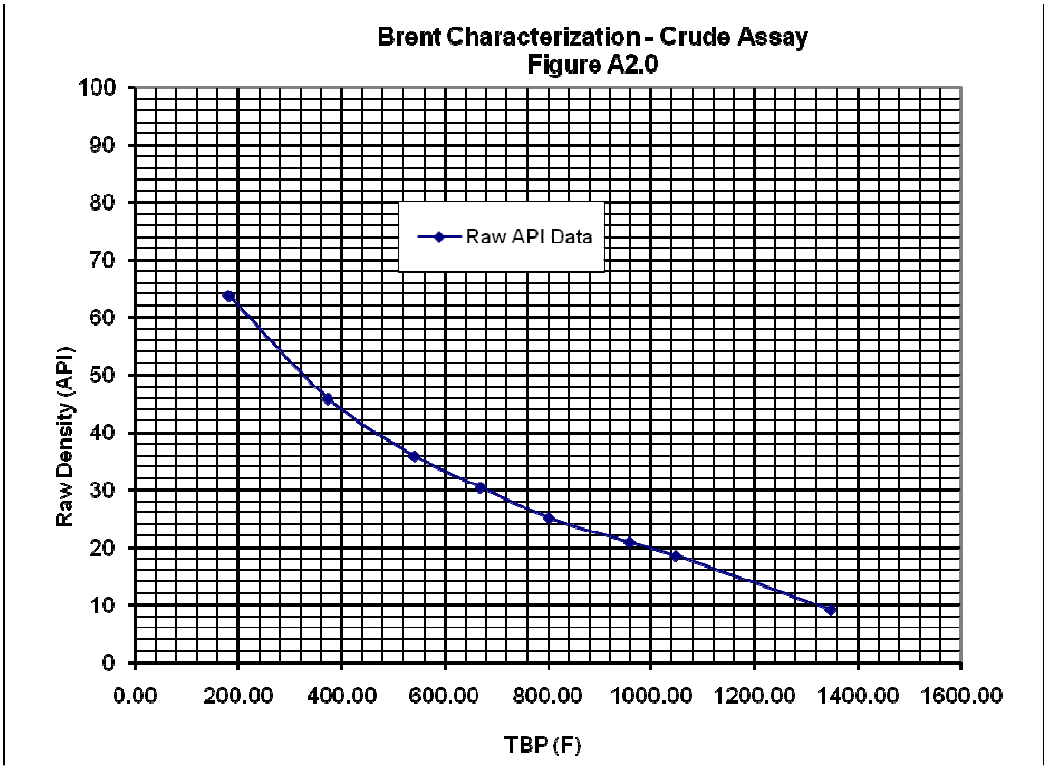

Figure A2.0 – Brent Characterization – Crude Assay – Raw Density vs. TBP

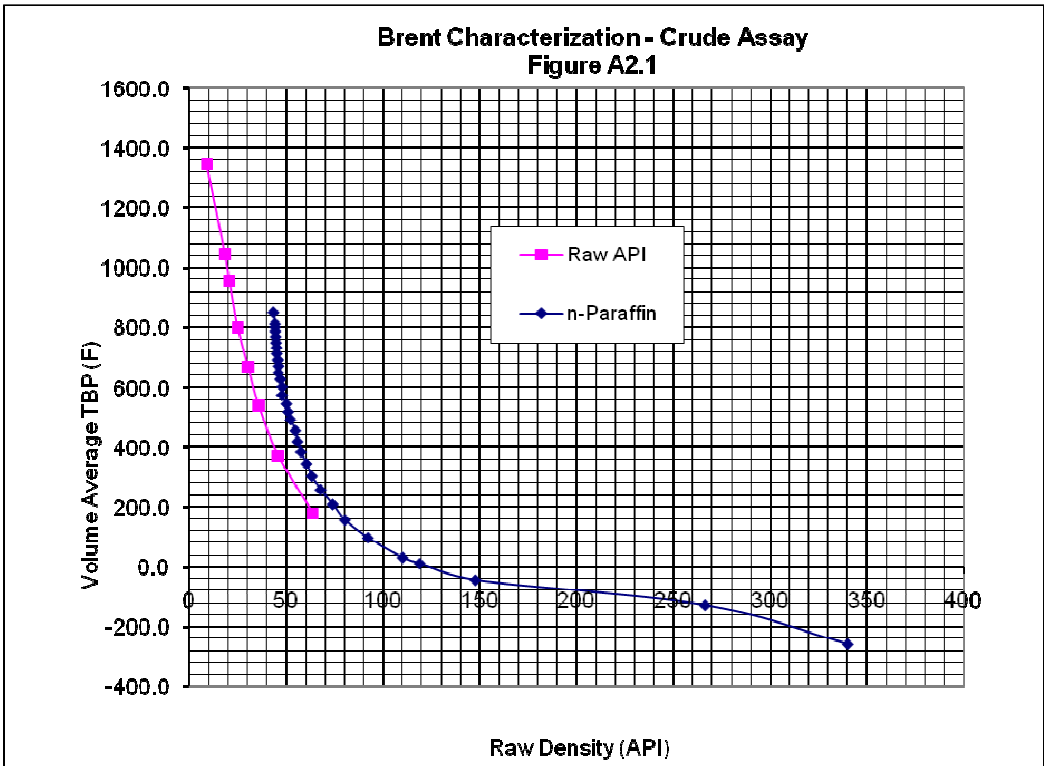

Figure A2.1 – Brent Characterization – Crude Assay – Vol Ave TBP vs. Ray Density

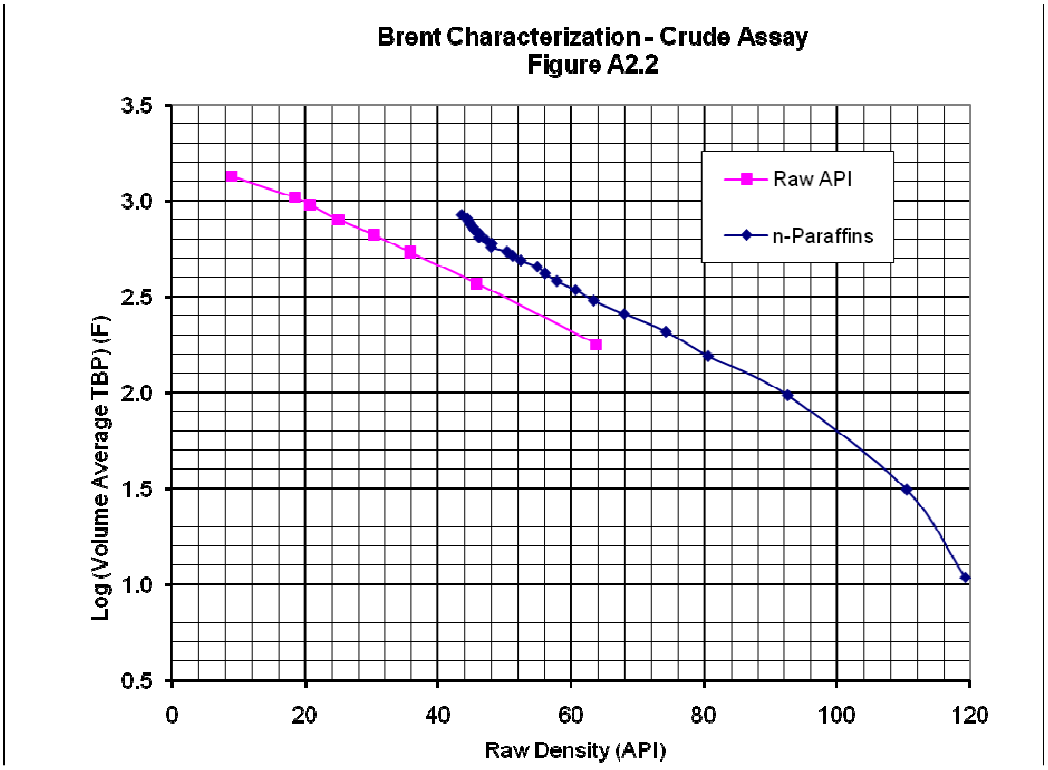

Figure A2.2 – Brent Characterization – Crude Assay – Log Vol Ave TBP vs. Raw Density

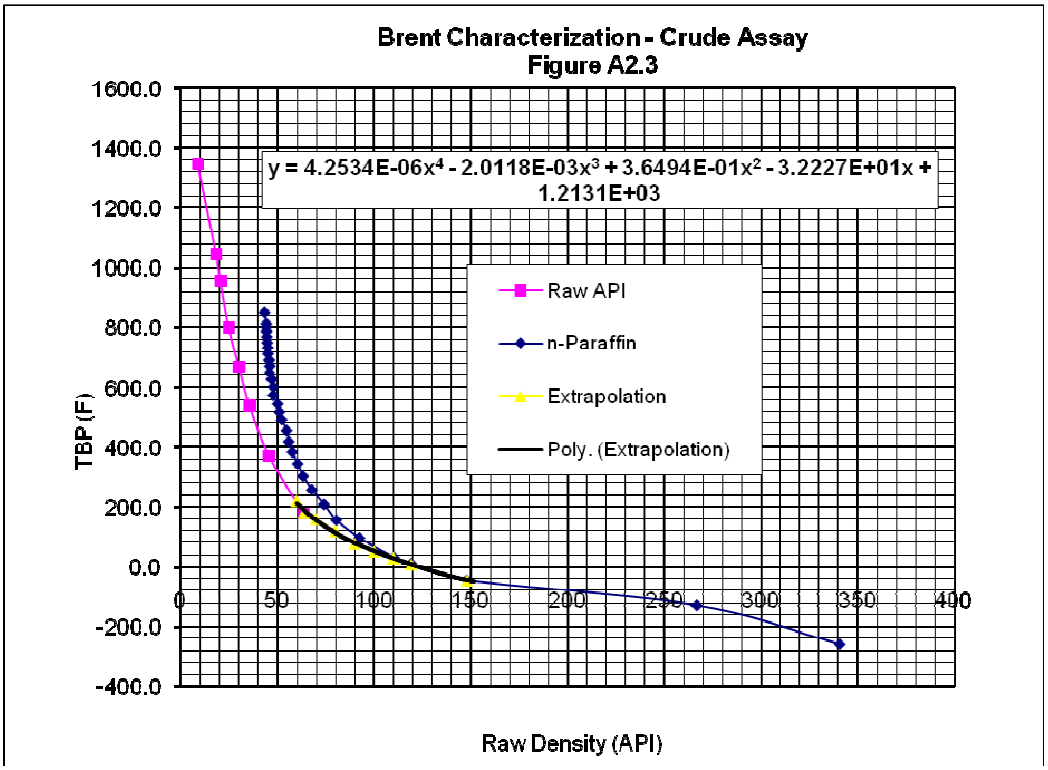

Figure A2.3 – Brent Characterization – Crude Assay – TBP vs. Raw Density

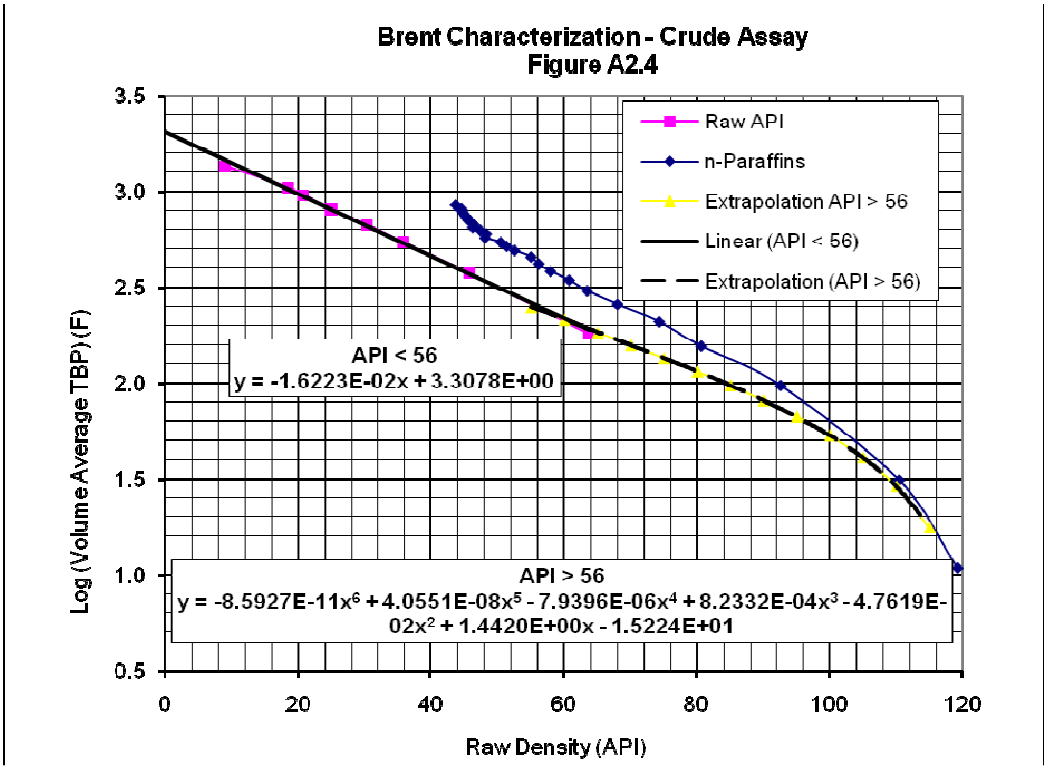

Figure A2.4 – Brent Characterization – Crude Assay – Log Vol Ave TBP vs. Raw Density

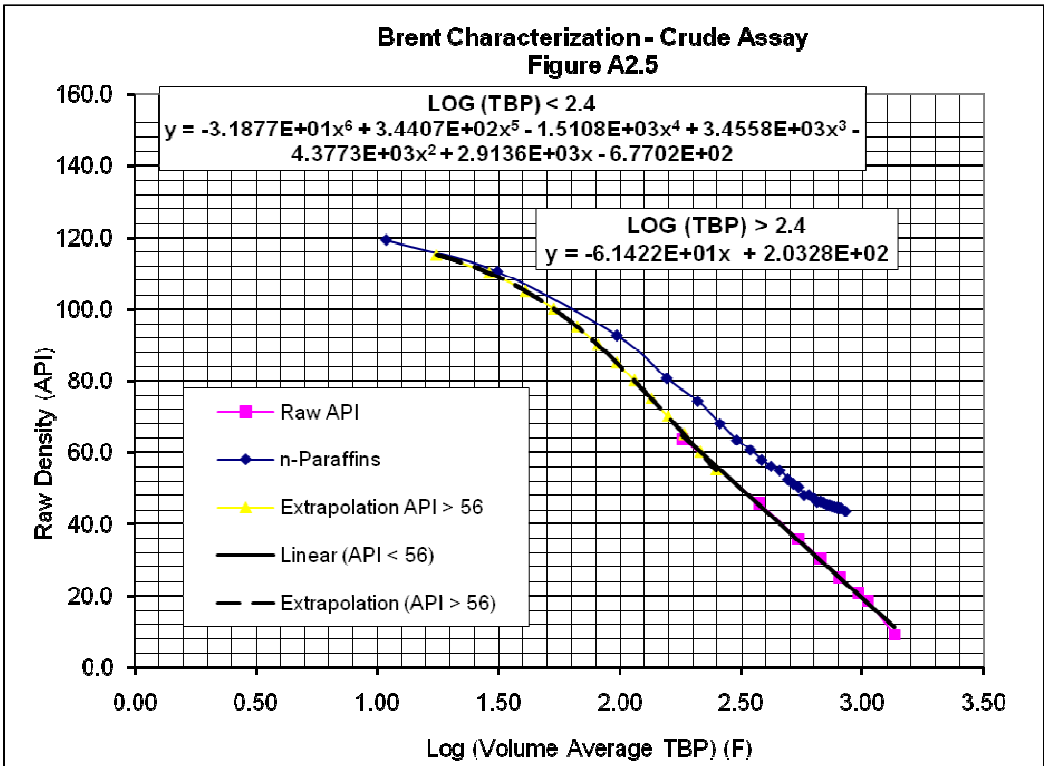

Figure A2.5 – Brent Characterization – Crude Assay – Raw Density vs. Log Vol Ave TBP

The gravity distribution across the whole crude as a function of percent distilled was obtained from the fitted gravity curve of Figure A2.5. The resulting gravity distribution curve is shown in Figure A3.0, which also shows crude assay data for reference. The calculated API curve in Figure A3.1 shows good agreement with the provided data.

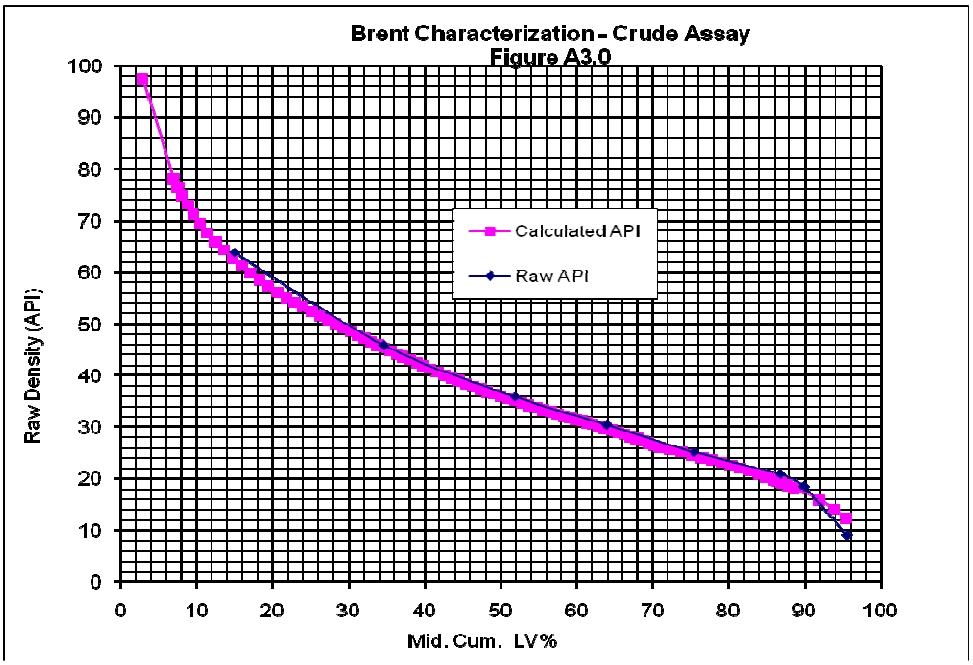

Figure A3.0 – Brent Characterization – Crude Assay – Raw Density vs. Mid Cum LV%

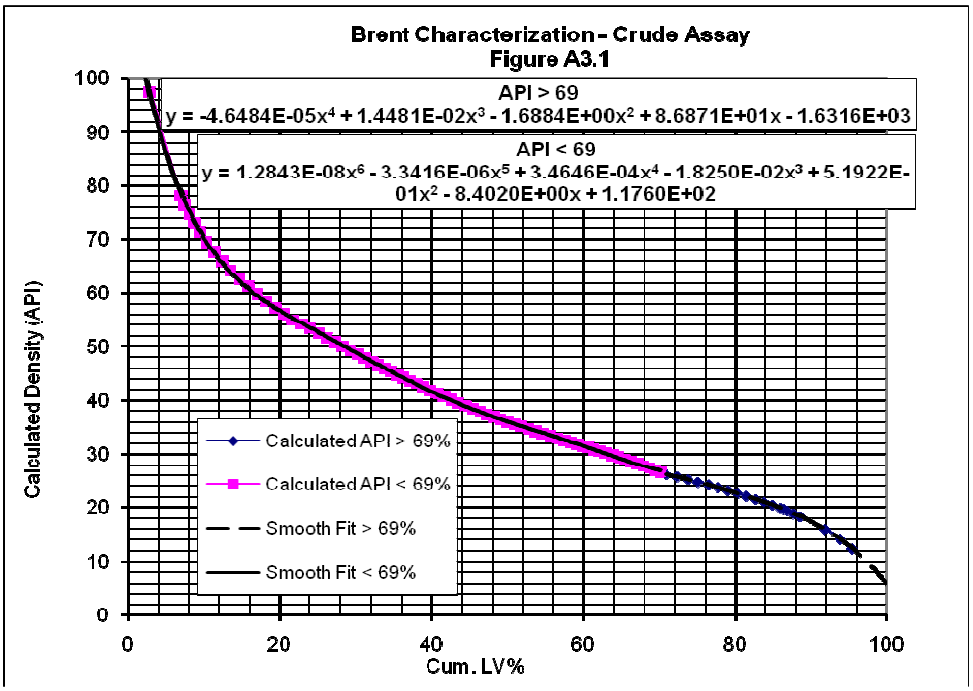

Figure A3.1 – Brent Characterization – Crude Assay – Calculated Density vs. Cum LV%

The generated API density curve was input to HYSYS and compared with the curve generated by HYSYS. As shown in Figure B2.0, the API density curve of Figure A3.0 matches the curve generated by HYSYS, except at the light ends and the 99% boiling point of the curve. The light ends consist of 7 LV% and API density should correspond to defined components such as propane, butane, etc. Since HYSYS calculates density of these components from a standard database, the deviation is acceptable. The deviation at the 99% boiling point will have no significant impact on the process simulation.

The provided viscosity data are shown in Figure A4.0. The same viscosity data were transformed to logarithmic coordinates and plotted against the provided gravity data as shown in Figure A4.1. Each set of viscosity data can be represented with a straight line of best fit through the data as shown in Figure A4.2. The viscosity distribution across the whole crude was generated using Figure A4.2. The resulting distribution curve is shown in Figure A4.3 and A4.4.

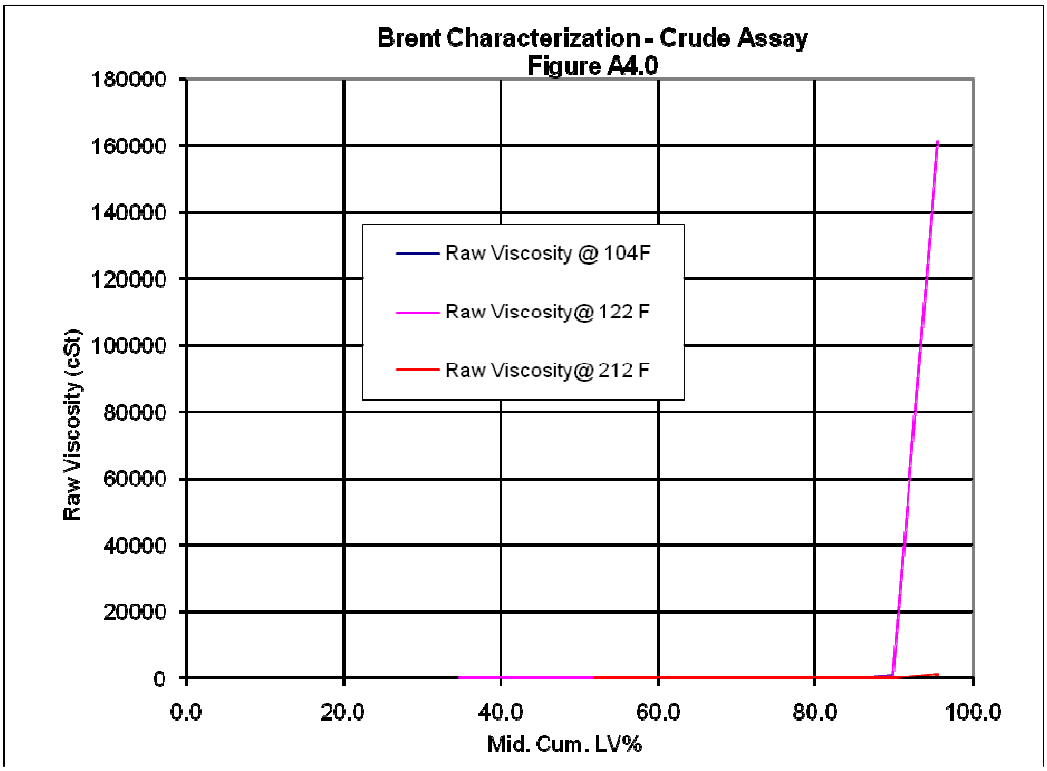

Figure A4.0 – Brent Characterization – Crude Assay – Raw Viscosity vs. Mid Cum LV%

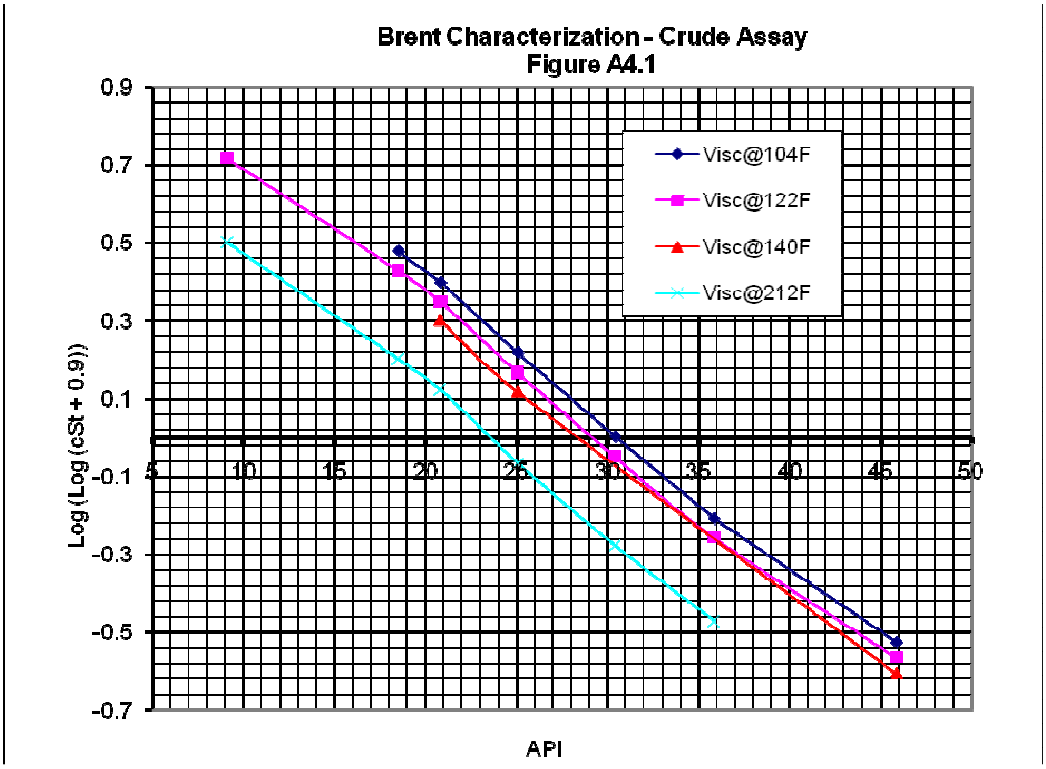

Figure A4.1 – Brent Characterization – Crude Assay – Log Viscosity vs. API Density

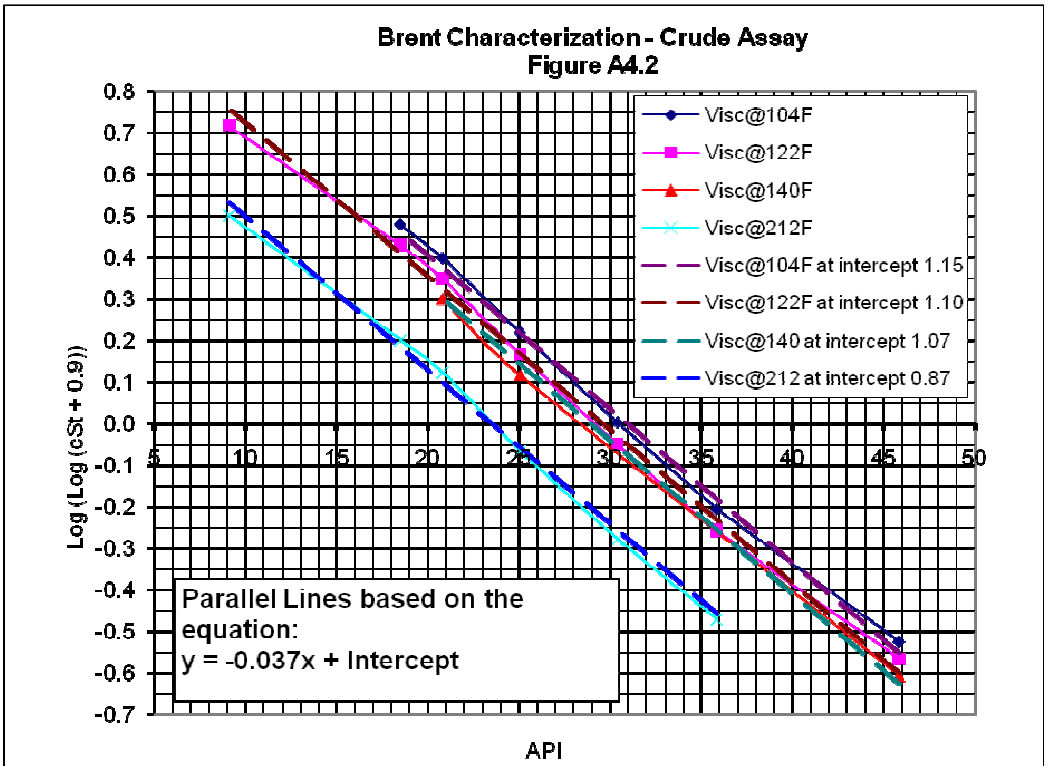

Figure A4.2 – Brent Characterization – Crude Assay – Log Viscosity vs. API Density

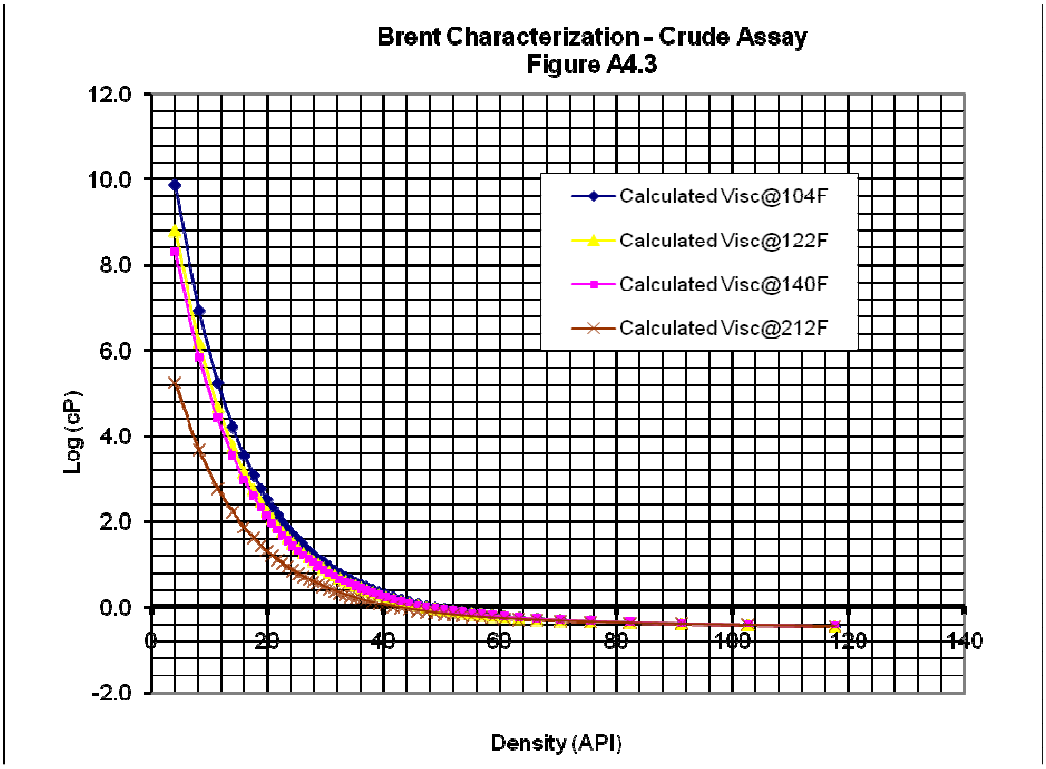

Figure A4.3 – Brent Characterization – Crude Assay – Log Viscosity vs. API Density

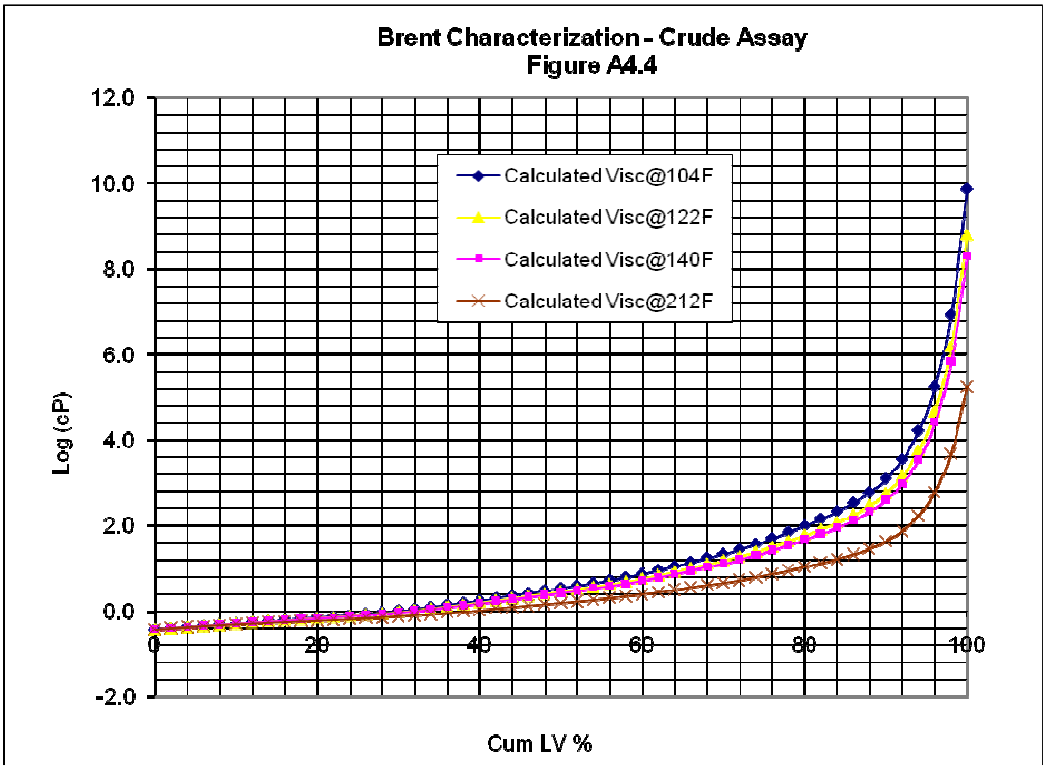

Figure A4.4 – Brent Characterization – Crude Assay – Log Viscosity vs. Cumulative LV%

The viscosity curve was also compared to the curve generated by HYSYS. As shown in Figure B3.0 and B3.1, the viscosity curve matches the HYSYS curve well, except for the light ends. The light ends consist of 7 LV% and viscosity should correspond to defined components such as propane, butane, etc. Since HYSYS calculates viscosity of these components from a standard database, the deviation is acceptable.

Figures B1.0, B2.0, B3.0 and B3.1 are presented below.

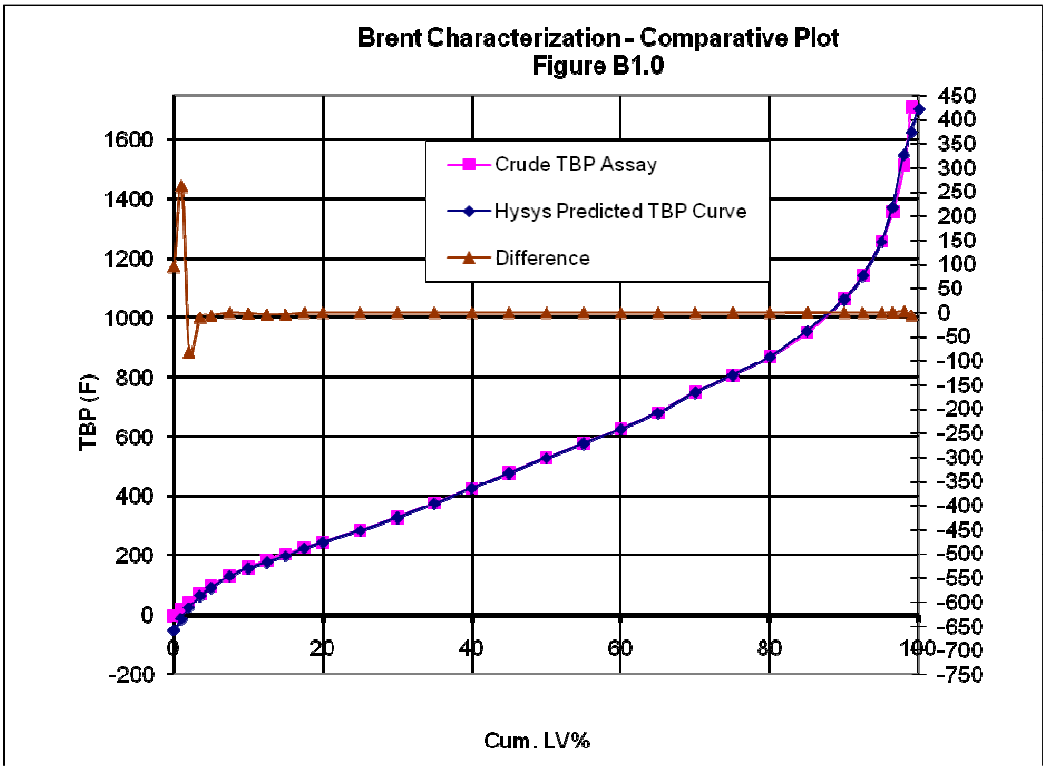

Figure B1.0 – Brent Characterization – Comparative Plot – TBP vs. Cum LV%

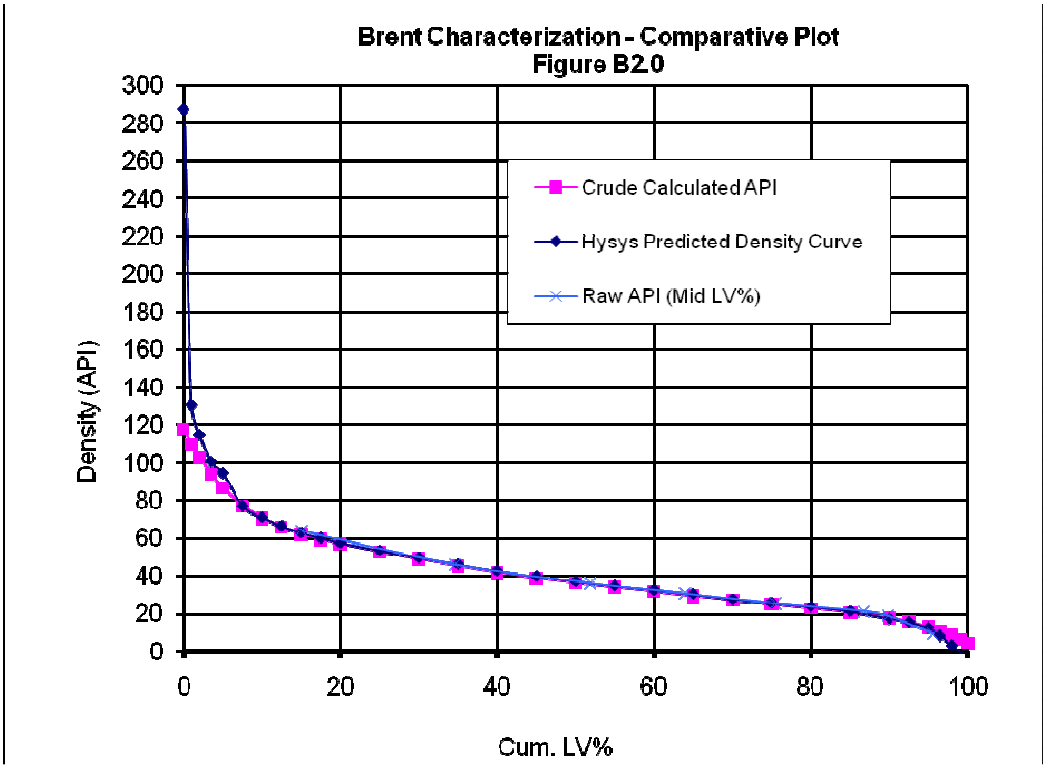

Figure B2.0 – Brent Characterization – Comparative Plot – Density vs. Cum LV%

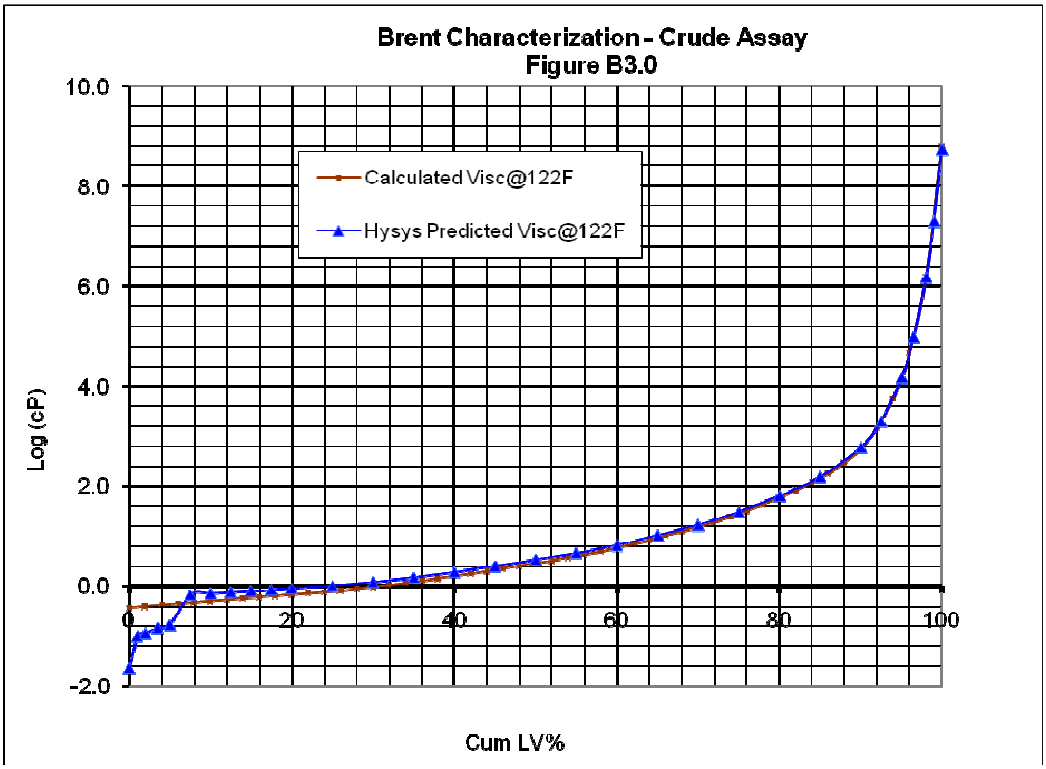

Figure B3.0 – Brent Characterization – Comparative Plot – Log Viscosity vs. Cum LV%

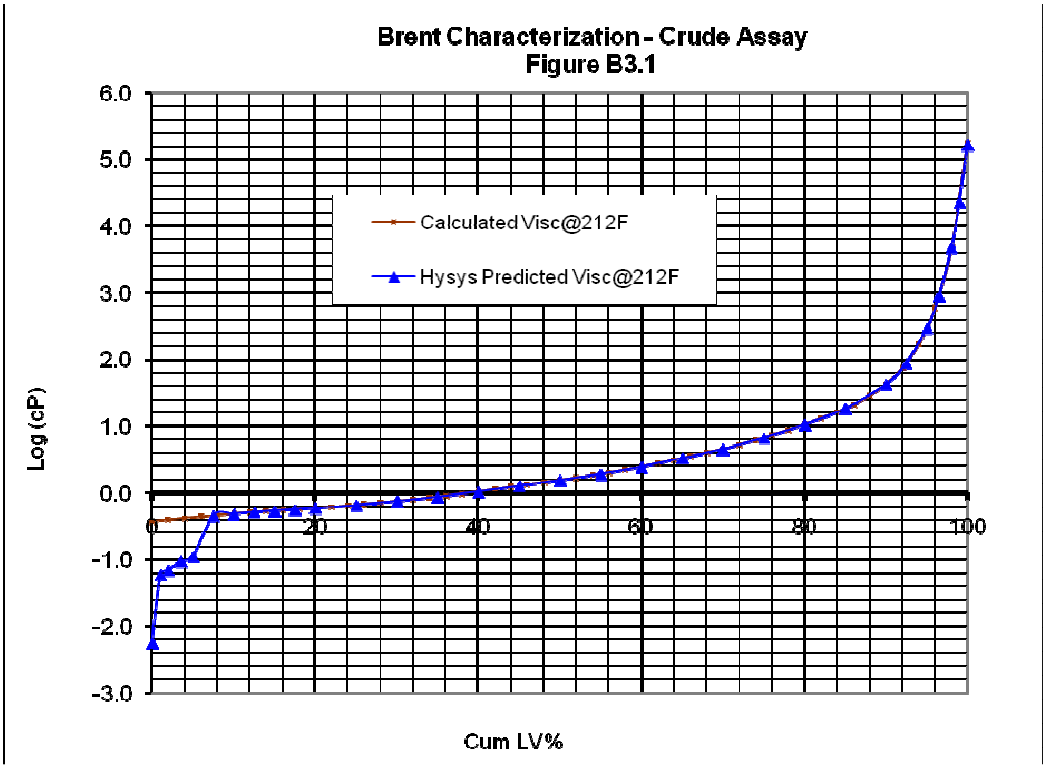

Figure B3.1 – Brent Characterization – Crude Assay – Log Viscosity vs. Cum LV%

The calculated Watson Characterization Factor (K_w) distribution is shown in Figure C1.0. The crude assay did not provide values of K_w but the curve shape displays a typical characterization factor curve. The usual curve starts with the high values of K_w for the light ends, decreases to a minimum, and then increases.

Values for several petroleum properties were calculated in similar fashion and are shown in Figures C2.0 through C5.0. Predicted values show a degree of agreement with the reported data for Cetane Index and Freezing Point as shown in C2.0 and C5.0. On the other hand, the calculated values of Cloud and Pour Points compare poorly to the provided values, as shown in Figures C3.0 and C4.0. No further action was taken. As a final check of the TBP and API curves, the weight of the whole crude used for the assay was calculated and compared against the actual weight. Table 4.4.1 shows a series of volume fractions and the corresponding TBP as determined from figure A1.4. For each TBP, the corresponding gravity was determined from the curve of Figure A3.1. The weight of each volume fraction was added to obtain the calculated weight of the whole crude.

Table 4.4.1 - Calculated Weight for Brent Crude

LV%	Cum LV%	API Calc	SG	Cut Vol mL	Cut Avg. Wt g	Cum Wt g
0	0	117.60	0.57	0.00	0.00	0.00
2	2	102.73	0.60	2.00	1.21	1.21
2	4	91.22	0.64	2.00	1.27	2.48
2	6	82.36	0.66	2.00	1.32	3.80
2	8	75.58	0.68	2.00	1.37	5.17
2	10	70.40	0.70	2.00	1.40	6.57
2	12	66.40	0.72	2.00	1.43	8.00
2	14	63.27	0.73	2.00	1.45	9.45
2	16	60.75	0.74	2.00	1.47	10.93
2	18	58.65	0.74	2.00	1.49	12.41
2	20	56.81	0.75	2.00	1.50	13.92
2	22	55.13	0.76	2.00	1.52	15.43
2	24	53.53	0.76	2.00	1.53	16.96
2	26	51.97	0.77	2.00	1.54	18.51
2	28	50.42	0.78	2.00	1.56	20.06
2	30	48.88	0.78	2.00	1.57	21.63
2	32	47.36	0.79	2.00	1.58	23.21
2	34	45.85	0.80	2.00	1.60	24.81
2	36	44.39	0.80	2.00	1.61	26.42
2	38	42.98	0.81	2.00	1.62	28.04
2	40	41.63	0.82	2.00	1.63	29.67
2	42	40.37	0.82	2.00	1.65	31.32
2	44	39.19	0.83	2.00	1.66	32.98
2	46	38.09	0.83	2.00	1.67	34.65
2	48	37.06	0.84	2.00	1.68	36.33
2	50	36.10	0.84	2.00	1.69	38.01
2	52	35.18	0.85	2.00	1.70	39.71
2	54	34.28	0.85	2.00	1.71	41.42
2	56	33.39	0.86	2.00	1.72	43.14
2	58	32.49	0.86	2.00	1.73	44.86
2	60	31.57	0.87	2.00	1.74	46.60
2	62	30.62	0.87	2.00	1.75	48.34
2	64	29.65	0.88	2.00	1.76	50.10
2	66	28.71	0.88	2.00	1.77	51.86
2	68	27.84	0.89	2.00	1.78	53.64
2	70	27.11	0.89	2.00	1.78	55.42
2	72	26.25	0.90	2.00	1.79	57.22
2	74	25.33	0.90	2.00	1.80	59.02
2	76	24.40	0.91	2.00	1.82	60.84
2	78	23.49	0.91	2.00	1.83	62.66
2	80	22.61	0.92	2.00	1.84	64.50
2	82	21.74	0.92	2.00	1.85	66.35
2	84	20.85	0.93	2.00	1.86	68.21
2	86	19.91	0.93	2.00	1.87	70.07
2	88	18.85	0.94	2.00	1.88	71.96
2	90	17.58	0.95	2.00	1.90	73.85
2	92	16.01	0.96	2.00	1.92	75.77
2	94	14.03	0.97	2.00	1.94	77.72
2	96	11.48	0.99	2.00	1.98	79.70
2	98	8.23	1.01	2.00	2.03	81.72
2	100	4.10	1.04	2.00	2.09	83.81

In view of the good weight balance and reasonable predictions for several petroleum properties, further adjustment of the TBP and gravity curves was deemed unnecessary.

The provided values for sulfur were also plotted and are shown in Figure C6.0. Figures C1.0, C2.0, C3.0, C4.0, C5.0 and C6.0 are presented here.

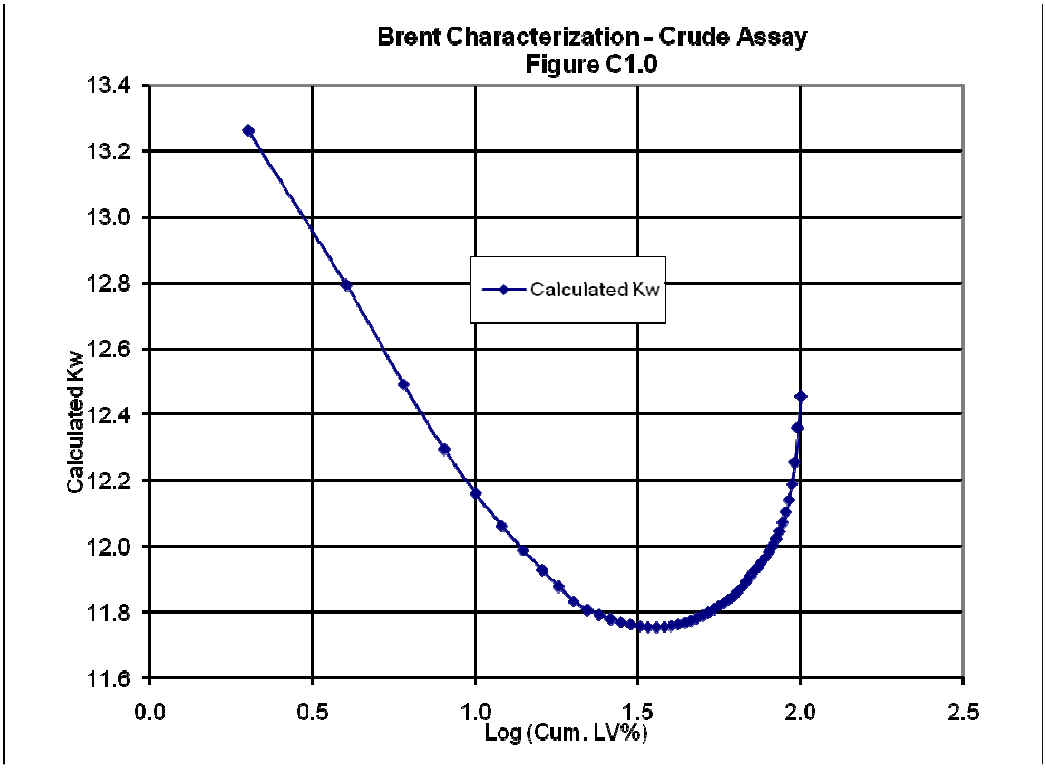

Figure C1.0 – Brent Characterization – Crude Assay – Calculated K_w vs. Log Cum LV%

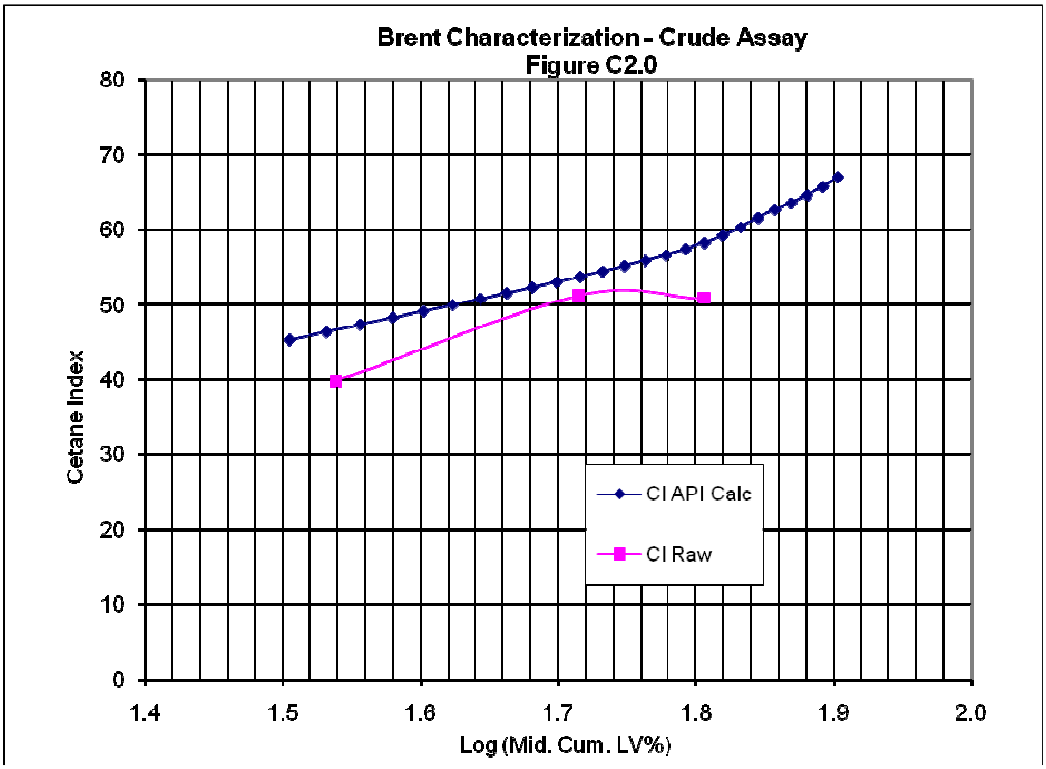

Figure C2.0 – Brent Characterization – Crude Assay – Cetane Index vs. Log Mid Cum LV%

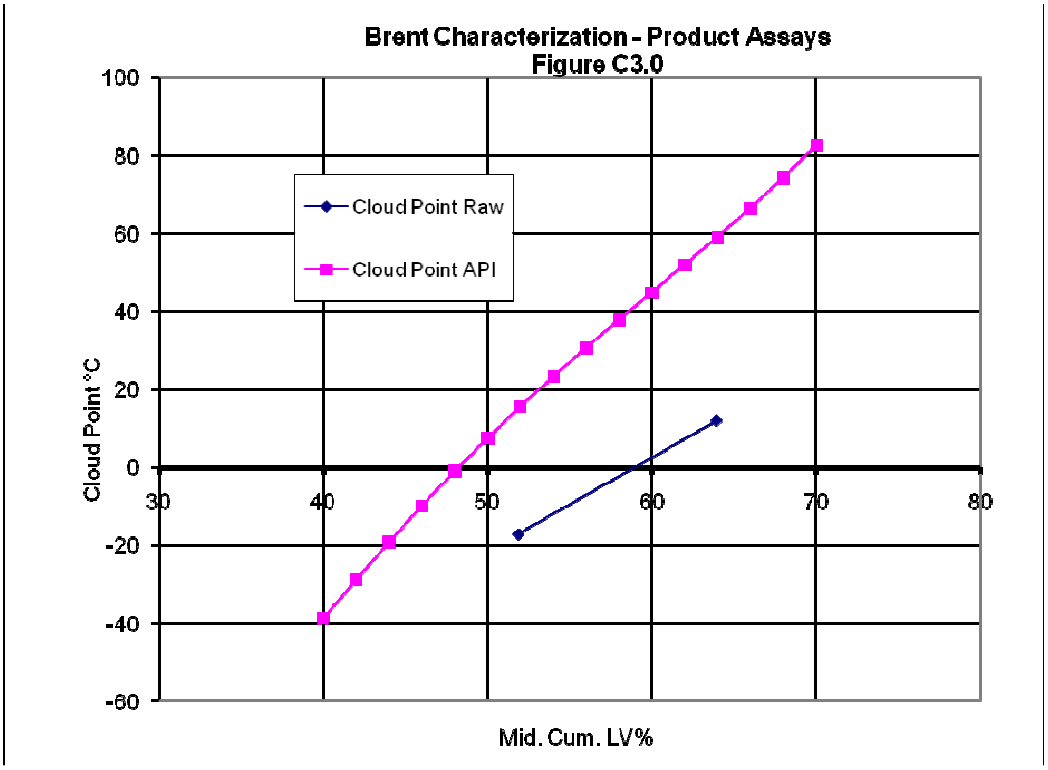

Figure C3.0 – Brent Characterization – Product Assays – Cloud Point vs. Mid Cum LV%

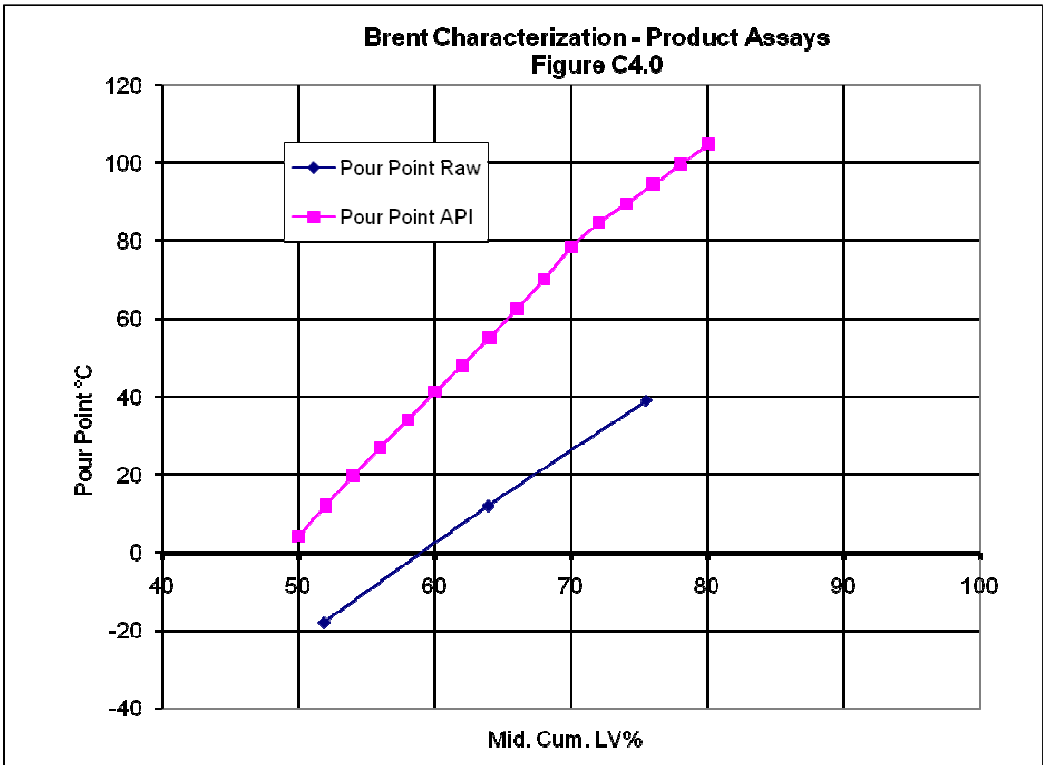

Figure C4.0 – Brent Characterization – Product Assays – Pour Point vs. Mid Cum LV%

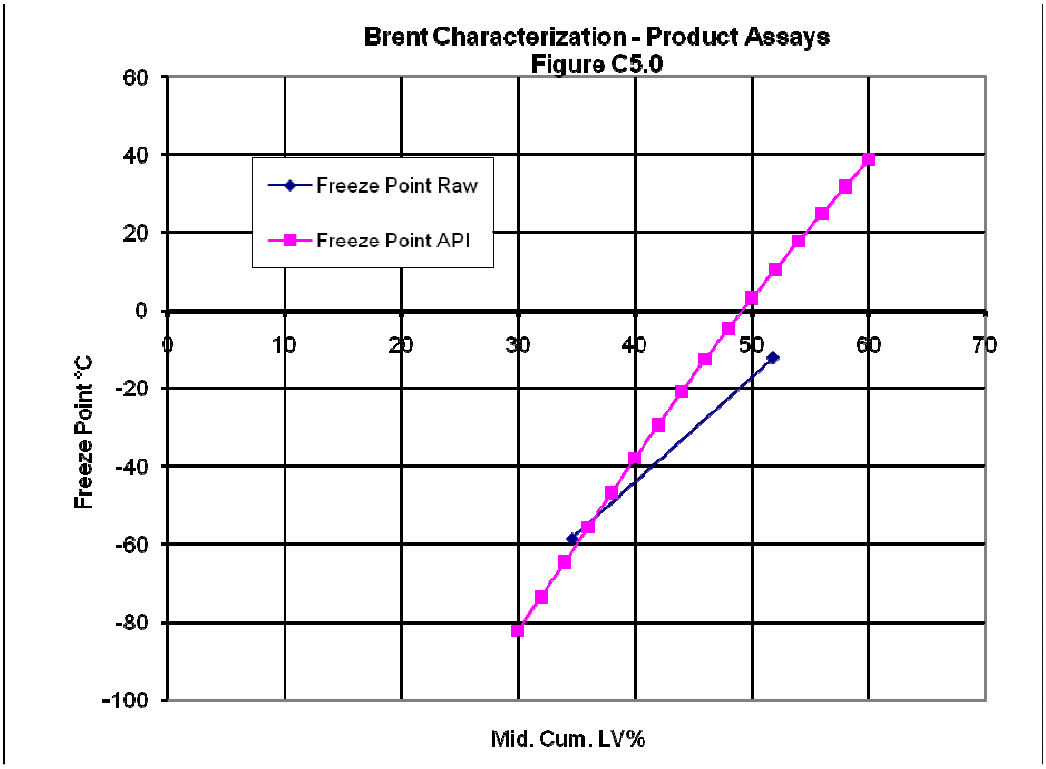

Figure C5.0 – Brent Characterization – Product Assays – Freeze Point vs. Mid Cum LV%

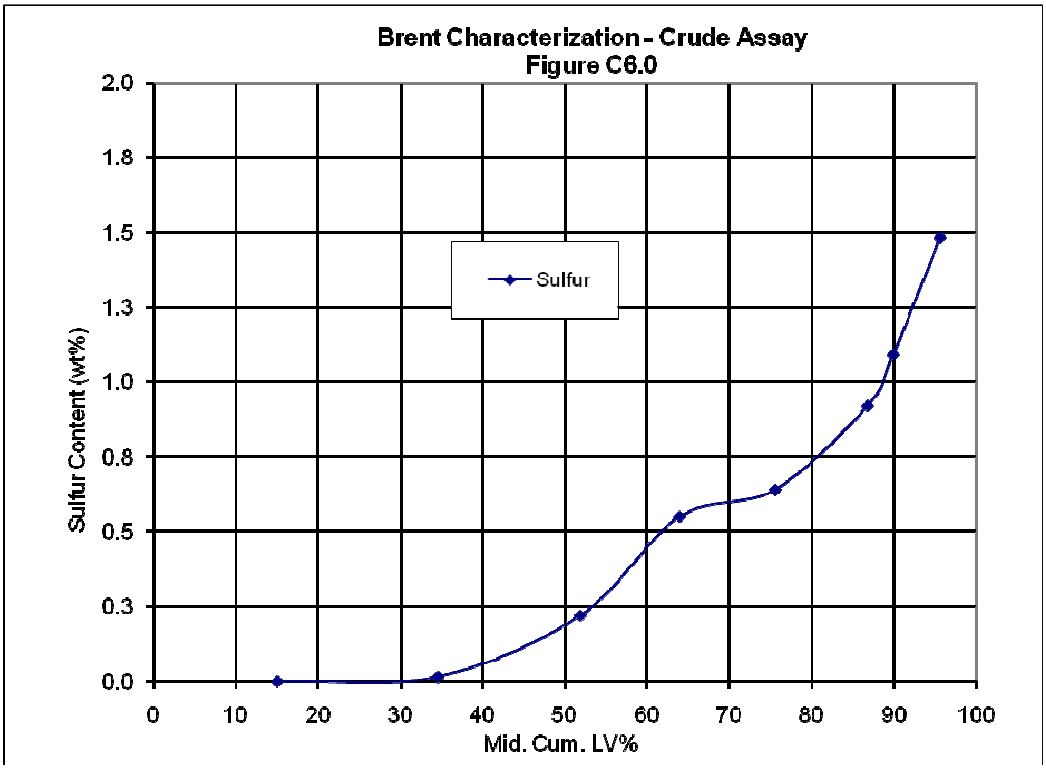

Figure C6.0 – Brent Characterization – Crude Assay – Sulfur Content wt% vs. Mid Cum LV%

4.4.2 Conclusions for Brent Crude

- The calculated crude assay data is entered into HYSYS.
- The adjusted gravity distribution is entered into HYSYS.
- Viscosity assays at $122^{o}F$ and $212^{o}F$ is entered into HYSYS.
- During process simulation, crude viscosity in the preheat train to be checked against this crude characterization for consistency.

4.4.3 Maya Crude

Crude assay data was provided in two forms: vendor lab data and calculated data or CAL II data. Since the vendor lab data provided is incomplete, CAL II is used to develop the Maya crude characterization.

The PCP CAL II data consists of an extensive set of boiling point curves and petroleum properties for distillate and residue cuts that closely match refinery products. These were generated from the crude assay by the PCP CAL II library, which is also used as input for the refinery's LP modeler.

This set of data is, in effect, an extrapolation of the raw crude assay data. The provided data was analyzed for consistency and accuracy in predicting selected petroleum properties. The result of this effort is represented in figures below.

The TBP data for each of the cuts is shown in Figure D1.0. This data was also plotted on logarithmic coordinates, as shown in Figures D1.1 and D1.2, to identify any irregularities. As shown by these curves, the data follows a smooth distribution across each fraction and requires no adjustment.

Each of the True Boiling Point (TBP) distributions was plotted to construct the whole crude, as shown in Figure D1.3. The composite TBP distribution curve for the whole crude was constructed by joining the mid-volume percent of the individual curves shown in Figure D1.3. Standard curve fitting procedures available in Excel were used to obtain a curve of best fit through the data points. Due to the nature of the distribution, it was not possible to adequately represent the whole crude with a single equation. Three separate equations were required and the resulting curve is shown in Figure D1.4.

The composite curve of Figure D1.4 and the raw distillation data from the crude assay are shown in Figure D1.5 for comparison. There is a perfect agreement between the two curves. The composite curve tends to over predict in the distillate range by up to 3 LV%, which is within the range of experimental error.

The composite curve was also compared to the blended curve generated by HYSYS from each of the cuts. As shown in Figure D1.6, the composite curve of Figure D1.4 matches the HYSYS curve well.

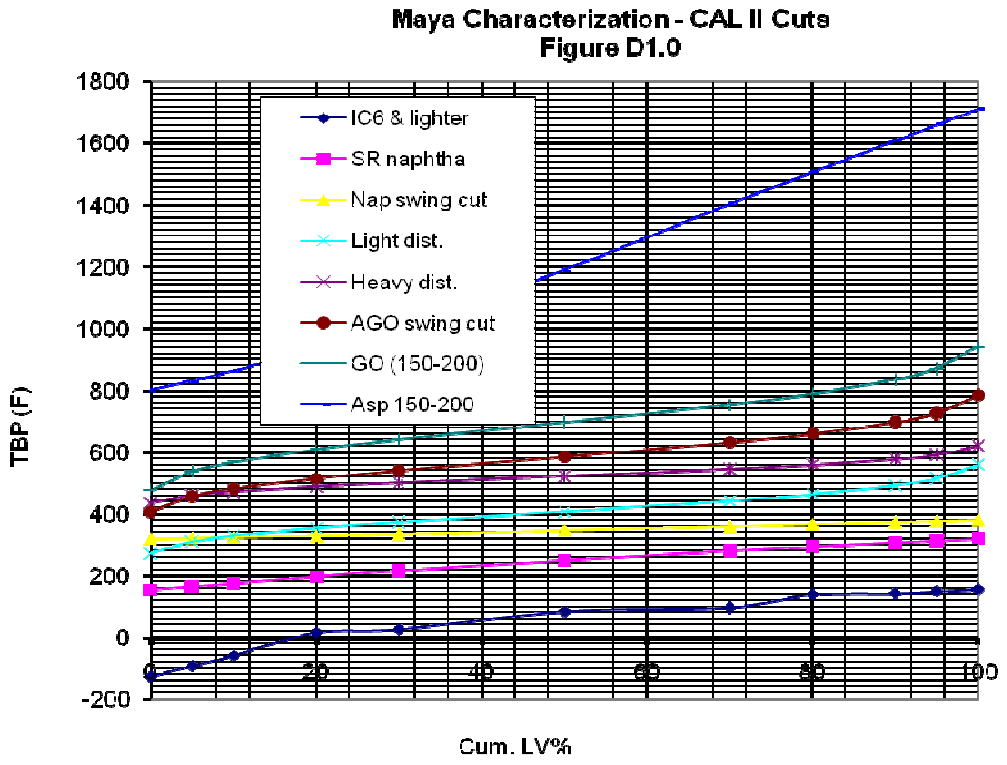

Figure D1.0 – Maya Characterization – CALII Cuts – TBP vs. Cumulative LV%

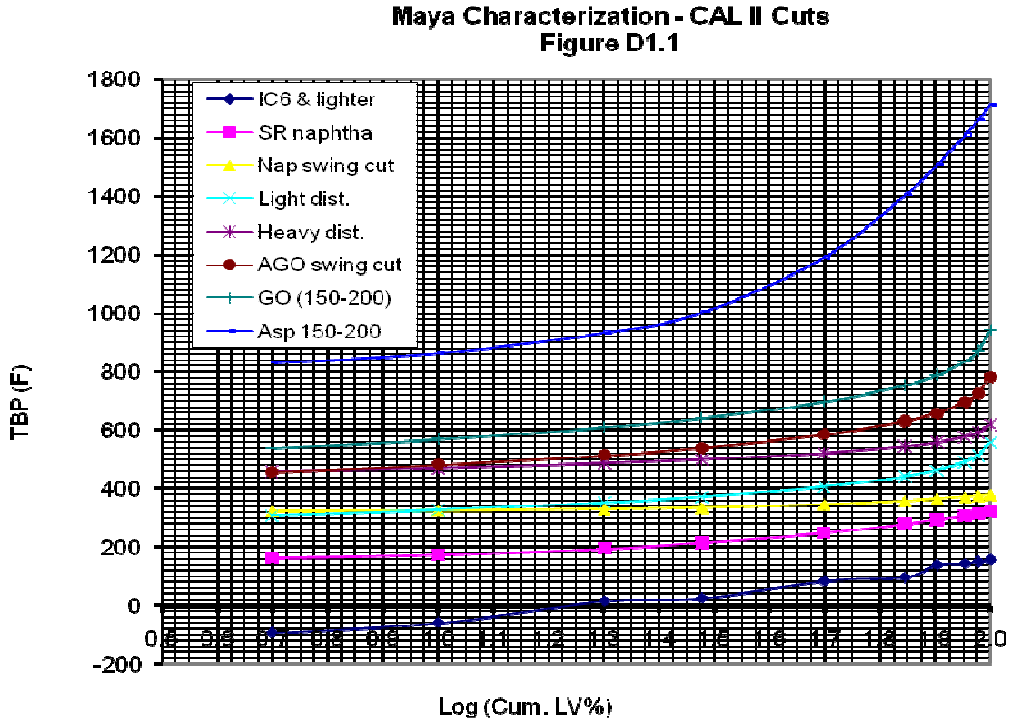

Figure D1.1 – Maya Characterization – CALII Cuts – TBP vs. Log Cumulative LV%

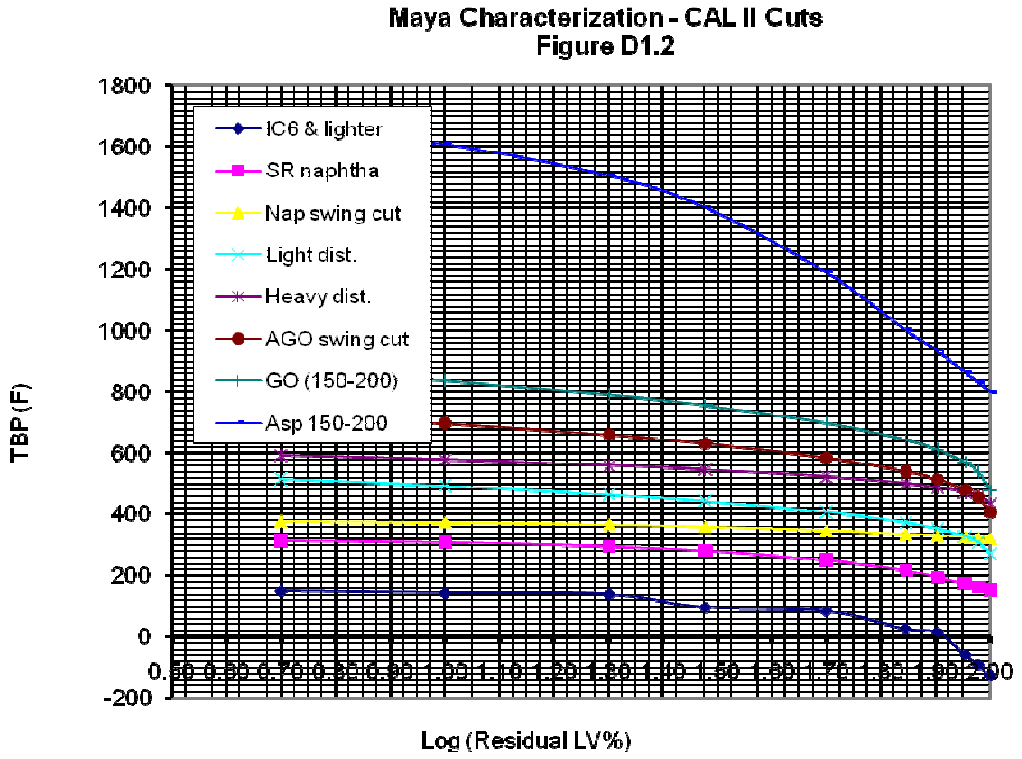

Figure D1.2 – Maya Characterization – CALII Cuts – TBP vs. Log Residual LV%

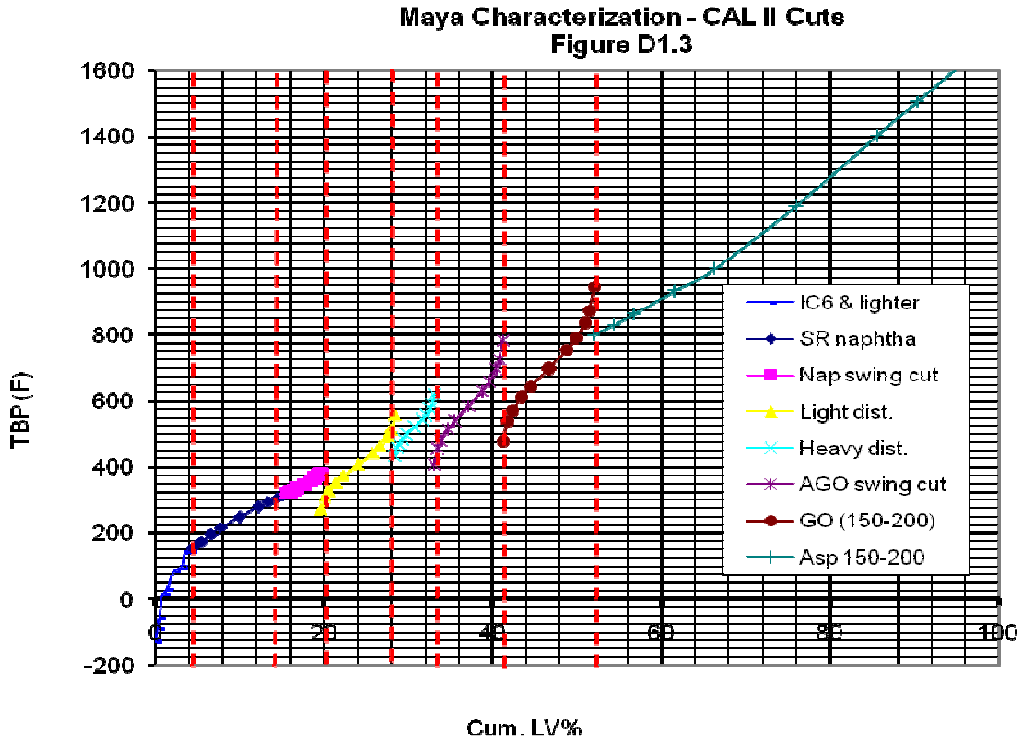

Figure D1.3 – Maya Characterization – CALII Cuts – TBP vs. Cumulative LV%

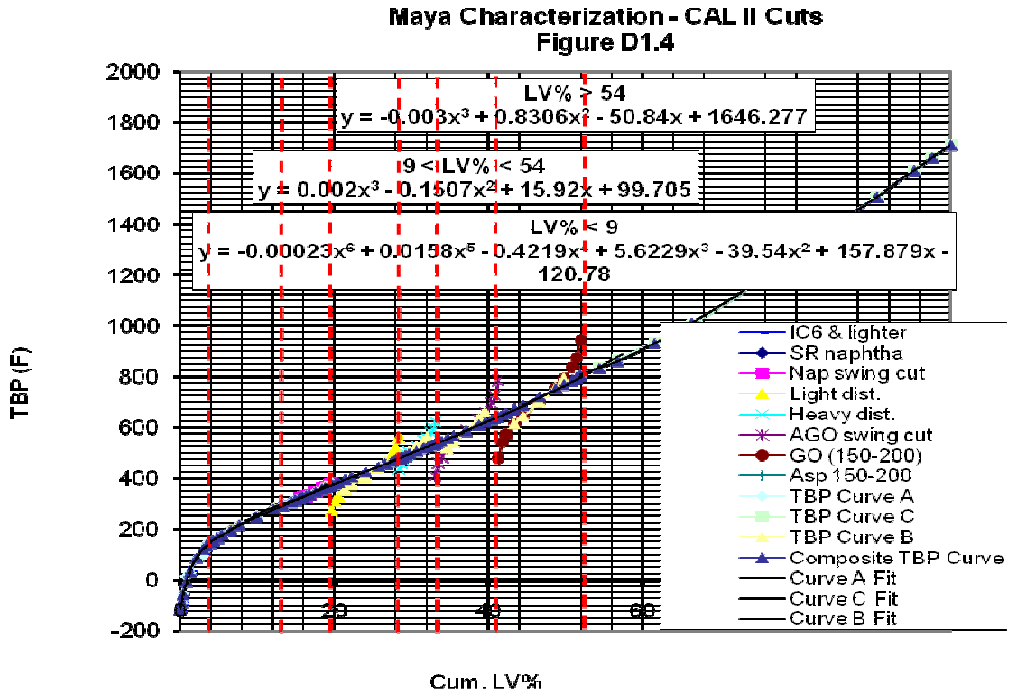

Figure D1.4 – Maya Characterization – CALII Cuts – TBP vs. Cumulative LV%

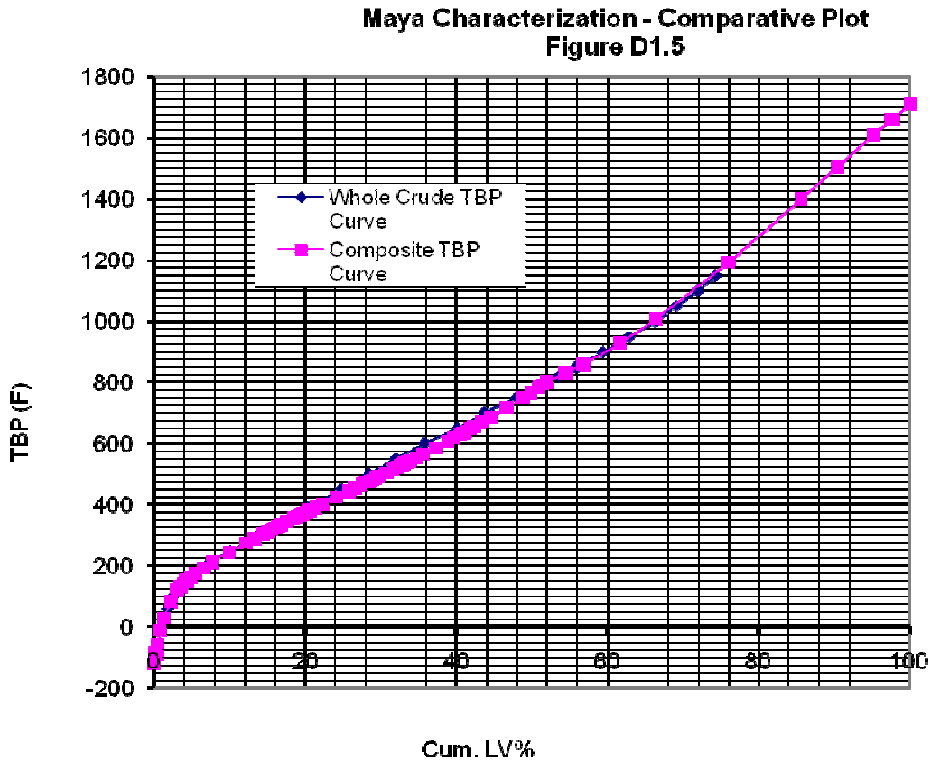

Figure D1.5 – Maya Characterization – Comparative Plot – TBP vs. Cumulative LV%

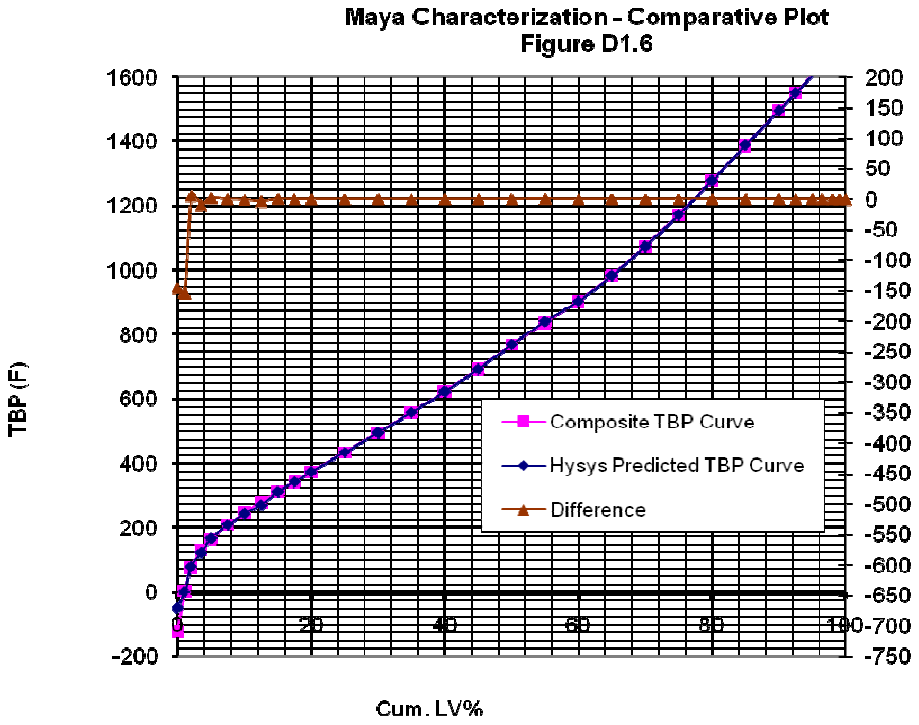

Figure D1.6 – Maya Characterization – Comparative Plot – TBP vs. Cumulative LV%

The provided gravity data was plotted against the volume average true boiling point of each cut as shown in Figure D2.0.

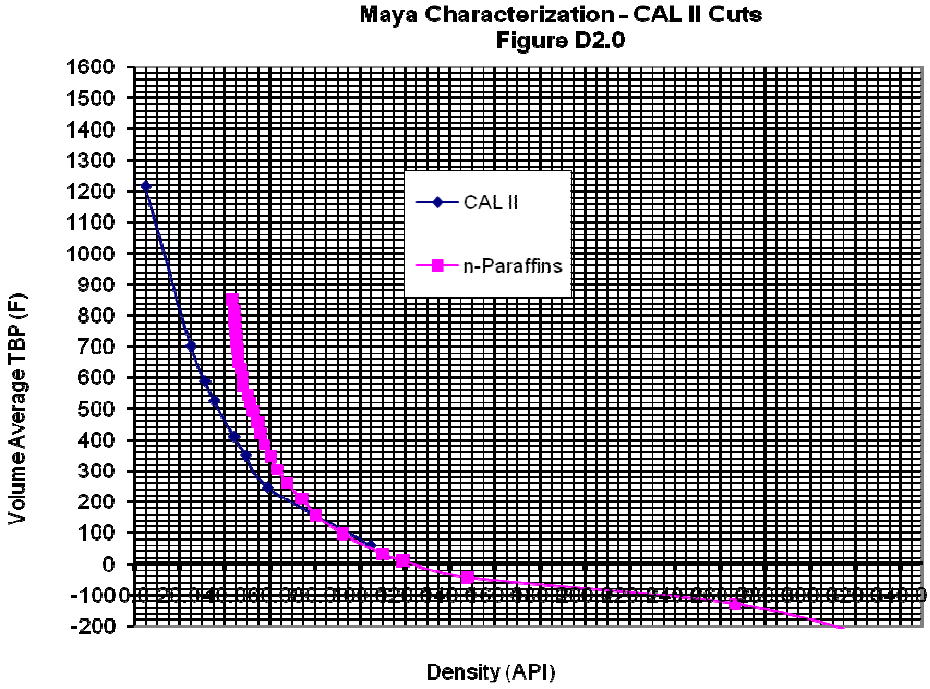

Figure D2.0 – Maya Characterization – CALII Cuts – Volume Ave TBP vs. Density

The same data was plotted on logarithmic coordinates in Figure D2.1, which shows that the provided gravity data is well behaved and follows very nearly a straight line.

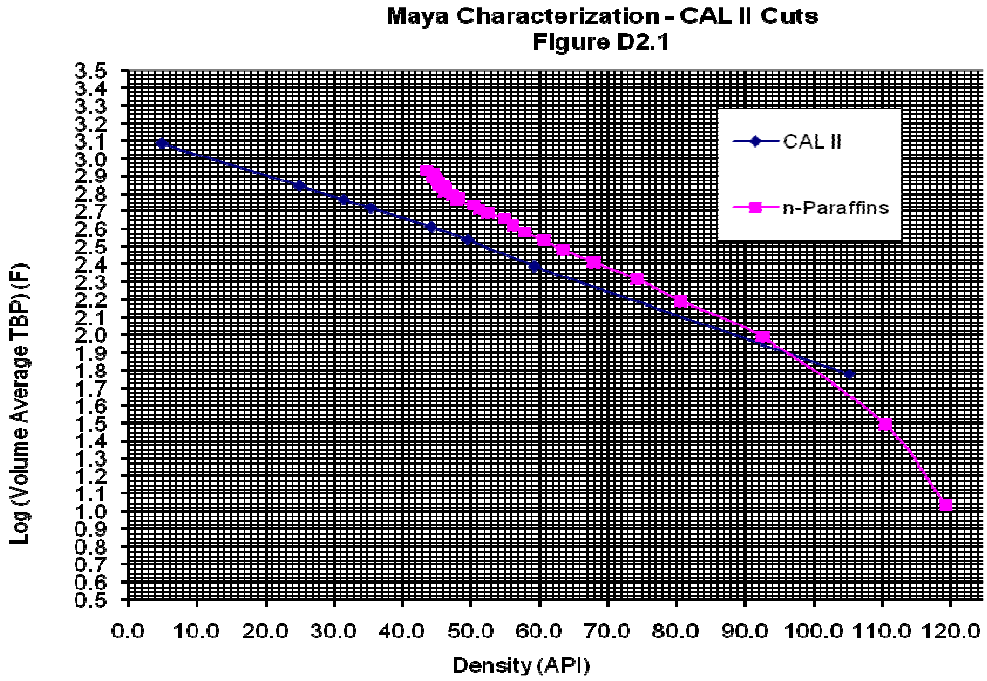

Figure D2.1 – Maya Characterization – CALII Cuts – Log Vol Ave TBP vs. Density

Next, the gravity curve was extended by a straight-line best fit through the raw data and extrapolation to 100 LV% to cover the full range of the crude. The curved portion of the gravity distribution was obtained by trial and error, using the n-paraffin line as reference, to converge with the n-paraffin line as shown in Figure D2.3. These steps were repeated until reasonable predictions for petroleum properties were obtained simultaneously with a weight balance on the whole crude.

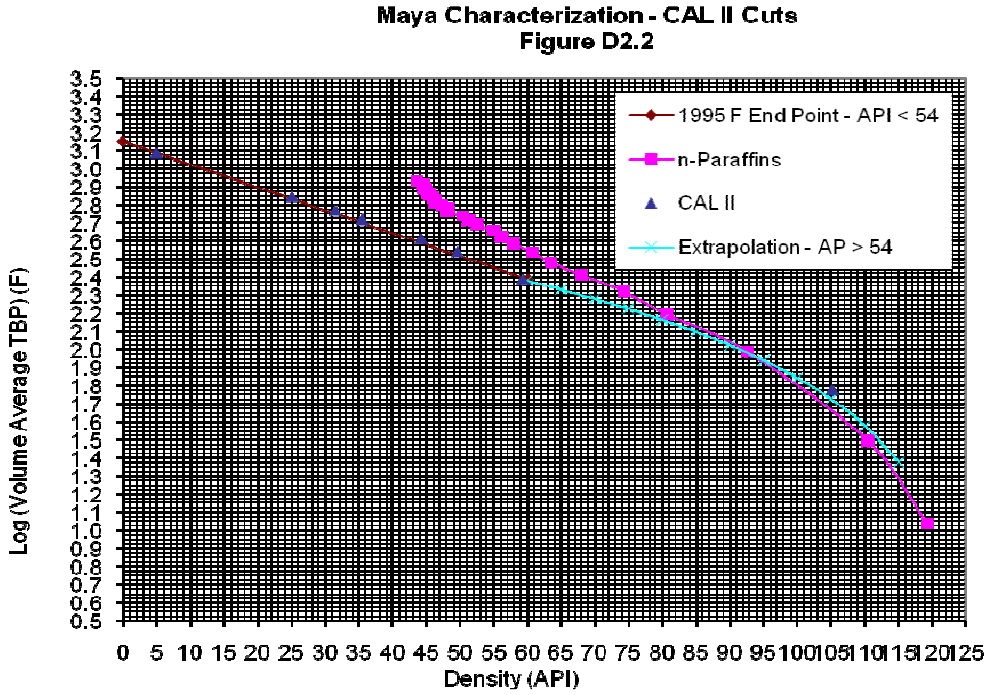

Figure D2.2 – Maya Characterization – CALII Cuts – Log Vol Ave TBP vs. Density

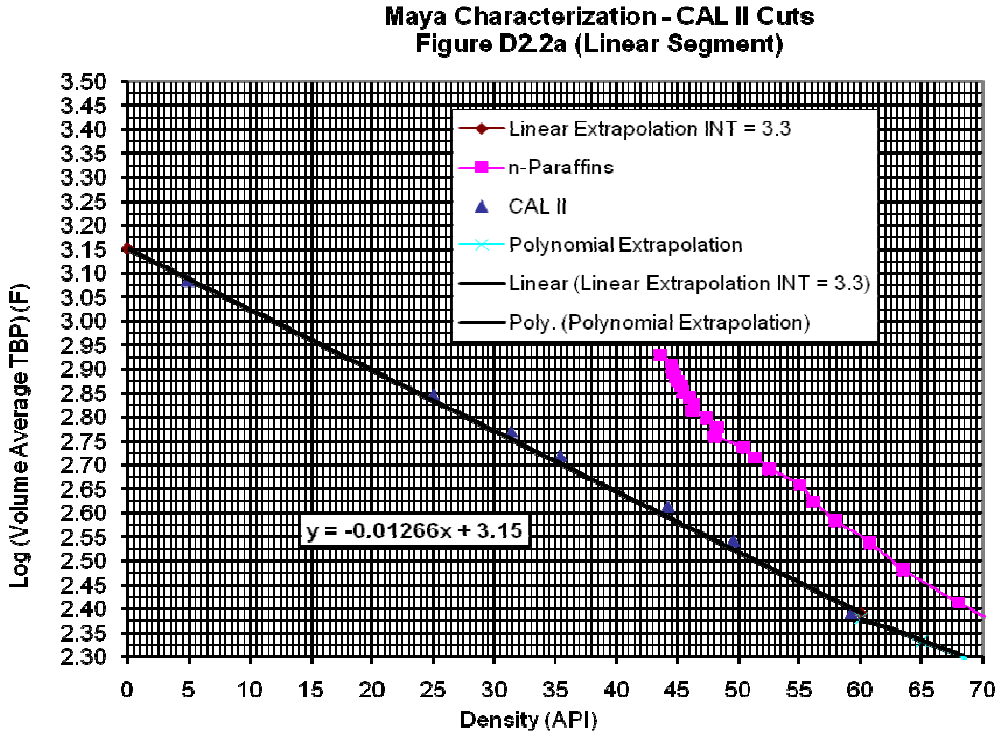

Figure D2.2a – Maya Characterization – CALII Cuts Linear Segment – Log Vol Ave TBP vs. Density

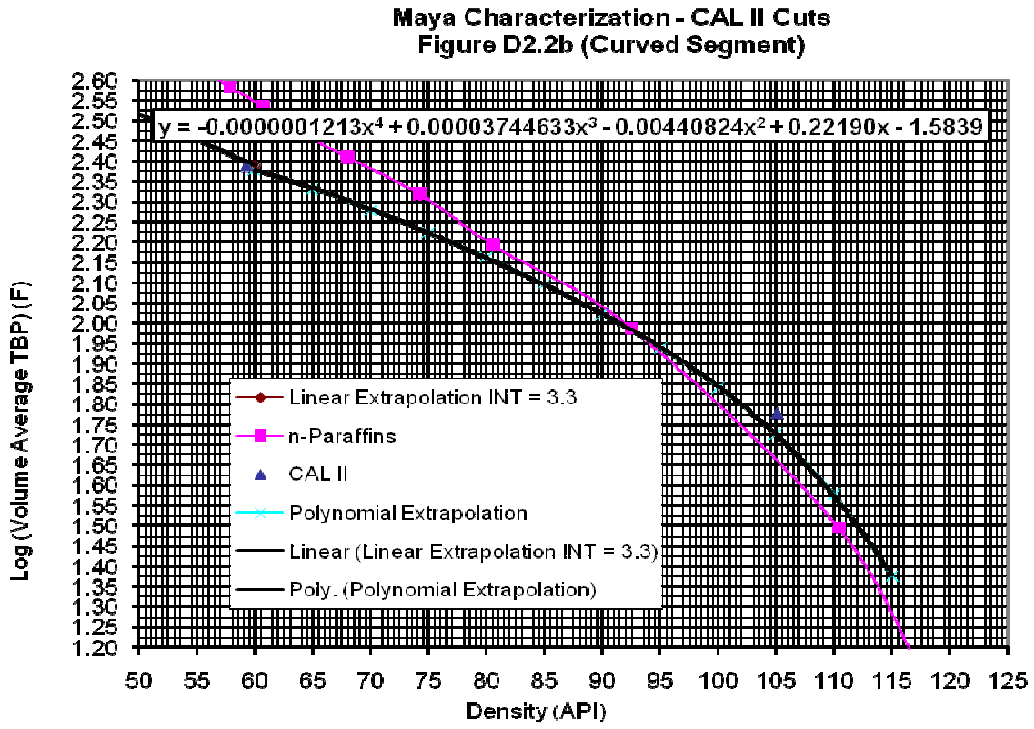

Figure D2.2b – Maya Characterization – CALII Cuts Curved Segment – Log Vol Ave TBP vs. Density

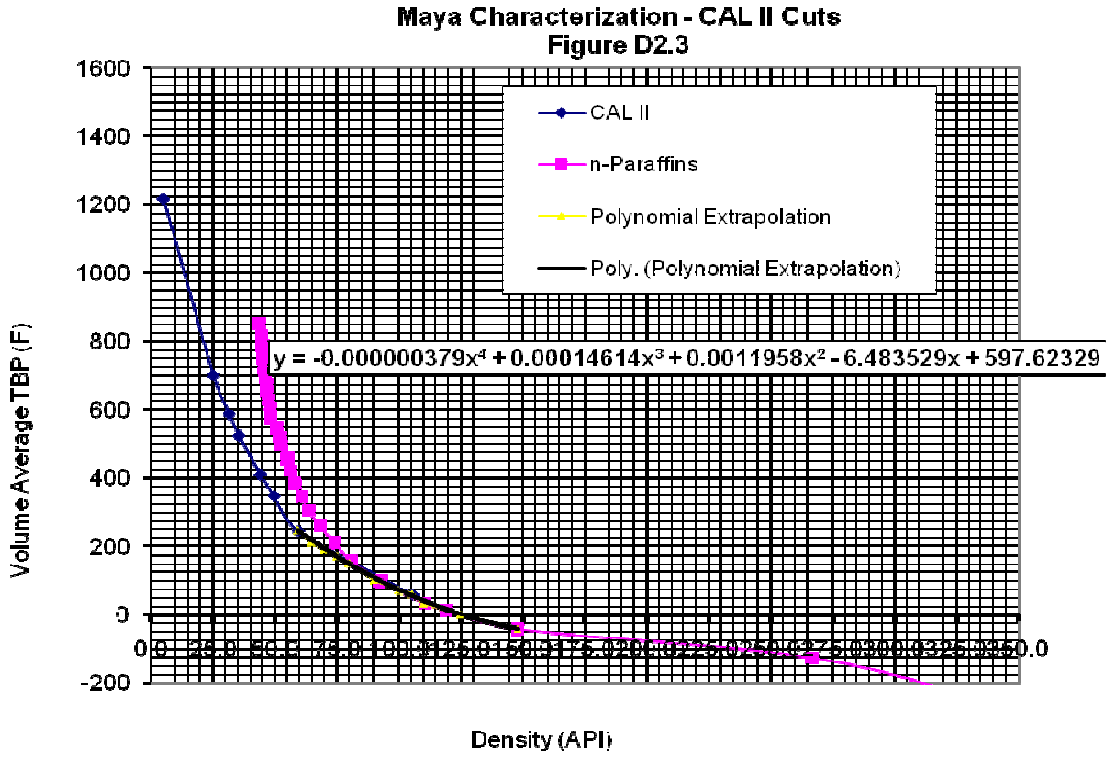

Figure D2.3 – Maya Characterization – CALII Cuts – Vol Ave TBP vs. Density

The gravity distribution across the whole crude as a function of percent distilled was obtained from the fitted gravity curve of Figure D2.2. The resulting gravity distribution curve is shown in Figure D3.0, which also shows the CAL II data for reference. The calculated API curve shows good agreement with the provided data.

Since many of the property prediction methods are based on empirical correlations between TBP and API, the adequacy of the fitted curves were checked through calculation of a series of petroleum properties as outlined in the API Technical Data Book.

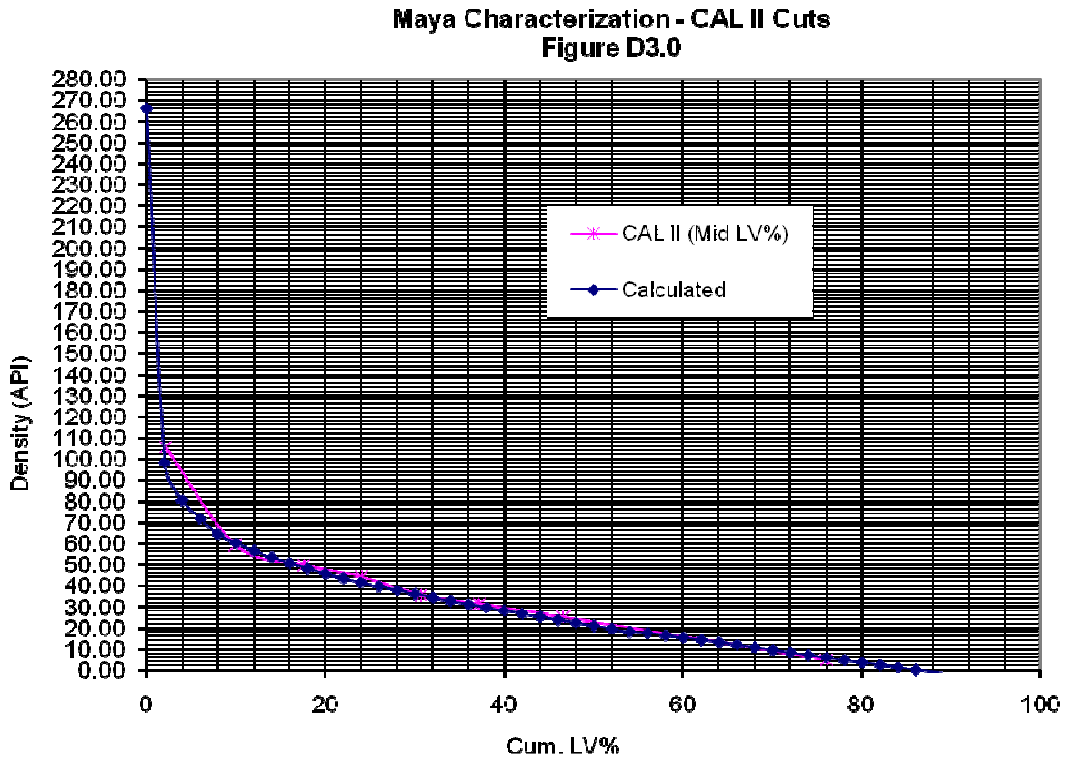

Figure D3.0 – Maya Characterization – CALII Cuts – Density vs. Cumulative LV%

The Watson Characterization factor (Kw) was calculated at each LV% distilled from the appropriate TBP curve shown in Figure D1.4 and the corresponding value of gravity from the curve of Figure D2.2. The calculated Kw distribution is shown in Figure D4.0. The provided values of Kw were plotted on the same figure for comparison. The results display a typical characterization factor curve and show good agreement between the calculated and provided data.

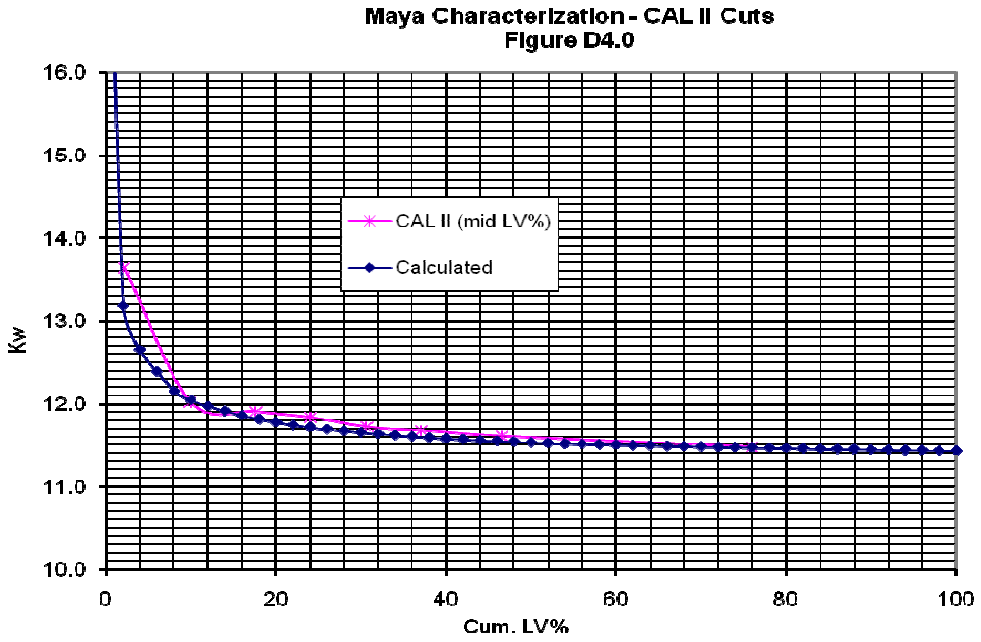

Figure D4.0 – Maya Characterization – CALII Cuts – Kw vs. Cumulative LV%

Values for several petroleum properties were calculated in similar fashion and are shown in Figures D5.0 through D8.0.

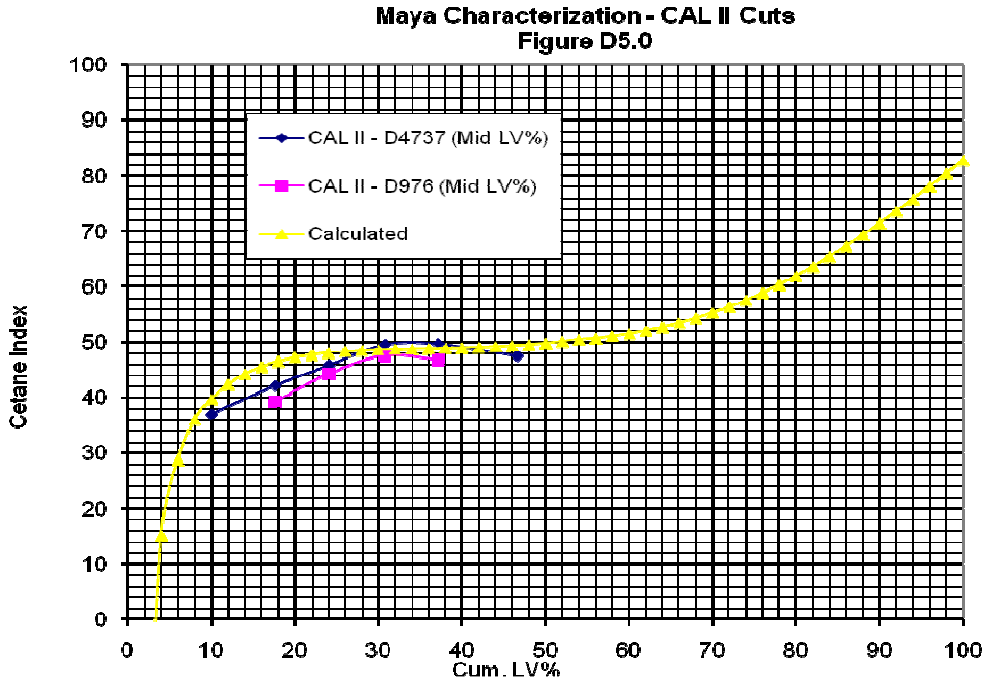

Figure D5.0 – Maya Characterization – CALII Cuts – Cetane Index vs. Cumulative LV%

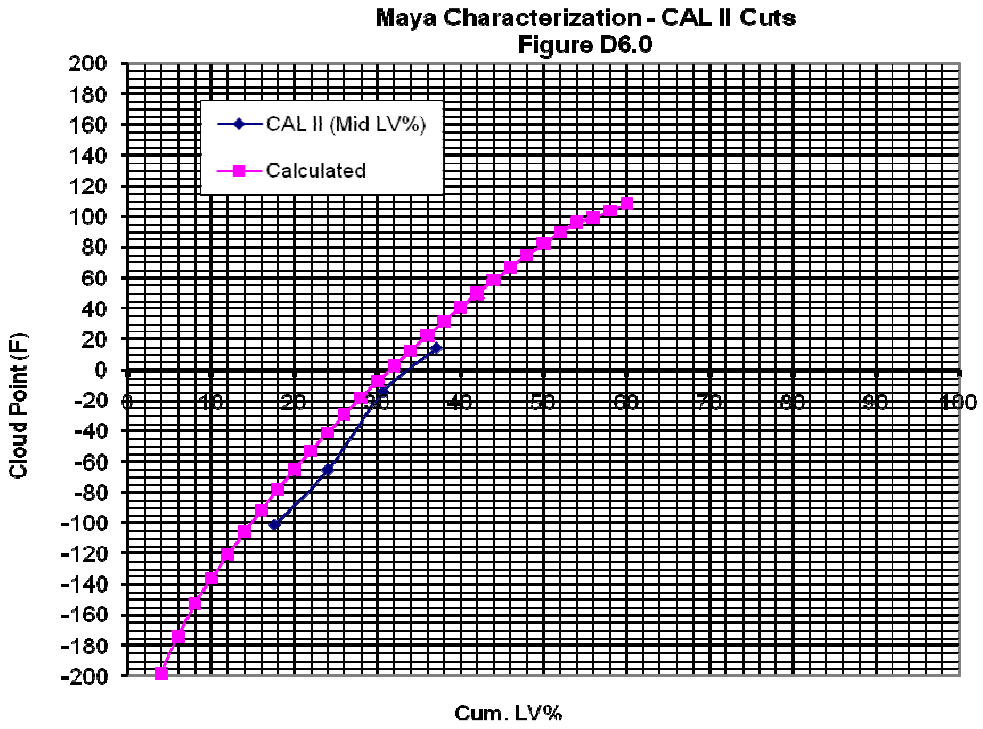

Figure D6.0 – Maya Characterization – CALII Cuts – Cloud Point vs. Cumulative LV%

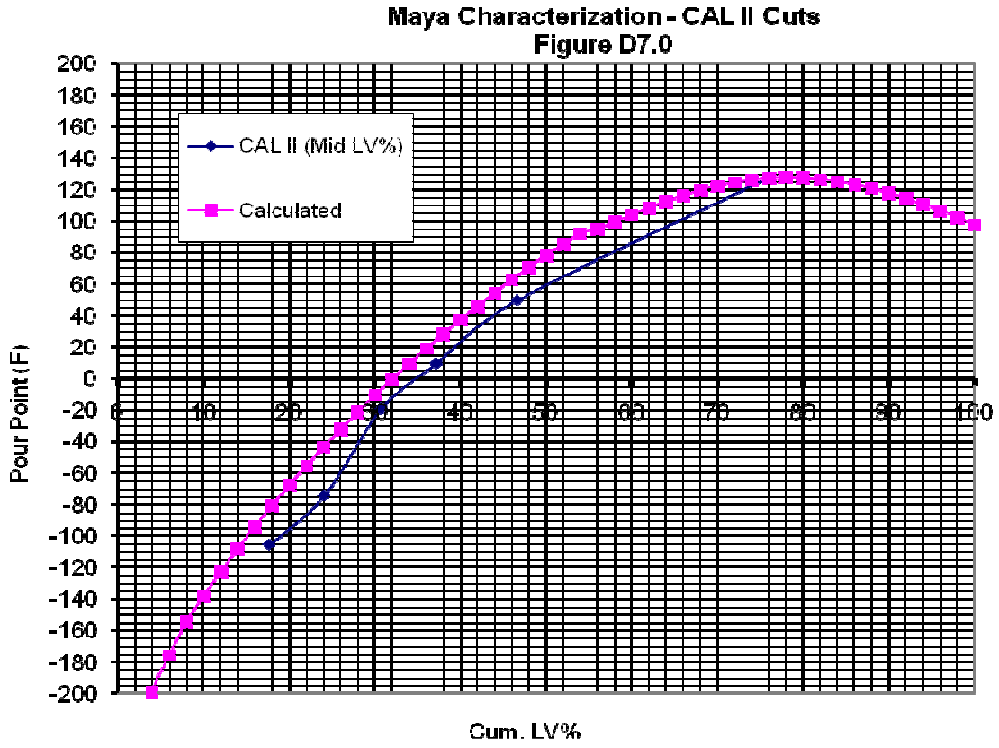

Figure D7.0 – Maya Characterization – CALII Cuts – Pour Point vs. Cumulative LV%

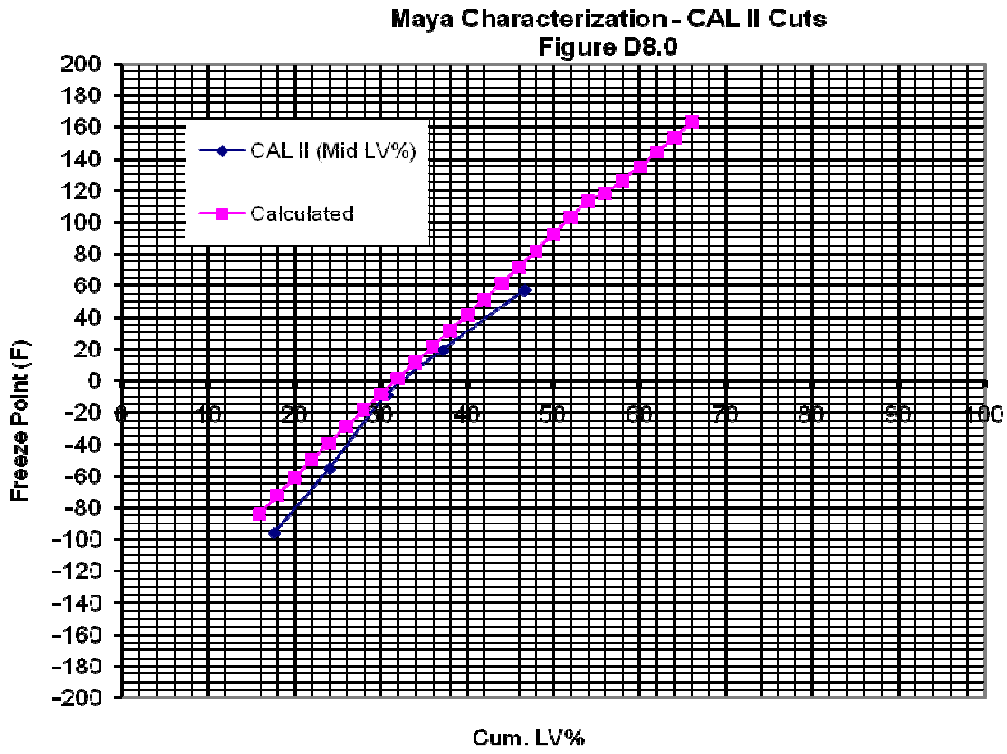

Figure D8.0 – Maya Characterization – CALII Cuts – Freeze Point vs. Cumulative LV%

With the exception of Cetane Index, each of the predicted values shows good agreement with the reported data in the range of interest that is 30-60 LV% distilled. This range corresponds to distillate fractions that have product specifications.

As a final check of the TBP and API curves, the weight of the whole crude used for the assay was calculated and compared against the actual weight. Table 4.4.3a shows a series of volume fractions and the corresponding TBP as determined from Figure D1.4. For each TBP, the corresponding gravity was determined from the curve of Figure D2.2. The weight of each volume fraction was added to obtain the calculated weight of the whole crude. The actual weight of the whole crude was determined from the measured whole crude gravity provided with the crude assay as shown in Table 4.4.3b. The results are summarized in Table 4.4.3c, which shows weight balance within 0.56%.

In view of the good weight balance and reasonable predictions for several petroleum properties, further adjustment of the TBP and gravity curves was deemed unnecessary.

Table 4.4.3a - Calculated Weight for Maya Crude

LV%	Cum LV%	API Calc	SG	Cut Vol mL	Cut Avg. Wt g	Cum Wt g
0	0	266.00	0.36	0.00	0.00	**0.00**
2	2	98.22	0.62	2.00	1.23	1.23
2	4	80.18	0.67	2.00	1.34	2.57
2	6	71.73	0.70	2.00	1.39	3.96
2	8	64.21	0.72	2.00	1.45	5.41
2	10	59.95	0.74	2.00	1.48	6.89
2	12	56.42	0.75	2.00	1.51	8.39
2	14	53.29	0.77	2.00	1.53	9.92
2	16	50.48	0.78	2.00	1.56	11.48
2	18	47.92	0.79	2.00	1.58	13.06
2	20	45.58	0.80	2.00	1.60	14.65
2	22	43.40	0.81	2.00	1.62	16.27
2	24	41.37	0.82	2.00	1.64	17.91
2	26	39.46	0.83	2.00	1.66	19.56
2	28	37.64	0.84	2.00	1.67	21.24
2	30	35.91	0.85	2.00	1.69	22.93
2	32	34.24	0.85	2.00	1.71	24.64
2	34	32.63	0.86	2.00	1.72	26.36
2	36	31.07	0.87	2.00	1.74	28.10
2	38	29.54	0.88	2.00	1.76	29.86
2	40	28.05	0.89	2.00	1.77	31.63
2	42	26.58	0.90	2.00	1.79	33.42
2	44	25.13	0.90	2.00	1.81	35.23
2	46	23.69	0.91	2.00	1.82	37.05
2	48	22.27	0.92	2.00	1.84	38.89
2	50	20.85	0.93	2.00	1.86	40.75
2	52	19.44	0.94	2.00	1.87	42.63
2	54	18.03	0.95	2.00	1.89	44.52
2	56	17.44	0.95	2.00	1.90	46.42
2	58	16.40	0.96	2.00	1.91	48.33
2	60	15.31	0.96	2.00	1.93	50.26
2	62	14.17	0.97	2.00	1.94	52.20
2	64	13.00	0.98	2.00	1.96	54.16
2	66	11.81	0.99	2.00	1.97	56.13
2	68	10.60	1.00	2.00	1.99	58.13
2	70	9.39	1.00	2.00	2.01	60.14
2	72	8.17	1.01	2.00	2.03	62.16
2	74	6.97	1.02	2.00	2.04	64.21
2	76	5.77	1.03	2.00	2.06	66.27
2	78	4.59	1.04	2.00	2.08	68.35
2	80	3.43	1.05	2.00	2.10	70.44
2	82	2.29	1.06	2.00	2.12	72.56
2	84	1.18	1.07	2.00	2.13	74.69
2	86	0.10	1.08	2.00	2.15	76.84
2	88	-0.96	1.08	2.00	2.17	79.01
2	90	-1.98	1.09	2.00	2.18	81.20
2	92	-2.97	1.10	2.00	2.20	83.40
2	94	-3.92	1.11	2.00	2.22	85.62
2	96	-4.84	1.12	2.00	2.23	87.85
2	98	-5.72	1.12	2.00	2.25	90.10
2	100	-6.56	1.13	2.00	2.27	92.36

Table 4.4.3b - Actual Cumulative Weight of the Whole Maya Crude

LV%	Cum LV%	API Raw	SG	Cut Vol mL	Cut Avg. Wt g	Cum Wt g
100	100	21.3	0.93	100	92.60	**92.60**

Table 4.4.3b – Summary of Results for Maya Crude Actual Weight

Calculated Wt g	Actual Wt g	Delta g	Delta %
92.36	92.60	0.24	0.26

The provided viscosity data are shown in Figure D9.0. The same viscosity data were transformed to logarithmic coordinates and plotted against the provided gravity data for each cut as shown in Figure D9.1.

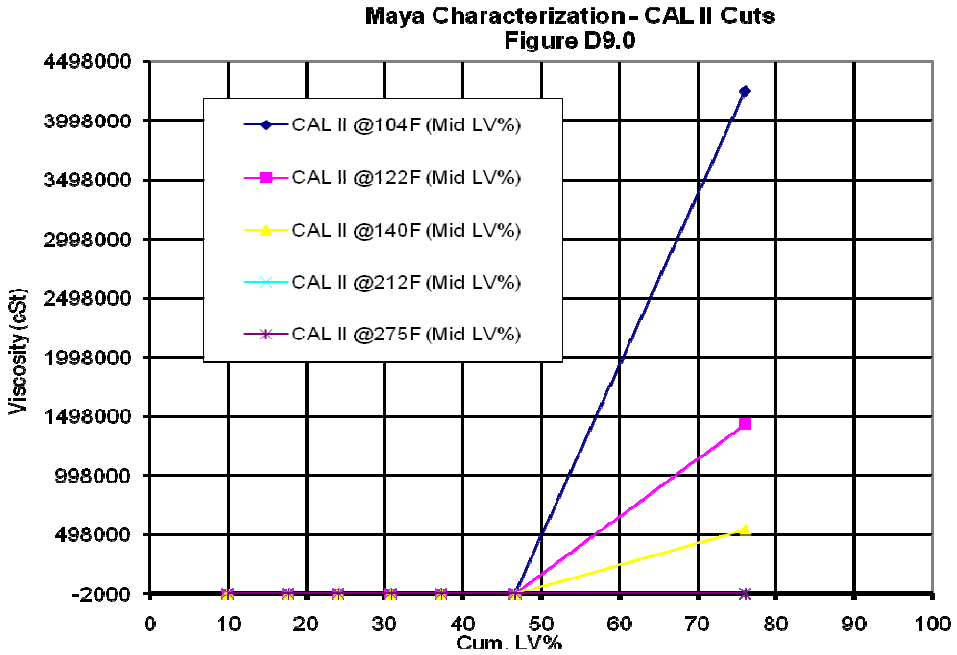

Figure D9.0 – Maya Characterization – CALII Cuts – Viscosity vs. Cumulative LV%

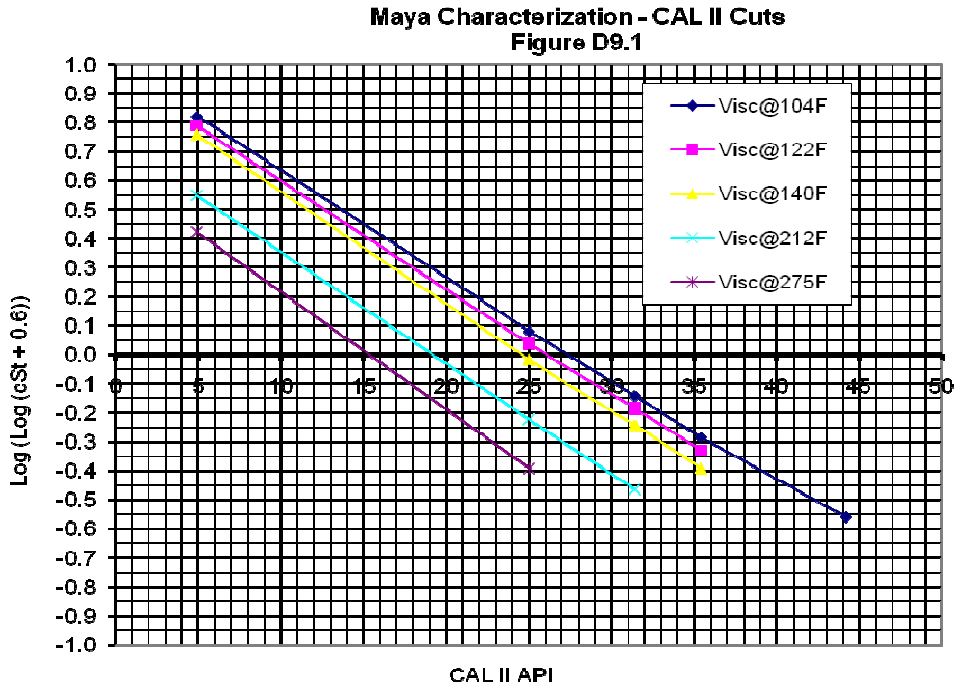

Figure D9.1 – Maya Characterization – CALII Cuts – Kinematic Viscosity vs. CAL II Density

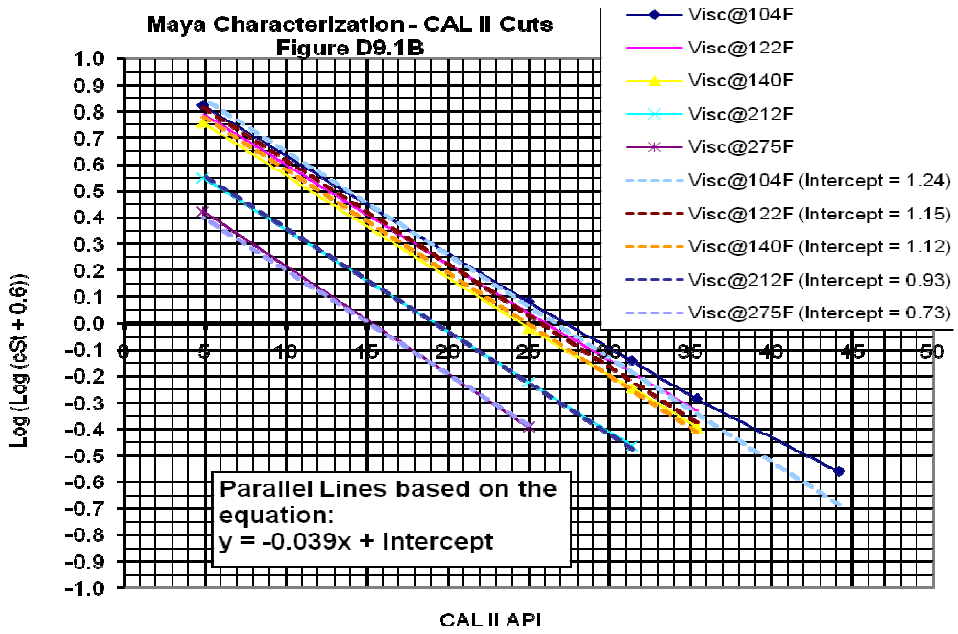

Figure D9.1B – Maya Characterization – CALII Cuts – Kinematic Viscosity vs. CAL II Density

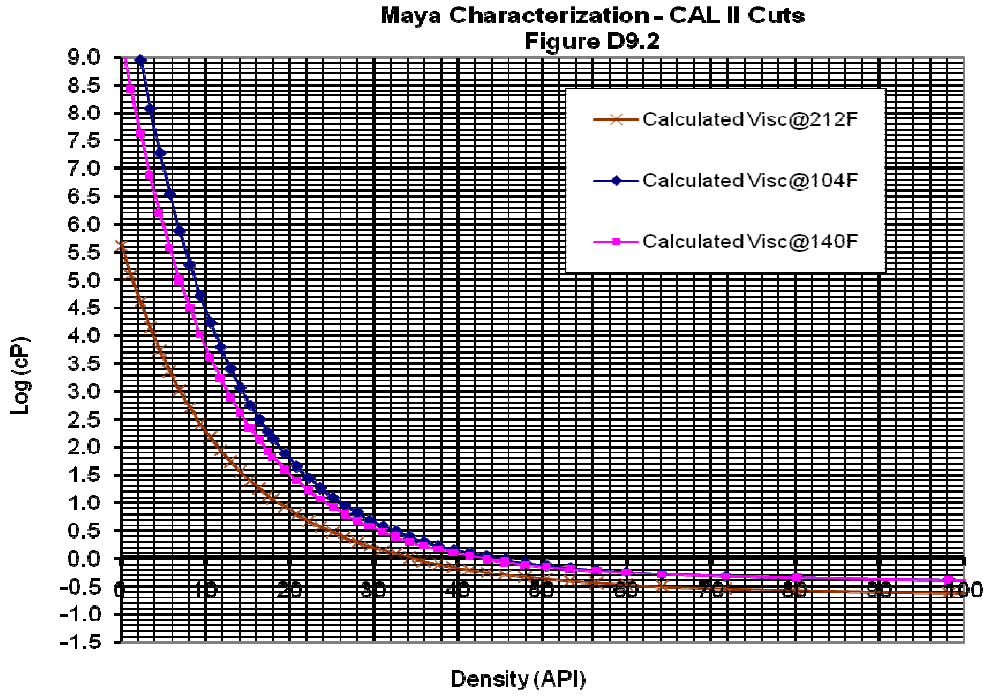

Figure D9.2 – Maya Characterization – CALII Cuts – Viscosity vs. Density

Each set of viscosity data can be represented with a straight line of best fit through the data as shown. The viscosity distribution across the whole crude was generated using Figures D2.2 and D1.4. The resulting distribution curve is shown in Figure D9.3.

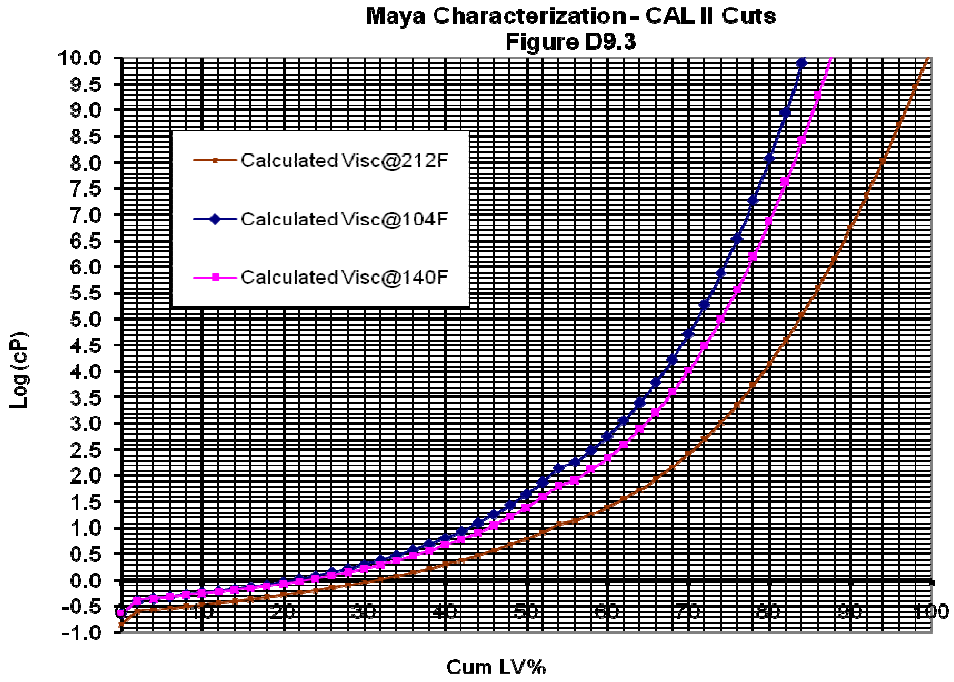

Figure D9.3 – Maya Characterization – CALII Cuts – Viscosity vs. Cumulative LV%

The provided values for sulfur, metals, flash point and molecular weight were also plotted and are shown in Figures D10.0 through D12.0.

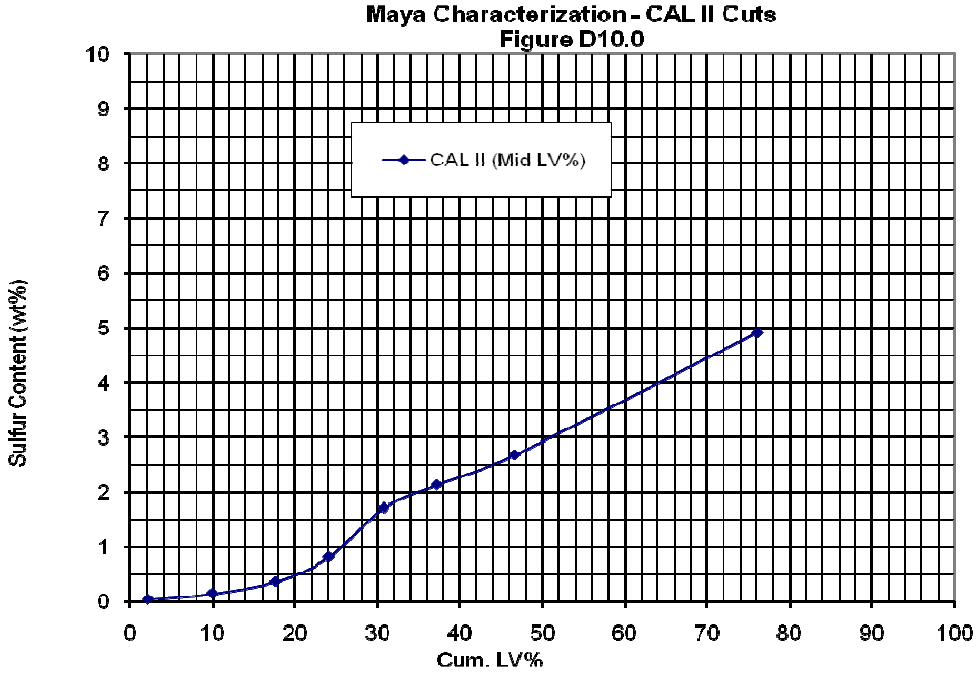

Figure D10.0 – Maya Characterization – CALII Cuts – Sulfur Content wt% vs. Cumulative LV%

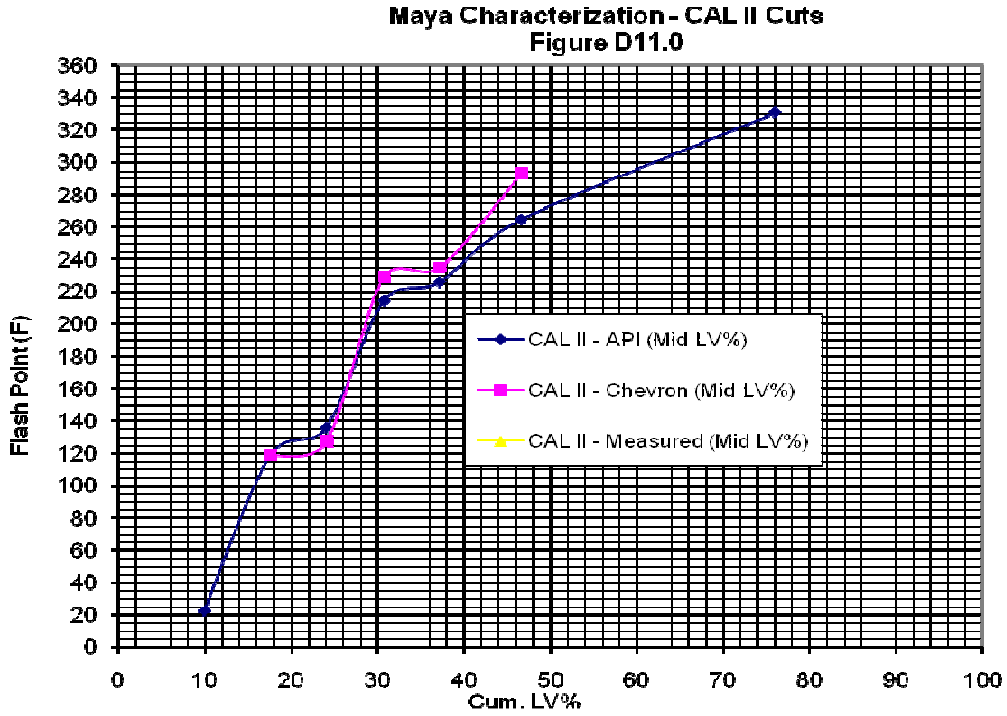

Figure D11.0 – Maya Characterization – CALII Cuts – Flash Point vs. Cumulative LV%

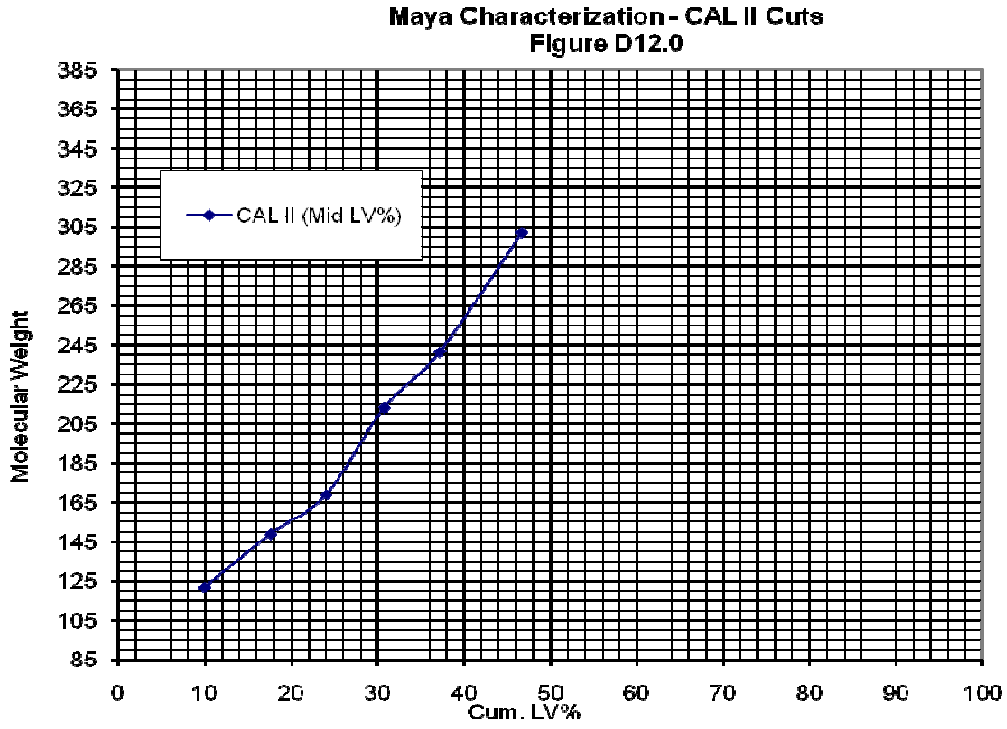

Figure D12.0 – Maya Characterization – CALII Cuts – Molecular Weight vs. Cumulative LV%

Figures E1.0 through to E5.0 show comparison of HYSYS generated properties vs. data generated in this crude characterization document.

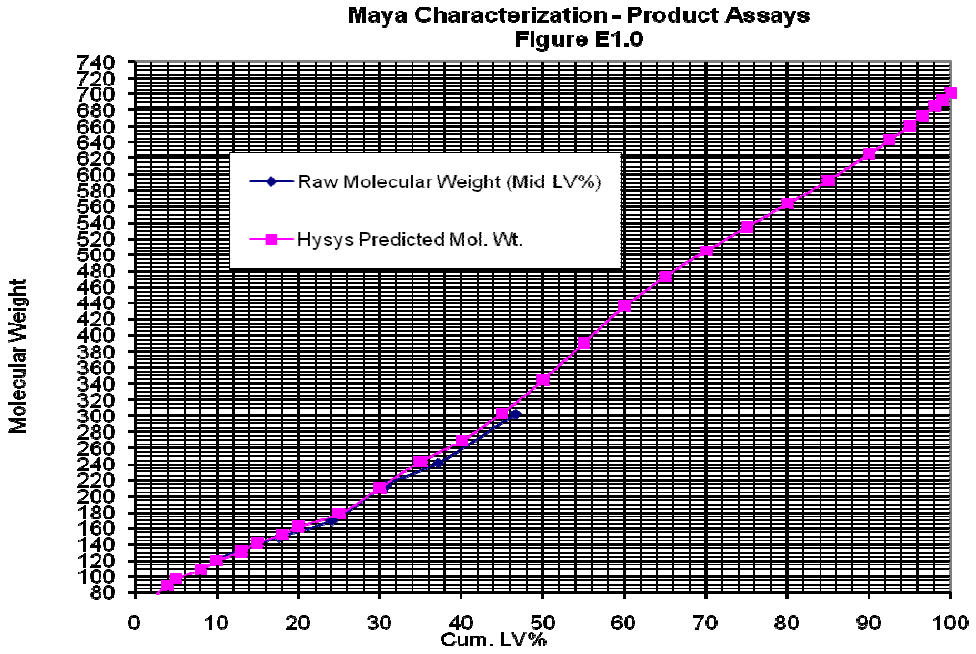

Figure E1.0 – Maya Characterization – Product Assays – Molecular Weight vs. Cumulative LV%

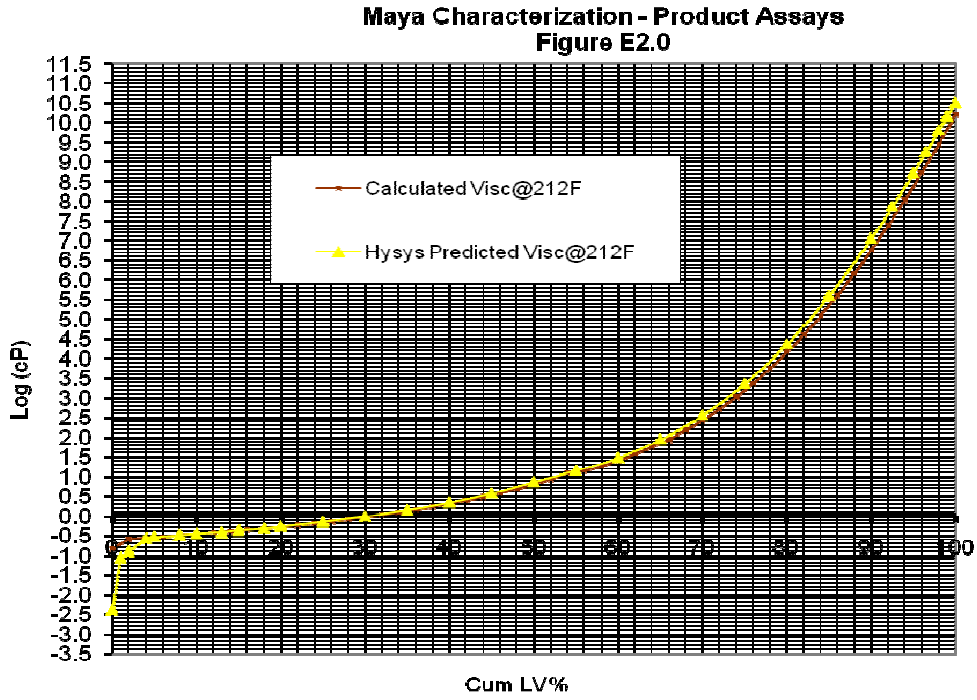

Figure E2.0 – Maya Characterization – Product Assays – Log Viscosity vs. Cumulative LV%

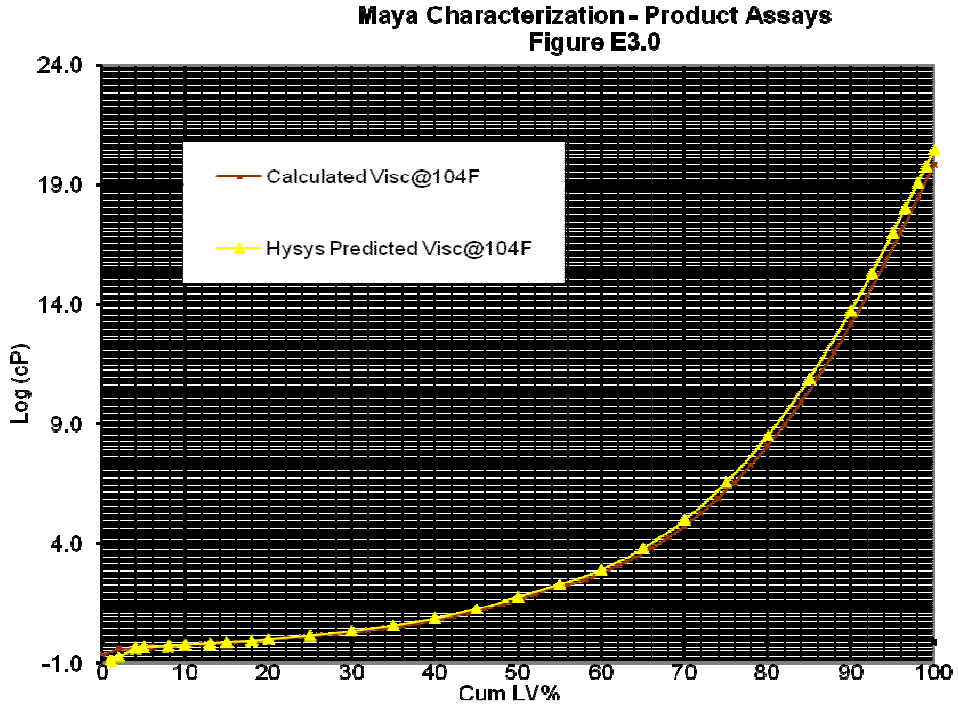

Figure E3.0 – Maya Characterization – Product Assays – Log Viscosity vs. Cumulative LV%

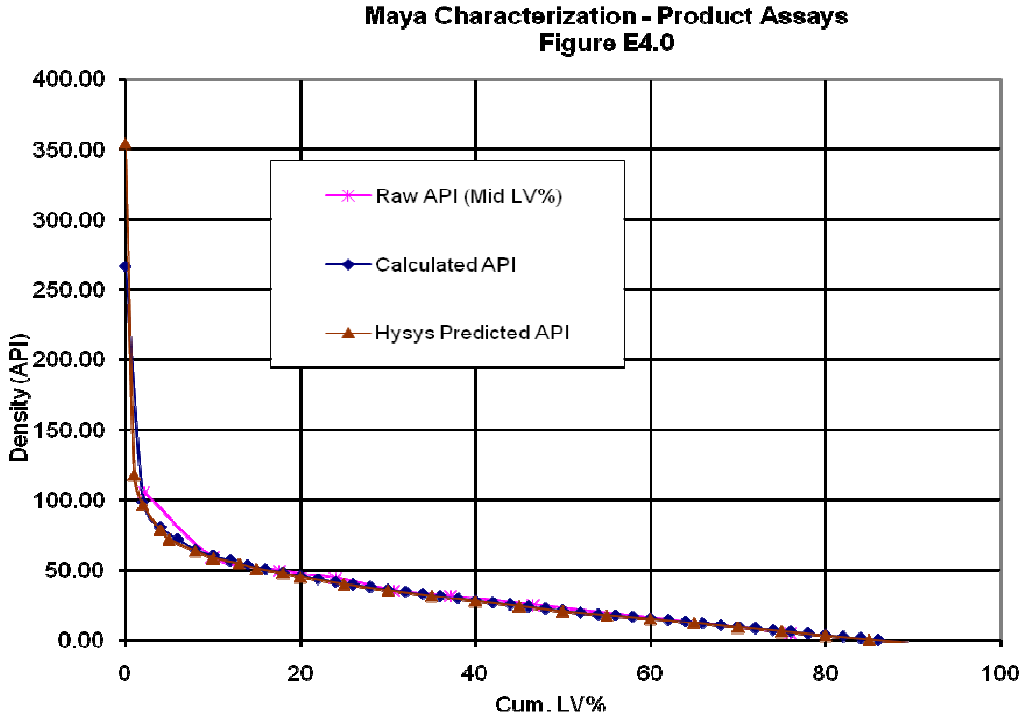

Figure E4.0 – Maya Characterization – Product Assays – Density vs. Cumulative LV%

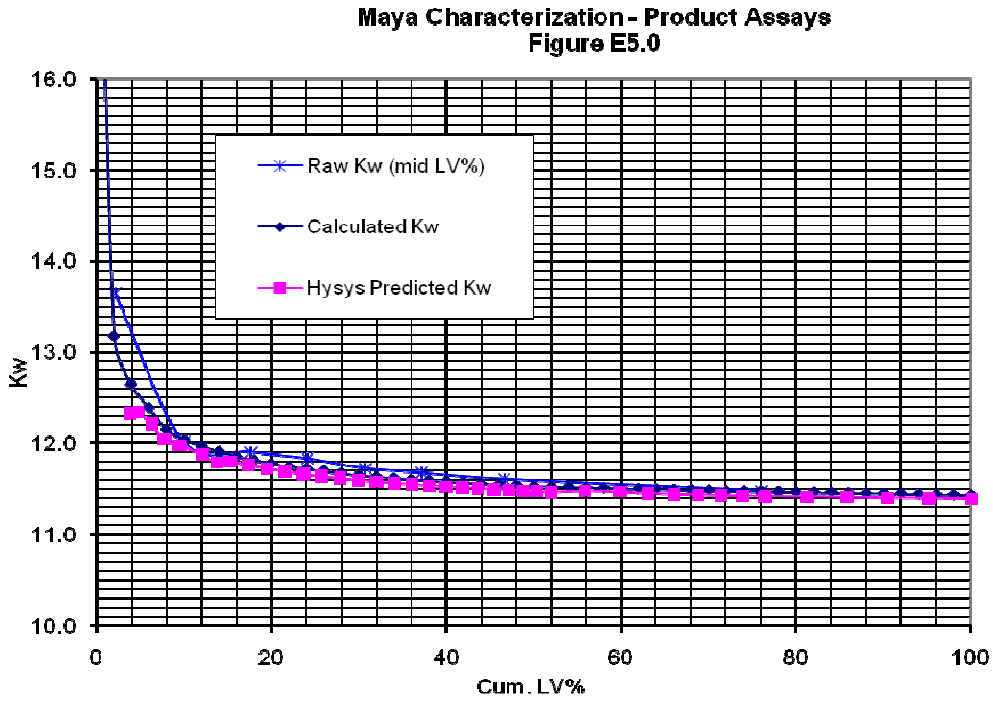

Figure E5.0 – Maya Characterization – Product Assays – Kw vs. Cumulative LV%

4.4.4 Conclusions for Maya Crude

- The adjusted CAL II TBP assays for the distillate and residue cuts is entered into HYSYS.
- The adjusted gravity distribution shown in Figure D3.0 is entered into HYSYS to generate consistent property data, as outlined here.
- Viscosity assays at 104^{o}F and 212^{o}F are entered into HYSYS based on the best fit lines shown in Figure D9.1.

4.5. Thermodynamic Package

When setting up the simulation, a great deal of attention should be paid to selection of thermodynamic package and the limitation of operating envelope in which one package can predict the simulation results. As far as crude distillation unit, the most widely used thermodynamic package in HYSYS is Peng-Robinson (PR). This package was used for the simulation of the crude distillation unit. However, this package does not produce accurate results for the vacuum section and hence the BK-10 thermodynamic package was used to simulate the vacuum section. Components of the vacuum tower that utilized the BK-10 thermo package are built in a sub-flowsheet and the rest of the process is simulated in the main flow sheet using PR thermodynamic package. The result of the simulation using these thermodynamic packages have been checked and benchmarked against actual operational data and satisfactory results have been achieved.

The Peng-Robinson Equation of State (EOS) uses binary interaction to tune the model to experimental data. The semi-theoretical basis for these factors is that they account for shape and size differences between components but they are effectively fudge factors used to tune the model to experimental data. There are two interaction coefficients for each pair of components in the mixture; the assumption is made that these interaction coefficients are not composition or temperature dependent though in practice they are. HYSYS contains a library of binary interactions coefficients. As the values used are often proprietary, different programs using the same EOS can give different Vapor/Liquid Equilibria (VLE). Discrepancies between programs may also be due to differences in the components mixing rules used. Interaction coefficients are close to unity for large non-polar, binary pairs such as alkanes, but deviate strongly if one or both of the components is small or polar, or both. Methane, Hydrogen, Nitrogen, Carbon Dioxide and Hydrogen Sulfide all fall into this category. Since the library binary interaction coefficients must cover the full range of mixtures, pressures and temperatures to which the simulation may be applied, the values may not be the best available for a specific system.

Binary interaction coefficients are calculated by regression analysis of the experimental data. HYSYS also has the capability to develop sets of binary interaction coefficients from experimental data.

4.6. Process Description

The process description entailed here only covers the desalting operation as per scope of this study. For better understanding of the process description, refer to Process Flow Diagrams in Appendix A.

Crude from the storage tanks is pumped through charge pumps P-1001A/B/C and goes through a number of heat exchangers in the pre-heat train to absorb the heat from hot products and the pump-around streams to elevate the temperature of the crude to the required temperature for desalting operation. Preheated crude will then enter the 1st stage desalter V-1001 and subsequently goes through to the 2nd stage desalter V-1002 for the salt content to be reduced to 1 PTB at the outlet of the 2nd stage desalter. The desalted crude will then go through the hot preheat train to be further heated against pump-around streams and VTB product to reach the required temperature before being fed to the pre-flash column C-1001.

In the desalting operation, the main supply of wash water is the Stripped Sour Water (SSW) coming from the Sour Water Treatment Unit. The SSW has traces of hydrocarbon and is rich in phenols. Using the SSW as wash water will allow the phenols to get reabsorbed in the crude oil before disposing of the wash water. The idea is to maximize use of the SSW in the desalting operation in order to minimize brine treatment and hence minimize any potential environmental impact. Some 300 USGPM of SSW is available in the plant and hence the idea is to use it as wash water for the desalting operation. The other source of water, which also contains phenols, is 25 USGPM of condensate coming from vacuum tower barometric condenser. Therefore 325 USGPM of water is available as wash water for the desalting operation.

Stripped sour water will go through wash water pumps P-1020A/B. Vacuum Steam Condensate will also be available for wash water and supplied to the discharge of wash water pumps and then the combined water will pass through the shell side of the wash water/brine exchangers E-1020A/B/C. The wash water is heated from about 100ºF to 236ºF through E-1020A/B/C and then subsequently through the wash water steam heater E-1021, raising the wash water temperature to about 373ºF by control on High Pressure (HP) steam supply from the header. The flow of wash water through the wash water steam heater can be adjusted by means of a bypass control valve.

In normal operation mode, the hot wash water from the outlet of E-1021 will be split and half of the flow will be fed to the crude stream just before going through the 1st stage mixing valve. The other half of the wash water flow is injected to the crude stream coming out of the 1st stage desalter and going through the 2nd stage mixing valve. The wash water and crude are mixed through the mixing valves and emulsified into fine droplets to be effectively demulsified in the desalter.

The desalters use electrostatic DC field to polarize the water droplets to increase the coalescence and hence the efficiency of the desalter. By removing the water from the crude, the crude is stripped of salts which are dissolved in the water. The brine will go to the bottom of the desalters and the crude will leave the desalter from the top. The brine streams from 1st and 2nd stage desalters will flow under desalter level control and will join together before going through the tube side of the wash water and brine exchanger E-1020A/B/C to be cooled down to 130ºF. The brine exit temperature is

determined by the constraints in the plant and is not allowed to be higher than 130^{o}F for safety reasons. The brine effluent will then leave the battery limit to go to the oily water sewer.

Desalter water can also be run in recycle mode. This will be done particularly when the SSW is in short supply. In this mode about 150 USGPM of SSW will be injected by pump P-1023 upstream of the 2nd stage desalter mixing valve through exchangers E-1021A/B/C and E-1021 and wash water from bottom of 2nd stage desalter will be injected by desalter recycle pump P-1023 to upstream of the 1st stage desalter mixing valve. The 2nd stage desalter will have a 2nd stage desalter mud wash pump P-1022 for mud washing.

4.7. Process Flow Diagrams (PFDs)

The Process Flow Diagrams are developed for better understanding of the process. The clouds indicate changes as part of the revamp project. Unclouded parts indicate unchanged existing facilities. The PFDs are presented in the Appendix A.

4.8. Heat and Material Balance (H&MB)

The result of simulation is a full H&MB for the crude distillation unit and is presented below in the next few pages. The H&MB contains the cold and hot preheat train streams, as well as the desalting unit streams. As discussed earlier, HYSYS cannot be used to produce a salt balance for the desalting operation. Therefore, Excel spreadsheet has been used to prepare Table 4.8.2a and Table 4.8.2b to present the salt and water balance for different streams of the desalting unit. For simulation of brine or salty streams in HYSYS, pure water assumption has been made. The energy or heat balance still holds for the salty water or brine streams as far as HYSYS simulation.

Table 4.8.1a: H&MB for CDU – Streams 2, 3, 4, 5, 6 and 7

Stream Name ***Stream Description*** ***Phase***		**2** **FEED** **Liquid**	**3** **CRUDE** **Liquid**	**4** **CRUDE** **Liquid**	**5** **CRUDE** **Liquid**	**6** **CRUDE** **Liquid**	**7** **CRUDE** **Liquid**
Total Stream Properties							
Vapour Fraction		0.00	0.00	0.00	0.00	0.00	0.00
Temperature	F	55.0	56.1	61.2	90.3	158.7	167.4
Pressure	psia	37.7	421.5	399.9	380.5	355.0	339.7
Molar Flow	lbmol/hr	3774.2	3774.2	3774.2	3774.2	3774.2	3774.2
Mass Flow	lb/hr	927806.7	927806.7	927806.7	927806.7	927806.7	927806.7
Std. Ideal Liquid Volume Flow	barrel/day	70001	70001	70001	70001	70001	70001
Molecular Weight		245.8	245.8	245.8	245.8	245.8	245.8
Heat Flow	Btu/hr	-8.7860E+08	-8.7706E+08	-8.7412E+08	-8.6273E+08	-8.3384E+08	-8.3000E+08
Molar Enthalpy	Btu/lbmole	-232791	-232381	-231605	-228585	-220931	-219912
Mass Heat Capacity	Btu/lb-F	0.408	0.407	0.414	0.434	0.479	0.485
Mass Density	lb/ft3	56.80	57.04	56.99	56.25	54.54	54.30
Watson K		11.312	11.312	11.312	11.312	11.312	11.312
Vapor Phase Properties							
Molar Flow	lbmol/hr						
Mass Flow	lb/hr						
Heat Flow	Btu/hr						
Actual Volume Flow	ft3/hr						
Mass Density	lb/ft3						
Compressibility							
Thermal Conductivity	Btu/hr-ft-F						
Viscosity	cP						
Molecular Weight							
Liquid Phase Properties							
Molar Flow	lbmol/hr	3774.2	3774.2	3774.2	3774.2	3774.2	3774.2
Mass Flow	lb/hr	927806.7	927806.7	927806.7	927806.7	927806.7	927806.7
Molecular Weight		245.8	245.8	245.8	245.8	245.8	245.8
Heat Flow	Btu/hr	-8.7860E+08	-8.7706E+08	-8.7412E+08	-8.6273E+08	-8.3384E+08	-8.3000E+08
Mass Heat Capacity	Btu/lb-F	0.408	0.407	0.414	0.434	0.479	0.485
Std. Ideal Liquid Volume Flow	barrel/day	70001	70001	70001	70001	70001	70001
Mass Density	lb/ft3	56.80	57.04	56.99	56.25	54.54	54.30
Thermal Conductivity	Btu/hr-ft-F	0.09	0.09	0.09	0.08	0.08	0.08
Viscosity	cP	83.00	80.00	68.00	28.00	7.80	6.80
Surface Tension	dyne/cm	74.21	74.10	30.50	29.24	26.36	25.97
Actual Volume Flow	ft3/hr	16335.7	16266.5	16280.3	16494.3	17012.8	17085.4
Aqueous Phase Properties							
Molar Flow	lbmol/hr						
Mass Flow	lb/hr						
Std. Ideal Liquid Volume Flow	barrel/day						
Heat Flow	Btu/hr						
Thermal Conductivity	Btu/hr-ft-F						
Viscosity	cP						
Surface Tension	dyne/cm						

Table 4.8.1b: H&MB for CDU – Streams 8, 8A, 8B, 9A, 9B and 10A

Stream Name ***Stream Description*** ***Phase***		**8** **CRUDE** **Liquid**	**8A** **CRUDE** **Liquid**	**8B** **CRUDE** **Liquid**	**9A** **CRUDE** **Liquid**	**9B** **CRUDE** **Liquid**	**10A** **CRUDE** **Liquid**
Total Stream Properties							
Vapour Fraction		0.00	0.00	0.00	0.00	0.00	0.00
Temperature	F	215.8	215.8	215.8	215.9	215.9	266.2
Pressure	psia	317.7	317.7	317.7	291.6	291.1	281.6
Molar Flow	lbmol/hr	3774.2	1924.8	1849.3	1924.8	1849.3	1924.8
Mass Flow	lb/hr	927806.7	473181.4	454625.3	473181.4	454625.3	473181.4
Std. Ideal Liquid Volume Flow	barrel/day	70001	35701	34301	35701	34301	35701
Molecular Weight		245.8	245.8	245.8	245.8	245.8	245.8
Heat Flow	Btu/hr	-8.0766E+08	-4.1191E+08	-3.9575E+08	-4.1191E+08	-3.9575E+08	-3.9935E+08
Molar Enthalpy	Btu/lbmole	-213994	-213994	-213994	-213994	-213994	-207470
Mass Heat Capacity	Btu/lb-F	0.514	0.514	0.514	0.515	0.515	0.544
Mass Density	lb/ft3	53.05	53.05	53.05	53.02	53.02	51.70
Watson K		11.312	11.312	11.312	11.312	11.312	11.312
Vapor Phase Properties							
Molar Flow	lbmol/hr						
Mass Flow	lb/hr						
Heat Flow	Btu/hr						
Actual Volume Flow	ft3/hr						
Mass Density	lb/ft3						
Compressibility							
Thermal Conductivity	Btu/hr-ft-F						
Viscosity	cP						
Molecular Weight							
Liquid Phase Properties							
Molar Flow	lbmol/hr	3774.2	1924.8	1849.3	1924.8	1849.3	1924.8
Mass Flow	lb/hr	927806.7	473181.4	454625.3	473181.4	454625.3	473181.4
Molecular Weight		245.8	245.8	245.8	245.8	245.8	245.8
Heat Flow	Btu/hr	-8.0766E+08	-4.1191E+08	-3.9575E+08	-4.1191E+08	-3.9575E+08	-3.9935E+08
Mass Heat Capacity	Btu/lb-F	0.514	0.514	0.514	0.515	0.515	0.544
Std. Ideal Liquid Volume Flow	barrel/day	70001	35701	34301	35701	34301	35701
Mass Density	lb/ft3	53.05	53.05	53.05	53.02	53.02	51.70
Thermal Conductivity	Btu/hr-ft-F	0.07	0.07	0.07	0.07	0.07	0.07
Viscosity	cP	3.90	2.04	3.90	3.90	3.90	2.40
Surface Tension	dyne/cm	23.79	23.79	23.79	23.78	23.78	21.50
Actual Volume Flow	ft3/hr	17489.5	8919.7	8569.9	8923.9	8574.0	9152.2
Aqueous Phase Properties							
Molar Flow	lbmol/hr						
Mass Flow	lb/hr						
Std. Ideal Liquid Volume Flow	barrel/day						
Heat Flow	Btu/hr						
Thermal Conductivity	Btu/hr-ft-F						
Viscosity	cP						
Surface Tension	dyne/cm						

Table 4.8.1c: H&MB for CDU – Streams 10B, 10, 111, 112, 113 and 118

Stream Name ***Stream Description*** ***Phase***		**10B** **CRUDE** **Liquid**	**10** **CRUDE** **Liquid**	**111** **NAPHTHA** **Liquid**	**112** **NAPHTHA** **Liquid**	**113** **NAPHTHA** **Liquid**	**118** **KERO.** **Liquid**
Total Stream Properties							
Vapour Fraction		0.00	0.00	0.00	0.00	0.00	0.00
Temperature	F	266.1	266.2	339.2	244.0	219.2	395.3
Pressure	psia	281.6	281.6	220.9	210.9	200.9	222.1
Molar Flow	lbmol/hr	1849.3	3774.2	2814.5	2814.5	2814.5	636.2
Mass Flow	lb/hr	454625.3	927806.7	409399.0	409399.0	409399.0	117952.1
Std. Ideal Liquid Volume Flow	barrel/day	34301	70001	35300	35300	35300	9660
Molecular Weight		245.8	245.8	145.5	145.5	145.5	185.4
Heat Flow	Btu/hr	-3.8370E+08	-7.8305E+08	-3.2397E+08	-3.4712E+08	-3.5285E+08	-8.9714E+07
Molar Enthalpy	Btu/lbmole	-207478	-207474	-115105	-123332	-125368	-141017
Mass Heat Capacity	Btu/lb-F	0.544	0.544	0.618	0.569	0.556	0.630
Mass Density	lb/ft3	51.70	51.70	41.68	44.44	45.11	43.34
Watson K		11.312	11.312	11.684	11.684	11.684	11.581
Vapor Phase Properties							
Molar Flow	lbmol/hr						
Mass Flow	lb/hr						
Heat Flow	Btu/hr						
Actual Volume Flow	ft3/hr						
Mass Density	lb/ft3						
Compressibility							
Thermal Conductivity	Btu/hr-ft-F						
Viscosity	cP						
Molecular Weight							
Liquid Phase Properties							
Molar Flow	lbmol/hr	1849.3	3774.2	2814.5	2814.5	2814.5	636.2
Mass Flow	lb/hr	454625.3	927806.7	409399.0	409399.0	409399.0	117952.1
Molecular Weight		245.8	245.8	145.5	145.5	145.5	185.4
Heat Flow	Btu/hr	-3.8370E+08	-7.8305E+08	-3.2397E+08	-3.4712E+08	-3.5285E+08	-8.9714E+07
Mass Heat Capacity	Btu/lb-F	0.544	0.544	0.618	0.569	0.556	0.630
Std. Ideal Liquid Volume Flow	barrel/day	34301	70001	35300	35300	35300	9660
Mass Density	lb/ft3	51.70	51.70	41.68	44.44	45.11	43.34
Thermal Conductivity	Btu/hr-ft-F	0.07	0.07	0.06	0.07	0.07	0.06
Viscosity	cP	2.40	2.40	0.05	0.10	0.12	0.05
Surface Tension	dyne/cm	21.51	21.50	12.88	17.47	18.70	13.90
Actual Volume Flow	ft3/hr	8793.1	17945.3	9822.3	9213.2	9076.0	2721.9
Aqueous Phase Properties							
Molar Flow	lbmol/hr						
Mass Flow	lb/hr						
Std. Ideal Liquid Volume Flow	barrel/day						
Heat Flow	Btu/hr						
Thermal Conductivity	Btu/hr-ft-F						
Viscosity	cP						
Surface Tension	dyne/cm						

Table 4.8.1d: H&MB for CDU – Streams 119, 128, 129, 208, 209 and 220

Stream Name		**119**	**128**	**129**	**208**	**209**	**220**
Stream Description		**KERO.**	**DIESEL**	**DIESEL**	**LVGO P/A**	**LVGO P/A**	**HVGO P/A**
Phase		**Liquid**	**Liquid**	**Liquid**	**Liquid**	**Liquid**	**Liquid**
Total Stream Properties							
Vapour Fraction		0.00	0.00	0.00	0.00	0.00	0.00
Temperature	F	231.7	458.7	160.0	243.6	164.1	223.7
Pressure	psia	212.1	222.8	212.8	200.3	190.3	180.4
Molar Flow	lbmol/hr	636.2	94.5	94.5	327.7	327.7	831.1
Mass Flow	lb/hr	117952.1	22465.7	22465.7	70436.8	70436.8	278991.3
Std. Ideal Liquid Volume Flow	barrel/day	9660	1765	1765	5624	5624	20654
Molecular Weight		185.4	237.7	237.7	215.0	215.0	335.7
Heat Flow	Btu/hr	-1.0111E+08	-1.6182E+07	-2.0027E+07	-5.9666E+07	-6.2596E+07	-2.3911E+08
Molar Enthalpy	Btu/lbmole	-158932	-171184	-211862	-182091	-191035	-287690
Mass Heat Capacity	Btu/lb-F	0.548	0.646	0.490	0.546	0.499	0.510
Mass Density	lb/ft3	47.63	44.29	51.62	48.71	50.60	53.48
Watson K		11.581	11.538	11.538	11.546	11.546	11.502
Vapor Phase Properties							
Molar Flow	lbmol/hr						
Mass Flow	lb/hr						
Heat Flow	Btu/hr						
Actual Volume Flow	ft3/hr						
Mass Density	lb/ft3						
Compressibility							
Thermal Conductivity	Btu/hr-ft-F						
Viscosity	cP						
Molecular Weight							
Liquid Phase Properties							
Molar Flow	lbmol/hr	636.2	94.5	94.5	327.7	327.7	831.1
Mass Flow	lb/hr	117952.1	22465.7	22465.7	70436.8	70436.8	278991.3
Molecular Weight		185.4	237.7	237.7	215.0	215.0	335.7
Heat Flow	Btu/hr	-1.0111E+08	-1.6182E+07	-2.0027E+07	-5.9666E+07	-6.2596E+07	-2.3911E+08
Mass Heat Capacity	Btu/lb-F	0.548	0.646	0.490	0.546	0.499	0.510
Std. Ideal Liquid Volume Flow	barrel/day	9660	1765	1765	5624	5624	20654
Mass Density	lb/ft3	47.63	44.29	51.62	48.71	50.60	53.48
Thermal Conductivity	Btu/hr-ft-F	0.08	0.07	0.09	0.08	0.08	0.09
Viscosity	cP	0.19	0.09	0.62	0.25	0.45	1.74
Surface Tension	dyne/cm	21.35	14.31	63.96	22.15	25.79	26.93
Actual Volume Flow	ft3/hr	2476.3	507.3	435.2	1446.0	1392.0	5217.2
Aqueous Phase Properties							
Molar Flow	lbmol/hr						
Mass Flow	lb/hr						
Std. Ideal Liquid Volume Flow	barrel/day						
Heat Flow	Btu/hr						
Thermal Conductivity	Btu/hr-ft-F						
Viscosity	cP						
Surface Tension	dyne/cm						

Table 4.8.1e: H&MB for CDU – Streams 232 and 240

Stream Name		**232**	**240**				
Stream Description		**VTB**	**VTB**				
Phase		**Liquid**	**Liquid**				
Total Stream Properties							
Vapour Fraction		0.00	0.00				
Temperature	F	405.8	420.6				
Pressure	psia	180.5	180.5				
Molar Flow	lbmol/hr	358.8	395.0				
Mass Flow	lb/hr	196115.9	215886.9				
Std. Ideal Liquid Volume Flow	barrel/day	12934	14238				
Molecular Weight		546.6	546.6				
Heat Flow	Btu/hr	-1.5322E+08	-1.6681E+08				
Molar Enthalpy	Btu/lbmole	-427045	-422349				
Mass Heat Capacity	Btu/lb-F	0.578	0.586				
Mass Density	lb/ft3	56.91	56.59				
Watson K		11.435	11.435				
Vapor Phase Properties							
Molar Flow	lbmol/hr						
Mass Flow	lb/hr						
Heat Flow	Btu/hr						
Actual Volume Flow	ft3/hr						
Mass Density	lb/ft3						
Compressibility							
Thermal Conductivity	Btu/hr-ft-F						
Viscosity	cP						
Molecular Weight							
Liquid Phase Properties							
Molar Flow	lbmol/hr	358.8	395.0				
Mass Flow	lb/hr	196115.9	215886.9				
Molecular Weight		546.6	546.6				
Heat Flow	Btu/hr	-1.5322E+08	-1.6681E+08				
Mass Heat Capacity	Btu/lb-F	0.578	0.586				
Std. Ideal Liquid Volume Flow	barrel/day	12934	14238				
Mass Density	lb/ft3	56.91	56.59				
Thermal Conductivity	Btu/hr-ft-F	0.09	0.09				
Viscosity	cP	13.32	12.12				
Surface Tension	dyne/cm	22.83	22.50				
Actual Volume Flow	ft3/hr	3446.3	3814.8				
Aqueous Phase Properties							
Molar Flow	lbmol/hr						
Mass Flow	lb/hr						
Std. Ideal Liquid Volume Flow	barrel/day						
Heat Flow	Btu/hr						
Thermal Conductivity	Btu/hr-ft-F						
Viscosity	cP						
Surface Tension	dyne/cm						

Table 4.8.1f: H&MB for CDU – Streams 129, 208, 209, 220, 232 and 240

Stream Name		**129**	**208**	**209**	**220**	**232**	**240**
Stream Description		**DIESEL**	**LVGO P/A**	**LVGO P/A**	**HVGO P/A**	**VTB**	**VTB**
Phase		**Liquid**	**Liquid**	**Liquid**	**Liquid**	**Liquid**	**Liquid**
Total Stream Properties							
Vapour Fraction		0.00	0.00	0.00	0.00	0.00	0.00
Temperature	F	160.0	243.6	164.1	223.7	405.8	420.6
Pressure	psia	212.8	200.3	190.3	180.4	180.5	180.5
Molar Flow	lbmol/hr	94.5	327.7	327.7	831.1	358.8	395.0
Mass Flow	lb/hr	22465.7	70436.8	70436.8	278991.3	196115.9	215886.9
Std. Ideal Liquid Volume Flow	barrel/day	1765	5624	5624	20654	12934	14238
Molecular Weight		237.7	215.0	215.0	335.7	546.6	546.6
Heat Flow	Btu/hr	-2.0027E+07	-5.9666E+07	-6.2596E+07	-2.3911E+08	-1.5322E+08	-1.6681E+08
Molar Enthalpy	Btu/lbmole	-211862	-182091	-191035	-287690	-427045	-422349
Mass Heat Capacity	Btu/lb-F	0.490	0.546	0.499	0.510	0.578	0.586
Mass Density	lb/ft3	51.62	48.71	50.60	53.48	56.91	56.59
Watson K		11.538	11.546	11.546	11.502	11.435	11.435
Vapor Phase Properties							
Molar Flow	lbmol/hr						
Mass Flow	lb/hr						
Heat Flow	Btu/hr						
Actual Volume Flow	ft3/hr						
Mass Density	lb/ft3						
Compressibility							
Thermal Conductivity	Btu/hr-ft-F						
Viscosity	cP						
Molecular Weight							
Liquid Phase Properties							
Molar Flow	lbmol/hr	94.5	327.7	327.7	831.1	358.8	395.0
Mass Flow	lb/hr	22465.7	70436.8	70436.8	278991.3	196115.9	215886.9
Molecular Weight		237.7	215.0	215.0	335.7	546.6	546.6
Heat Flow	Btu/hr	-2.0027E+07	-5.9666E+07	-6.2596E+07	-2.3911E+08	-1.5322E+08	-1.6681E+08
Mass Heat Capacity	Btu/lb-F	0.490	0.546	0.499	0.510	0.578	0.586
Std. Ideal Liquid Volume Flow	barrel/day	1765	5624	5624	20654	12934	14238
Mass Density	lb/ft3	51.62	48.71	50.60	53.48	56.91	56.59
Thermal Conductivity	Btu/hr-ft-F	0.09	0.08	0.08	0.09	0.09	0.09
Viscosity	cP	0.62	0.25	0.45	1.74	13.32	12.12
Surface Tension	dyne/cm	63.96	22.15	25.79	26.93	22.83	22.50
Actual Volume Flow	ft3/hr	435.2	1446.0	1392.0	5217.2	3446.3	3814.8
Aqueous Phase Properties							
Molar Flow	lbmol/hr						
Mass Flow	lb/hr						
Std. Ideal Liquid Volume Flow	barrel/day						
Heat Flow	Btu/hr						
Thermal Conductivity	Btu/hr-ft-F						
Viscosity	cP						
Surface Tension	dyne/cm						

Table 4.8.1g: H&MB for CDU – Streams 11, 12, 14, 70, 70A and 70B

Stream Name		**11**	**12**	**14**	**70**	**70A**	**70B**
Stream Description		**CRUDE WW**	**CRUDE WW**	**DESALTED CRUDE**	**WASH WATER**	**WASH WATER**	**WASH WATER**
Phase		**Liquid**	**Liquid**	**Liquid**	**Liquid**	**Liquid**	**Liquid**
Total Stream Properties							
Vapour Fraction		0.00	0.00	0.00	0.00	0.00	0.00
Temperature	F	269.9	270.0	272.1	100.0	100.0	101.4
Pressure	psia	281.6	263.6	243.6	114.7	29.7	370.7
Molar Flow	lbmol/hr	8201.4	8201.4	4152.9	8321.5	8321.5	8321.5
Mass Flow	lb/hr	1008692.5	1008692.5	936887.5	149913.5	149913.5	149913.5
Std. Ideal Liquid Volume Flow	barrel/day	75573	75573	70668	10286	10286	10286
Molecular Weight		123.0	123.0	225.6	18.0	18.0	18.0
Heat Flow	Btu/hr	-1.3089E+09	-1.3089E+09	-8.2592E+08	-1.0163E+09	-1.0163E+09	-1.0161E+09
Molar Enthalpy	Btu/lbmole	-159595	-159595	-198876	-122127	-122127	-122103
Mass Heat Capacity	Btu/lb-F	0.586	0.586	0.553	0.998	0.998	0.998
Mass Density	lb/ft3	52.04	52.02	51.55	62.30	62.28	62.29
Watson K		11.312	11.312	11.312			
Vapor Phase Properties							
Molar Flow	lbmol/hr						
Mass Flow	lb/hr						
Heat Flow	Btu/hr						
Actual Volume Flow	ft3/hr						
Mass Density	lb/ft3						
Compressibility							
Thermal Conductivity	Btu/hr-ft-F						
Viscosity	cP						
Molecular Weight							
Liquid Phase Properties							
Molar Flow	lbmol/hr	3857.0	3857.2	3868.4			
Mass Flow	lb/hr	930428.6	930432.1	931763.2			
Molecular Weight		241.2	241.2	240.9			
Heat Flow	Btu/hr	-7.9172E+08	-7.9175E+08	-7.9207E+08			
Mass Heat Capacity	Btu/lb-F	0.549	0.549	0.550			
Std. Ideal Liquid Volume Flow	barrel/day	70203	70203	70316			
Mass Density	lb/ft3	51.63	51.61	51.52			
Thermal Conductivity	Btu/hr-ft-F	0.07	0.07	0.07			
Viscosity	cP	1.29	1.29	1.27			
Surface Tension	dyne/cm	18.62	18.62	18.54			
Actual Volume Flow	ft3/hr	18021.9	18028.4	18084.2			
Aqueous Phase Properties							
Molar Flow	lbmol/hr	4344.3	4344.2	284.4	8321.5	8321.5	8321.5
Mass Flow	lb/hr	78263.9	78260.4	5124.3	149913.5	149913.5	149913.5
Std. Ideal Liquid Volume Flow	barrel/day	5369.8	5369.5	351.6	10285.7	10285.7	10285.7
Heat Flow	Btu/hr	-5.1719E+08	-5.1716E+08	-3.3851E+07	-1.0163E+09	-1.0163E+09	-1.0161E+09
Thermal Conductivity	Btu/hr-ft-F	0	0	0	0	0	0
Viscosity	cP	0.207	0.207	0.205	0.680	0.680	0.670
Surface Tension	dyne/cm	52.324	52.317	52.077	69.881	69.881	69.750

Table 4.8.1h: H&MB for CDU – Streams 71, 72, 73, 74, 75 and 78

Stream Name		**71**	**72**	**73**	**74**	**75**	**78**
Stream Description		**VAC. COND.**	**WASH WATER**	**WASH WATER**	**WASH WATER**	**WASH WATER**	**WASH WATER**
Phase		**Liquid**	**Liquid**	**Liquid**	**Liquid**	**Liquid**	**Liquid**
Total Stream Properties							
Vapour Fraction		0.00	0.00	0.00	0.00	0.00	0.00
Temperature	F	102.3	101.4	236.1	236.1	236.1	373.6
Pressure	psia	328.7	328.7	318.7	318.7	318.7	308.7
Molar Flow	lbmol/hr	532.9	8854.4	8854.4	3099.0	5755.4	3099.0
Mass Flow	lb/hr	11858.2	161771.6	161771.6	56620.1	105151.6	56620.1
Std. Ideal Liquid Volume Flow	barrel/day	857	11143	11143	3900	7243	3900
Molecular Weight		22.3	18.3	18.3	18.3	18.3	18.3
Heat Flow	Btu/hr	-6.5324E+07	-1.0814E+09	-1.0597E+09	-3.7090E+08	-6.8882E+08	-3.6290E+08
Molar Enthalpy	Btu/lbmole	-122587	-122132	-119682	-119682	-119682	-117100
Mass Heat Capacity	Btu/lb-F	0.887	0.990	1.004	1.004	1.004	1.056
Mass Density	lb/ft3	58.78	62.02	58.26	58.26	58.26	53.77
Watson K		11.646	11.646	11.646	11.646	11.646	11.646
Vapor Phase Properties							
Molar Flow	lbmol/hr						
Mass Flow	lb/hr						
Heat Flow	Btu/hr						
Actual Volume Flow	ft3/hr						
Mass Density	lb/ft3						
Compressibility							
Thermal Conductivity	Btu/hr-ft-F						
Viscosity	cP						
Molecular Weight							
Liquid Phase Properties							
Molar Flow	lbmol/hr	17.1	17.1	17.3	6.0	11.2	6.4
Mass Flow	lb/hr	2566.4	2564.5	2567.5	898.6	1668.9	904.8
Molecular Weight		149.7	150.0	148.7	148.7	148.7	141.7
Heat Flow	Btu/hr	-2.3658E+06	-2.3656E+06	-2.2053E+06	-7.7186E+05	-1.4335E+06	-7.3856E+05
Mass Heat Capacity	Btu/lb-F	0.484	0.483	0.563	0.563	0.563	0.636
Std. Ideal Liquid Volume Flow	barrel/day	219	219	219	77	143	77
Mass Density	lb/ft3	48.86	48.86	45.38	45.38	45.38	41.55
Thermal Conductivity	Btu/hr-ft-F	0.08	0.08	0.07	0.07	0.07	0.07
Viscosity	cP	0.29	0.29	0.12	0.12	0.12	0.05
Surface Tension	dyne/cm	24.67	24.77	18.31	18.31	18.31	13.29
Actual Volume Flow	ft3/hr	52.5	52.5	56.6	19.8	36.8	21.8
Aqueous Phase Properties							
Molar Flow	lbmol/hr	515.7	8837.3	8837.2	3093.0	5744.2	3092.7
Mass Flow	lb/hr	9291.8	159207.1	159204.1	55721.4	103482.6	55715.2
Std. Ideal Liquid Volume Flow	barrel/day	637.6	10923.4	10923.2	3823.1	7100.1	3822.7
Heat Flow	Btu/hr	-6.2958E+07	-1.0791E+09	-1.0575E+09	-3.7013E+08	-6.8739E+08	-3.6216E+08
Thermal Conductivity	Btu/hr-ft-F	0	0	0	0	0	0
Viscosity	cP	0.664	0.670	0.244	0.244	0.244	0.141
Surface Tension	dyne/cm	69.655	69.743	56.035	56.035	56.035	40.109

Table 4.8.1i: H&MB for CDU – Streams 79, 82, 83, 84, 85 and 86

Stream Name		**79**	**82**	**83**	**84**	**85**	**86**
Stream Description		**WASH WATER**	**WASH WATER**	**WASH WATER**	**WASH WATER**	**CRUDE**	**CRUDE WW**
Phase		**Liquid**	**Liquid**	**Liquid**	**Liquid**	**Liquid**	**Liquid**
Total Stream Properties							
Vapour Fraction		0.00	0.00	0.00	0.00	0.00	0.00
Temperature	F	236.1	285.0	285.0	285.0	270.0	272.1
Pressure	psia	308.7	308.7	281.6	263.6	263.6	263.6
Molar Flow	lbmol/hr	5755.4	8854.4	4427.2	4427.2	3857.2	8284.4
Mass Flow	lb/hr	105151.6	161771.6	80885.8	80885.8	930432.1	1011317.9
Std. Ideal Liquid Volume Flow	barrel/day	7243	11143	5571	5571	70203	75774
Molecular Weight		18.3	18.3	18.3	18.3	241.2	122.1
Heat Flow	Btu/hr	-6.8882E+08	-1.0517E+09	-5.2586E+08	-5.2586E+08	-7.9175E+08	-1.3176E+09
Molar Enthalpy	Btu/lbmole	-119682	-118778	-118778	-118778	-205261	-159045
Mass Heat Capacity	Btu/lb-F	1.004	1.017	1.017	1.017	0.549	0.587
Mass Density	lb/ft3	58.26	56.76	56.75	56.75	51.61	51.96
Watson K		11.646	11.646	11.646	11.646	11.312	11.312
Vapor Phase Properties							
Molar Flow	lbmol/hr						
Mass Flow	lb/hr						
Heat Flow	Btu/hr						
Actual Volume Flow	ft3/hr						
Mass Density	lb/ft3						
Compressibility							
Thermal Conductivity	Btu/hr-ft-F						
Viscosity	cP						
Molecular Weight							
Liquid Phase Properties							
Molar Flow	lbmol/hr	11.2	17.5	8.7	8.7	3857.2	3868.2
Mass Flow	lb/hr	1668.9	2571.0	1285.5	1285.5	930432.1	931759.3
Molecular Weight		148.7	147.3	147.3	147.3	241.2	240.9
Heat Flow	Btu/hr	-1.4335E+06	-2.1562E+06	-1.0782E+06	-1.0783E+06	-7.9175E+08	-7.9204E+08
Mass Heat Capacity	Btu/lb-F	0.563	0.589	0.589	0.589	0.549	0.550
Std. Ideal Liquid Volume Flow	barrel/day	143	220	110	110	70203	70316
Mass Density	lb/ft3	45.37	44.05	44.02	44.00	51.61	51.54
Thermal Conductivity	Btu/hr-ft-F	0.07	0.07	0.07	0.07	0.07	0.07
Viscosity	cP	0.12	0.09	0.09	0.09	1.29	1.28
Surface Tension	dyne/cm	18.31	16.30	16.30	16.30	18.62	18.55
Actual Volume Flow	ft3/hr	36.8	58.4	29.2	29.2	18028.4	18076.9
Aqueous Phase Properties							
Molar Flow	lbmol/hr	5744.2	8837.0	4418.5	4418.5		4416.2
Mass Flow	lb/hr	103482.6	159200.6	79600.3	79600.3		79558.6
Std. Ideal Liquid Volume Flow	barrel/day	7100.1	10923.0	5461.5	5461.5		5458.6
Heat Flow	Btu/hr	-6.8739E+08	-1.0496E+09	-5.2478E+08	-5.2478E+08		-5.2557E+08
Thermal Conductivity	Btu/hr-ft-F	0	0	0	0		0
Viscosity	cP	0.244	0.194	0.194	0.194		0.205
Surface Tension	dyne/cm	56.035	50.626	50.626	50.626		52.085

Table 4.8.1j: H&MB for CDU – Streams 87, 88, 90, 91, 91A and 92

Stream Name		**87**	**88**	**90**	**91**	**91A**	**92**
Stream Description		**CRUDE**					
Phase		**WW Liquid**	**BRINE Liquid**	**BRINE Liquid**	**BRINE Liquid**	**BRINE Liquid**	**BRINE Liquid**
Total Stream Properties							
Vapour Fraction		0.00	0.00	0.00	0.00	0.00	0.00
Temperature	F	272.1	272.1	272.1	270.0	270.0	271.0
Pressure	psia	243.6	243.6	238.6	263.6	238.6	238.6
Molar Flow	lbmol/hr	8284.4	4131.6	4131.6	4344.2	4344.2	8475.7
Mass Flow	lb/hr	1011317.9	74430.4	74430.4	78260.4	78260.4	152690.8
Std. Ideal Liquid Volume Flow	barrel/day	75774	5107	5107	5370	5370	10476
Molecular Weight		122.1	18.0	18.0	18.0	18.0	18.0
Heat Flow	Btu/hr	-1.3176E+09	-4.9169E+08	-4.9169E+08	-5.1716E+08	-5.1716E+08	-1.0089E+09
Molar Enthalpy	Btu/lbmole	-159045	-119007	-119007	-119047	-119047	-119028
Mass Heat Capacity	Btu/lb-F	0.587	1.020	1.020	1.020	1.020	1.020
Mass Density	lb/ft3	51.94	57.41	57.41	57.48	57.48	57.45
Watson K		11.312	9.718	9.718	10.206	10.206	9.894
Vapor Phase Properties							
Molar Flow	lbmol/hr						
Mass Flow	lb/hr						
Heat Flow	Btu/hr						
Actual Volume Flow	ft3/hr						
Mass Density	lb/ft3						
Compressibility							
Thermal Conductivity	Btu/hr-ft-F						
Viscosity	cP						
Molecular Weight							
Liquid Phase Properties							
Molar Flow	lbmol/hr	3868.4					
Mass Flow	lb/hr	931763.2					
Molecular Weight		240.9					
Heat Flow	Btu/hr	-7.9207E+08					
Mass Heat Capacity	Btu/lb-F	0.550					
Std. Ideal Liquid Volume Flow	barrel/day	70316					
Mass Density	lb/ft3	51.52					
Thermal Conductivity	Btu/hr-ft-F	0.07					
Viscosity	cP	1.27					
Surface Tension	dyne/cm	18.54					
Actual Volume Flow	ft3/hr	18084.2					
Aqueous Phase Properties							
Molar Flow	lbmol/hr	4416.0	4131.6	4131.6	4344.2	4344.2	8475.7
Mass Flow	lb/hr	79554.6	74430.4	74430.4	78260.4	78260.4	152690.8
Std. Ideal Liquid Volume Flow	barrel/day	5458.3	5106.7	5106.7	5369.5	5369.5	10476.3
Heat Flow	Btu/hr	-5.2554E+08	-4.9169E+08	-4.9169E+08	-5.1716E+08	-5.1716E+08	-1.0089E+09
Thermal Conductivity	Btu/hr-ft-F	0	0	0	0	0	0
Viscosity	cP	0.205	0.205	0.205	0.207	0.207	0.206
Surface Tension	dyne/cm	52.077	52.077	52.077	52.317	52.317	52.200

Table 4.8.1k: H&MB for CDU – Streams 93, 94, 98 and 99

Stream Name		**93**	**94**	**98**	**99**
Stream Description		**BRINE**	**BRINE**	**HP STEAM**	**STEAM COND.**
Phase		**Liquid**	**Liquid**	**Vapour**	**Liquid**
Total Stream Properties					
Vapour Fraction		0.00	0.00	1.00	0.00
Temperature	F	130.0	130.0	520.0	399.7
Pressure	psia	228.6	25.0	254.7	244.7
Molar Flow	lbmol/hr	8475.7	8475.7	493.5	493.5
Mass Flow	lb/hr	152690.8	152690.8	8890.7	8890.7
Std. Ideal Liquid Volume Flow	barrel/day	10476	10476	610	610
Molecular Weight		18.0	18.0	18.0	18.0
Heat Flow	Btu/hr	-1.0305E+09	-1.0305E+09	-4.9542E+07	-5.7543E+07
Molar Enthalpy	Btu/lbmole	-121587	-121587	-100386	-116598
Mass Heat Capacity	Btu/lb-F	0.999	0.999	0.571	1.080
Mass Density	lb/ft3	61.51	61.48	0.46	53.02
Watson K		9.894	9.894		
Vapor Phase Properties					
Molar Flow	lbmol/hr			493.5	
Mass Flow	lb/hr			8890.7	
Heat Flow	Btu/hr			-4.9542E+07	
Actual Volume Flow	ft3/hr			19267.9	
Mass Density	lb/ft3			0.46	
Compressibility				0.95	
Thermal Conductivity	Btu/hr-ft-F			0.02	
Viscosity	cP			0.02	
Molecular Weight				18.0	
Liquid Phase Properties					
Molar Flow	lbmol/hr				
Mass Flow	lb/hr				
Molecular Weight					
Heat Flow	Btu/hr				
Mass Heat Capacity	Btu/lb-F				
Std. Ideal Liquid Volume Flow	barrel/day				
Mass Density	lb/ft3				
Thermal Conductivity	Btu/hr-ft-F				
Viscosity	cP				
Surface Tension	dyne/cm				
Actual Volume Flow	ft3/hr				
Aqueous Phase Properties					
Molar Flow	lbmol/hr	8475.7	8475.7		493.5
Mass Flow	lb/hr	152690.8	152690.8		8890.7
Std. Ideal Liquid Volume Flow	barrel/day	10476.3	10476.3		610.0
Heat Flow	Btu/hr	-1.0305E+09	-1.0305E+09		-5.7543E+07
Thermal Conductivity	Btu/hr-ft-F	0	0		0
Viscosity	cP	0.505	0.505		0.131
Surface Tension	dyne/cm	66.949	66.949		36.833

Table 4.8.1l: H&MB for CDU – Streams 14A, 14B, 14C, 15A, 15B and 15C

Stream Name *Stream Description* *Phase*		14A CRUDE Liquid	14B CRUDE Liquid	14C CRUDE Liquid	15A CRUDE Liquid	15B CRUDE Mixed	15C CRUDE Mixed
Total Stream Properties							
Vapour Fraction		0.00	0.00	0.00	0.00	0.07	0.17
Temperature	F	272.1	272.1	272.1	291.9	334.8	372.0
Pressure	psia	243.6	243.6	243.6	144.0	191.3	118.7
Molar Flow	lbmol/hr	1930.3	1134.6	1088.1	1930.3	1134.6	1088.1
Mass Flow	lb/hr	435465.3	255957.7	245464.5	435465.3	255957.7	245464.5
Std. Ideal Liquid Volume Flow	barrel/day	32846	19306	18515	32846	19306	18515
Molecular Weight		225.6	225.6	225.6	225.6	225.6	225.6
Heat Flow	Btu/hr	-3.8389E+08	-2.2564E+08	-2.1639E+08	-3.7917E+08	-2.1566E+08	-2.0030E+08
Molar Enthalpy	Btu/lbmole	-198876	-198876	-198876	-196430	-190079	-184085
Mass Heat Capacity	Btu/lb-F	0.553	0.553	0.553	0.564	0.583	0.596
Mass Density	lb/ft3	51.55	51.55	51.55	50.94	31.36	13.70
Watson K		11.312	11.312	11.312	11.312	11.312	11.312
Vapor Phase Properties							
Molar Flow	lbmol/hr					75.6	186.2
Mass Flow	lb/hr					3076.4	10340.8
Heat Flow	Btu/hr					-6.2128E+06	-1.4229E+07
Actual Volume Flow	ft3/hr					3108.4	13154.5
Mass Density	lb/ft3					0.99	0.79
Compressibility						0.92	0.94
Thermal Conductivity	Btu/hr-ft-F					0.02	0.02
Viscosity	cP					0.01	0.01
Molecular Weight						40.7	55.5
Liquid Phase Properties							
Molar Flow	lbmol/hr	1798.1	1056.9	1013.5	1809.8	1050.4	901.9
Mass Flow	lb/hr	433083.6	254557.7	244122.0	433294.5	252727.5	235123.7
Molecular Weight		240.9	240.9	240.9	239.4	240.6	260.7
Heat Flow	Btu/hr	-3.6815E+08	-2.1639E+08	-2.0752E+08	-3.6487E+08	-2.0844E+08	-1.8607E+08
Mass Heat Capacity	Btu/lb-F	0.550	0.550	0.550	0.562	0.583	0.598
Std. Ideal Liquid Volume Flow	barrel/day	32683	19210	18423	32697	18993	17502
Mass Density	lb/ft3	51.52	51.52	51.52	50.91	50.03	49.42
Thermal Conductivity	Btu/hr-ft-F	0.07	0.07	0.07	0.07	0.07	0.06
Viscosity	cP	1.27	1.27	1.27	1.15	1.01	0.99
Surface Tension	dyne/cm	18.54	18.54	18.54	17.91	17.04	15.75
Actual Volume Flow	ft3/hr	8405.5	4940.6	4738.1	8510.8	5051.5	4757.3
Aqueous Phase Properties							
Molar Flow	lbmol/hr	132.2	77.7	74.5	120.5	8.5	
Mass Flow	lb/hr	2381.8	1399.9	1342.6	2170.8	153.8	
Std. Ideal Liquid Volume Flow	barrel/day	163.4	96.1	92.1	148.9	10.6	
Heat Flow	Btu/hr	-1.5734E+07	-9.2481E+06	-8.8690E+06	-1.4296E+07	-1.0060E+06	
Thermal Conductivity	Btu/hr-ft-F	0	0	0	0	0	
Viscosity	cP	0.205	0.205	0.205	0.189	0.160	
Surface Tension	dyne/cm	52.077	52.077	52.077	49.838	44.828	

Table 4.8.1m: H&MB for CDU – Streams 16A, 16B, 16C, 17, 17A, 17B

Stream Name ***Stream Description*** ***Phase***		**16A CRUDE Mixed**	**16B CRUDE Mixed**	**16C CRUDE Mixed**	**17 CRUDE Mixed**	**17A CRUDE Mixed**	**17B CRUDE Mixed**
Total Stream Properties							
Vapour Fraction		0.08	0.15	0.19	0.14	0.14	0.14
Temperature	F	284.5	327.5	370.1	317.4	317.4	317.4
Pressure	psia	102.5	102.5	102.5	102.5	102.5	102.5
Molar Flow	lbmol/hr	1930.3	1134.6	1088.1	4152.9	2076.4	2076.4
Mass Flow	lb/hr	435465.3	255957.7	245464.5	936887.5	468443.7	468443.7
Std. Ideal Liquid Volume Flow	barrel/day	32846	19306	18515	70668	35334	35334
Molecular Weight		225.6	225.6	225.6	225.6	225.6	225.6
Heat Flow	Btu/hr	-3.7917E+08	-2.1566E+08	-2.0030E+08	-7.9512E+08	-3.9756E+08	-3.9756E+08
Molar Enthalpy	Btu/lbmole	-196430	-190079	-184085	-191461	-191461	-191461
Mass Heat Capacity	Btu/lb-F	0.557	0.574	0.593	0.569	0.569	0.569
Mass Density	lb/ft3	21.51	14.18	11.36	14.92	14.92	14.92
Watson K		11.312	11.312	11.312	11.312	11.312	11.312
Vapor Phase Properties							
Molar Flow	lbmol/hr	161.0	168.1	205.8	580.4	290.2	290.2
Mass Flow	lb/hr	6897.2	8200.3	11830.3	27170.8	13585.4	13585.4
Heat Flow	Btu/hr	-1.2793E+07	-1.3200E+07	-1.5601E+07	-4.5996E+07	-2.2998E+07	-2.2998E+07
Actual Volume Flow	ft3/hr	11897.2	13144.4	16888.2	44821.0	22410.5	22410.5
Mass Density	lb/ft3	0.58	0.62	0.70	0.61	0.61	0.61
Compressibility		0.95	0.95	0.94	0.95	0.95	0.95
Thermal Conductivity	Btu/hr-ft-F	0.02	0.02	0.02	0.02	0.02	0.02
Viscosity	cP	0.01	0.01	0.01	0.01	0.01	0.01
Molecular Weight		42.8	48.8	57.5	46.8	46.8	46.8
Liquid Phase Properties							
Molar Flow	lbmol/hr	1725.6	966.4	882.3	3572.5	1786.2	1786.2
Mass Flow	lb/hr	427782.4	247757.4	233634.2	909716.7	454858.3	454858.3
Molecular Weight		247.9	256.4	264.8	254.6	254.6	254.6
Heat Flow	Btu/hr	-3.6119E+08	-2.0246E+08	-1.8470E+08	-7.4913E+08	-3.7456E+08	-3.7456E+08
Mass Heat Capacity	Btu/lb-F	0.556	0.575	0.595	0.570	0.570	0.570
Std. Ideal Liquid Volume Flow	barrel/day	32095	18495	17357	67975	33988	33988
Mass Density	lb/ft3	51.33	50.44	49.57	50.67	50.67	50.67
Thermal Conductivity	Btu/hr-ft-F	0.07	0.07	0.07	0.07	0.07	0.07
Viscosity	cP	1.28	1.19	1.09	1.23	1.23	1.23
Surface Tension	dyne/cm	18.75	20.25	18.61	20.67	20.67	20.67
Actual Volume Flow	ft3/hr	8333.4	4911.5	4713.7	17955.4	8977.7	8977.7
Aqueous Phase Properties							
Molar Flow	lbmol/hr	43.6					
Mass Flow	lb/hr	785.6					
Std. Ideal Liquid Volume Flow	barrel/day	53.9					
Heat Flow	Btu/hr	-5.1800E+06					
Thermal Conductivity	Btu/hr-ft-F	0					
Viscosity	cP	0.195					
Surface Tension	dyne/cm	50.684					

Table 4.8.1n: H&MB for CDU – Streams 18A, 18B, 18, 20, 77 and 123

Stream Name		**18A**	**18B**	**18**	**20**	**77**	**123**
Stream Description		**CRUDE**	**CRUDE**	**CRUDE**	**CRUDE**	**DE-C4**	**DIESEL**
Phase		**Mixed**	**Mixed**	**Mixed**	**Mixed**	**Mixed**	**Liquid**
Total Stream Properties							
Vapour Fraction		0.24	0.25	0.32	0.32	0.00	0.00
Temperature	F	378.6	385.2	375.2	372.1	110.2	521.1
Pressure	psia	78.5	78.5	43.3	43.3	45.0	123.0
Molar Flow	lbmol/hr	2076.4	2076.4	4152.9	4229.6	76.7	729.3
Mass Flow	lb/hr	468443.7	468443.7	936887.5	947140.3	10252.9	163879.4
Std. Ideal Liquid Volume Flow	barrel/day	35334	35334	70668	71568	900	13000
Molecular Weight		225.6	225.6	225.6	223.9	133.7	224.7
Heat Flow	Btu/hr	-3.7887E+08	-3.7686E+08	-7.5572E+08	-7.6515E+08	-9.4286E+06	-1.1085E+08
Molar Enthalpy	Btu/lbmole	-182457	-181489	-181973	-180903	-122965	-152009
Mass Heat Capacity	Btu/lb-F	0.595	0.598	0.588	0.587	0.498	0.676
Mass Density	lb/ft3	7.47	7.21	3.28	3.31	42.12	41.61
Watson K		11.312	11.312	11.312	11.314	11.717	11.540
Vapor Phase Properties							
Molar Flow	lbmol/hr	495.1	512.4	1346.9	1353.6	0.2	
Mass Flow	lb/hr	32003.3	33858.5	101334.3	101961.2	2.7	
Heat Flow	Btu/hr	-3.6913E+07	-3.8094E+07	-1.0043E+08	-1.0098E+08	-2.7313E+03	
Actual Volume Flow	ft3/hr	53940.9	56231.2	268801.2	269019.8	26.4	
Mass Density	lb/ft3	0.59	0.60	0.38	0.38	0.10	
Compressibility		0.95	0.95	0.96	0.96	1.00	
Thermal Conductivity	Btu/hr-ft-F	0.02	0.02	0.02	0.02	0.05	
Viscosity	cP	0.01	0.01	0.01	0.01	0.01	
Molecular Weight		64.6	66.1	75.2	75.3	13.9	
Liquid Phase Properties							
Molar Flow	lbmol/hr	1581.4	1564.0	2806.0	2876.0	76.5	729.3
Mass Flow	lb/hr	436440.5	434585.2	835553.2	845179.1	10250.2	163879.4
Molecular Weight		276.0	277.9	297.8	293.9	134.0	224.7
Heat Flow	Btu/hr	-3.4195E+08	-3.3876E+08	-6.5529E+08	-6.6417E+08	-9.4258E+06	-1.1085E+08
Mass Heat Capacity	Btu/lb-F	0.598	0.601	0.593	0.592	0.498	0.676
Std. Ideal Liquid Volume Flow	barrel/day	32231	32060	61011	61850	899	13000
Mass Density	lb/ft3	49.66	49.55	50.38	50.32	47.23	41.61
Thermal Conductivity	Btu/hr-ft-F	0.07	0.07	0.07	0.07	0.07	0.06
Viscosity	cP	1.13	1.10	1.34	1.32	0.20	0.05
Surface Tension	dyne/cm	18.60	18.40	19.55	19.56	22.68	10.87
Actual Volume Flow	ft3/hr	8788.1	8770.2	16583.8	16797.1	217.0	3938.3
Aqueous Phase Properties							
Molar Flow	lbmol/hr						
Mass Flow	lb/hr						
Std. Ideal Liquid Volume Flow	barrel/day						
Heat Flow	Btu/hr						
Thermal Conductivity	Btu/hr-ft-F						
Viscosity	cP						
Surface Tension	dyne/cm						

Table 4.8.1o: H&MB for CDU – Streams 124, 132, 133, 218, 219 and 231

Stream Name		**124**	**132**	**133**	**218**	**219**	**231**
Stream Description		**DIESEL**	**AGO P/A**	**AGO P/A**	**HVGO P/A**	**HVGO P/A**	**VTB**
Phase		**Liquid**	**Liquid**	**Liquid**	**Liquid**	**Liquid**	**Liquid**
Total Stream Properties							
Vapour Fraction		0.00	0.00	0.00	0.00	0.00	0.00
Temperature	F	368.3	606.8	281.4	427.9	368.7	512.0
Pressure	psia	113.0	124.0	114.0	200.4	190.4	190.5
Molar Flow	lbmol/hr	729.3	81.3	81.3	831.1	831.1	358.8
Mass Flow	lb/hr	163879.4	23028.3	23028.3	278991.5	278991.5	196115.7
Std. Ideal Liquid Volume Flow	barrel/day	13000	1752	1752	20654	20654	12934
Molecular Weight		224.7	283.1	283.1	335.7	335.7	546.6
Heat Flow	Btu/hr	-1.2695E+08	-1.4305E+07	-1.9026E+07	-2.0680E+08	-2.1678E+08	-1.4066E+08
Molar Enthalpy	Btu/lbmole	-174078	-175852	-233893	-248809	-260817	-392044
Mass Heat Capacity	Btu/lb-F	0.607	0.700	0.553	0.618	0.590	0.629
Mass Density	lb/ft3	45.89	42.08	50.50	48.78	50.17	54.64
Watson K		11.540	11.498	11.498	11.502	11.502	11.435
Vapor Phase Properties							
Molar Flow	lbmol/hr						
Mass Flow	lb/hr						
Heat Flow	Btu/hr						
Actual Volume Flow	ft3/hr						
Mass Density	lb/ft3						
Compressibility							
Thermal Conductivity	Btu/hr-ft-F						
Viscosity	cP						
Molecular Weight							
Liquid Phase Properties							
Molar Flow	lbmol/hr	729.3	81.3	81.3	831.1	831.1	358.8
Mass Flow	lb/hr	163879.4	23028.3	23028.3	278991.5	278991.5	196115.7
Molecular Weight		224.7	283.1	283.1	335.7	335.7	546.6
Heat Flow	Btu/hr	-1.2695E+08	-1.4305E+07	-1.9026E+07	-2.0680E+08	-2.1678E+08	-1.4066E+08
Mass Heat Capacity	Btu/lb-F	0.607	0.700	0.553	0.618	0.590	0.629
Std. Ideal Liquid Volume Flow	barrel/day	13000	1752	1752	20654	20654	12934
Mass Density	lb/ft3	45.89	42.08	50.50	48.78	50.17	54.64
Thermal Conductivity	Btu/hr-ft-F	0.07	0.06	0.08	0.08	0.08	0.09
Viscosity	cP	0.14	0.12	0.56	0.44	0.60	7.40
Surface Tension	dyne/cm	17.09	10.49	23.03	19.09	21.31	20.69
Actual Volume Flow	ft3/hr	3571.2	547.2	456.0	5719.1	5561.1	3589.0
Aqueous Phase Properties							
Molar Flow	lbmol/hr						
Mass Flow	lb/hr						
Std. Ideal Liquid Volume Flow	barrel/day						
Heat Flow	Btu/hr						
Thermal Conductivity	Btu/hr-ft-F						
Viscosity	cP						
Surface Tension	dyne/cm						

Table 4.8.1p: H&MB for CDU – Streams 236, 237 and 239

Stream Name		**236**	**237**	**239**			
Stream Description		**VTB**	**VTB**	**VTB**			
Phase		**Liquid**	**Liquid**	**Liquid**			
Total Stream Properties							
Vapour Fraction		0.00	0.00	0.00			
Temperature	F	512.6	512.6	512.6			
Pressure	psia	190.5	190.5	190.5			
Molar Flow	lbmol/hr	398.9	4.0	395.0			
Mass Flow	lb/hr	218067.4	2180.7	215886.8			
Std. Ideal Liquid Volume Flow	barrel/day	14381	144	14238			
Molecular Weight		546.6	546.6	546.6			
Heat Flow	Btu/hr	-1.5632E+08	-1.5632E+06	-1.5476E+08			
Molar Enthalpy	Btu/lbmole	-391838	-391838	-391838			
Mass Heat Capacity	Btu/lb-F	0.630	0.630	0.630			
Mass Density	lb/ft3	54.63	54.63	54.63			
Watson K		11.435	11.435	11.435			
Vapor Phase Properties							
Molar Flow	lbmol/hr						
Mass Flow	lb/hr						
Heat Flow	Btu/hr						
Actual Volume Flow	ft3/hr						
Mass Density	lb/ft3						
Compressibility							
Thermal Conductivity	Btu/hr-ft-F						
Viscosity	cP						
Molecular Weight							
Liquid Phase Properties							
Molar Flow	lbmol/hr	398.9	4.0	395.0			
Mass Flow	lb/hr	218067.4	2180.7	215886.8			
Molecular Weight		546.6	546.6	546.6			
Heat Flow	Btu/hr	-1.5632E+08	-1.5632E+06	-1.5476E+08			
Mass Heat Capacity	Btu/lb-F	0.630	0.630	0.630			
Std. Ideal Liquid Volume Flow	barrel/day	14381	144	14238			
Mass Density	lb/ft3	54.63	54.63	54.63			
Thermal Conductivity	Btu/hr-ft-F	0.09	0.09	0.09			
Viscosity	cP	7.38	7.38	7.38			
Surface Tension	dyne/cm	20.67	20.67	20.67			
Actual Volume Flow	ft3/hr	3991.7	39.9	3951.7			
Aqueous Phase Properties							
Molar Flow	lbmol/hr						
Mass Flow	lb/hr						
Std. Ideal Liquid Volume Flow	barrel/day						
Heat Flow	Btu/hr						
Thermal Conductivity	Btu/hr-ft-F						
Viscosity	cP						
Surface Tension	dyne/cm						

Table 4.8.2a: System Salt Balance - Parallel Wash Water Injection (Normal Operation)

Stream Description	Stream #	lb/hr	bbl/d	Salt PTB	Salt lb/hr
Crude Oil Stream	10	927806.7	70001.0	100.0	291.7
Stripped Sour Water	70	149913.5	10286.0	0.0	0.0
River Water (NNF)	-	0.0	0.0	0.0	0.0
Vacuum Steam Condensate	71	11858.2	857.0	0.0	0.0
Wash Water to 1st Stage	83	80885.8	5571.0	0.0	0.0
Crude+Wash Water at Inlet to 1st Stage	11	1008692.5	75573.0	92.6	291.7
Wash Water to 2nd Stage	84	80885.8	5571.0	0.0	0.0
Crude from 1st Stage Desalter	85	930432.1	70203.0	13.9	40.6
Crude+Wash Water at Inlet to 2nd Stage	86	1011317.9	75774.0	12.9	40.6
Desalted Crude Oil	14	936887.5	70668.0	1.0	2.8
Brine from 1st Stage Desalter	91	78260.4	5370.0	1121.9	251.0
Brine from 2nd Stage Desalter	90	74430.4	5107.0	177.6	37.8
Brine from Both Desalters	93	152690.8	10476.0	661.7	288.8

1st Stage Desalter Efficiency	85.00%
2nd Stage Desalter Efficiency	92.50%

Table 4.8.2b: System Salt Balance - Recycle Wash Water Injection (Counter-current Mode)

Stream Description	Stream #	lb/hr	bbl/d	Salt PTB	Salt lb/hr
Crude Oil Stream	10	927806.7	70001.0	100.0	291.7
Stripped Sour Water	70	0.0	0.0	0.0	0.0
River Water (NNF)	-	74956.8	5143.0	0.0	0.0
Vacuum Steam Condensate	71	11858.2	857.0	0.0	0.0
Wash Water to 1st Stage	83	77734.1	5333.0	0.0	0.0
Crude+Wash Water at Inlet to 1st Stage	11	1005540.9	75334.0	92.9	291.7
Wash Water to 2nd Stage	84	86815.0	6000.0	0.0	0.0
Crude from 1st Stage Desalter	85	927806.7	70001.0	13.9	40.7
Crude+Wash Water at Inlet to 2nd Stage	86	1014621.7	76001.0	12.8	40.7
Desalted Crude Oil	14	936887.5	70668.0	1.0	2.8
Brine from 1st Stage Desalter	91	77734.1	5333.0	1129.6	251.0
Brine from 2nd Stage Desalter	90	77734.1	5333.0	165.9	37.8
Brine from Both Desalters	93	77734.1	5333.0	1295.6	288.8

1st Stage Desalter Efficiency	85.00%
2nd Stage Desalter Efficiency	92.50%

4.9. Equipment Design Consideration

The existing desalter is chosen to be the 1st stage desalter followed by the new desalter to be the 2nd stage desalter. To maximize the phenolic water consumption in the desalters, the following two configurations are considered for the injection of wash water. For schematic view of the configurations, refer to the PFD in Appendix A.

4.9.1 Parallel Wash Water Injection to Both Desalters

In this configuration the wash water from Battery Limit is heated through brine wash water and VTB wash water exchangers to reach the required operating temperature of 275°F. It is then split in equal amounts (7 vol% each) and injected to crude streams just before the mixing valves for each desalter. This configuration will insure maximum consumption of wash-water and hence maximum absorption of phenols from the wash water into the crude oil.

4.9.2 Counter-Current (Recycle) Injection of Wash Water

In this configuration the wash water is heated through brine wash water and VTB wash water exchangers to reach the required operating temperature of 275°F. The heated wash water (7 vol%) is injected to the 2nd stage desalter and the salty water effluent from the 2nd stage desalter is routed to the 1st stage as wash water for the 1st stage desalter, from where it will exit as brine stream going out of the system. This configuration is the most typical configuration used in refinery operations.

Under normal conditions, operation will be based on parallel injection mode. In case of unavailability of wash water, the desalters will operate in recycle mode.

4.9.3 Heat Exchange for Increased Desalter Temperature

As per the results in Chapter 3, the optimum temperature for desalting of Maya crude is 275ºF. The current operating temperature in the desalter is 256 ºF. Therefore, the temperature of the desalter should be increased. There are a few ways to achieve a higher temperature in the desalter, as following:

a) Increased pump-around flow rates; By increasing the pump-around flow rate the temperature of the crude in the pre-heat train could increase as there would be more heat available through the increased flow rate for given temperatures. However, increasing the pump-around flow rates will affect the atmospheric and vacuum column reboiler duties as the product specification should be met. Also increased pump-around flow rates, would result in additional capacity on the pumps, increased column diameter, and increased pipe sizes. These changes are very costly and not considered as a suitable option by the refinery.

b) Relocation of existing and new desalters further downstream in the preheat train where the temperatures are higher; By moving the desalters from the existing location further downstream in the pre-heat train where there is higher crude temperature it is possible to meet the required temperature in the desalters. However this option requires major change in piping as well as plot preparation for moving around existing equipment. This is too costly for the

refinery. Also the additional pressure drop through moving the exchangers upstream of the desalters will decrease the pressure in the desalter and this is not favorable as the desalter works under pressure control to prevent vapor production in the desalter. If the existing pressure is to be kept under the new proposed configuration, the charge pumps should be changed and increased in size. Overall, this is an expensive option and therefore not considered by the refinery.

c) Addition of utility exchangers to heat up crude or water; A third option could be increasing the temperature of the wash water or crude stream to achieve the optimum temperature of 275^{o}F in the desalter. Adding utility exchanger to the crude stream will cause pressure drop in the crude preheat train and hence reduced pressure in the desalter. Also there is no space available in the plot for fitting in an exchanger next to the existing desalter. Therefore this option is not feasible. Addition of utility exchanger to the wash water section seems to be the only feasible option as the above problems are not encountered. Also due to increased wash water flow rates the existing wash water/brine heat exchanger needs to be revamped. Therefore integration of wash water/brine exchanger together with new utility exchanger is considered for revamp design of the desalters.

4.9.4 Heat Integration

In the current operation, the wash water is first heated through the brine wash water exchanger before mixing with crude oil at the entrance of 1st stage desalter V-1001. The size of this exchanger is not sufficient for the new service as the wash water flow rate will increase in new operation, The increased wash water rate means increased brine flow rate and hence a bigger wash water/brine exchanger required as the existing exchanger would produce too much pressure drop under new conditions and also wouldn't be able to meet the optimum heat transfer required.

Even when the wash water/brine exchanger is sized sufficiently for the new service it wouldn't be able deliver the required (optimum) temperature for the desalter on itself because the wash water is being heated by the brine stream. In the new operation the brine is coming out of the desalter at 275^{o}F, so assuming a temperature approach of 35^{o}F the wash water temperature coming out of the wash water/brine exchanger would be at 240^{o}F. To increase the temperature of wash water from 240^{o}F to optimum temperature of 275^{o}F, a utility exchanger would be required.

The utility available in the refinery is High Pressure (HP) steam and therefore the new exchanger would be designed as a steam pre-heater to increase the temperature of the wash water sufficiently so that after wash water is mixed with the crude oil, the optimum temperature in the desalter is met.

Although the mathematical model in chapter 3 shows that the optimum temperature of the Maya crude is 275^{o}F, operating temperature chosen for 1st stage desalter is 270^{o}F in order to have a margin to prevent vapor production in the desalter as the pressure of the existing desalter cannot be increased. Also a reasonably lower temperature would decrease the size of new utility exchanger required.

The results of HYSYS simulation for new temperatures are given in the H&MB section in this chapter.

4.10. Environmental Considerations

The potential environmental concerns for revamp of the desalting unit are as follows:

- Carry-over of phenols into the salty water (brine) stream in an upset condition
- Carry-over of oil into the brine

These potential environmental concerns are considered when designing the new desalters explained below.

4.10.1 Loss of Phenols into Brine

The wash water used will be phenolic stripped sour water from the refinery. One of the primary reasons for using this stream as wash water in the desalter is that phenols can be reabsorbed from the water into the oil and the brine going to the effluent treatment will be free from phenols.

One of the concerns is that upset in the desalter operation can lead to phenols going into the brine. This malfunction is controlled by shutting off the stripped sour water as source of water to the desalters and switching the desalters operation from a parallel wash water injection mode into countercurrent mode and use of river water instead of the stripped sour water. This change will temporarily prevent rejection of phenols into the brine stream until normal operation is restored. In addition to this control scheme, the rag layer in the desalter is physically removed by draining and therefore any emulsion material including phenol will be removed from the desalter. Vendors will provide special piped systems to drain the rag layer. Disposal of this emulsion is also an environmental issue.

4.10.2 Loss of Oil into Brine

In the event of upsets or while mud washing, there is a strong possibility of some loss of oil into the brine. This could be prevented by level control of the interface layer. AGAR control could potentially help with minimizing the potential risks with this matter and hence prevent economical and environmental concerns. Therefore to control the level in the desalter, AGAR control has been chosen.

Chapter 5: Conclusions

In this thesis work, a history of dehydration and desalting, its importance, the global trend in crude quality and sources of wet crudes were reviewed. As a result it was concluded that as the oil industry is maturing, the crude sources are becoming more heavy and more salty and also the specifications by refiners are becoming more stringent. Therefore, the need for desalting is increasing.

As crude oil emulsions make the desalting process more difficult and more energy intensive, it is of utmost importance to understand the fundamentals of emulsion and how to remove them in an oil system. This subject was studied in Chapter 2. The information provided is based on experimental data from other works. A few common techniques to break up emulsion or to facilitate separation in emulsion systems are discussed in this chapter. The two most important factors in breaking up the emulsion are heating and application of electrostatic field, which become the cornerstone of later chapters of this thesis.

Different technologies were compared to understand the best available means for desalting the heavy crude oils. To this end, two major desalter vendors, Cameron and NATCO, were contacted for their technologies. Based on the experience history of the two vendors it was concluded that Cameron provides a more suitable technology for desalting the Maya crude. Details of the two technologies as well as pros and cons for each technology are provided in sufficient detail in Chapter 2.

The effect of different variables on the desalting process were investigated and studied in Chapter 3. As a result, it was found that the properties of Maya crude i.e. density, viscosity and electrical conductivity seem to be strong functions of temperature. This functionality needs to be further studied through statistical data analysis and further lab data are needed to support the results. This could be subject of future studies.

The functionality of Maya crude on temperature was used to mathematically model and determine the optimum operating temperature for this type of crude. The mathematical model prepared for this study is a linear model with profit and cost terms and the optimum temperature is achieved at maximum profit or minimum cost for the overall system. The results show that the objective function is satisfied at operating temperature of 275 ºF. It is worthwhile to prepare a detailed mathematical model to forecast the optimum desalting temperature of any crude in the market and this could be the subject of future research work.

To achieve the optimum temperature in the desalter and in order to maximize the heat integration in the system the available heat sources in the process were looked into. The Cold Preheat Train and the Hot Preheat Train in the crude distillation unit were both studied to find potential heat sources. Although it was found that heat sources are available or could be made available by reconfiguration of equipment, it was not justified to make these modifications due to system constraints such as pressure drop and additional costs for the project. Therefore, to achieve the optimum temperature in the desalter, it was proposed to increase the temperature of the wash water to effectively elevate the temperature of the crude and wash water mix in the desalter to that of the optimum temperature. This can be achieved by installing a new steam pre-heater online for the wash water and reconfiguring the existing wash water heat exchangers. The heat integration and equipment design considerations are discussed

in Chapter 4. As a future complimentary work for this study, Pinch Technology can be used to analyze and quantify the heat integration in the cold and hot preheat trains of the crude distillation unit and conclude whether the current heat integration is optimum regardless of the constraints in the system.

As far as desalting specification, it was concluded that a second stage desalter is needed for achieving the 1 PTB at the outlet of the desalter for the Maya crude in the refinery. Two configurations were studied; Parallel injection of wash water to both desalters and/or counter current operation of the two desalters. Based on the availability of the wash water and the need for maximizing the wash water consumption in the desalters, parallel injection of wash water to desalters was chosen as normal operation. In the meantime the system is designed to operate in recycle or counter current mode at wash water turn down.

In order to start the HYSYS simulation of the crude distillation unit, a full characterization of Brent and Maya crudes, which form the blend for the refinery, were accomplished in Chapter 4. The two sets of data i.e. lab data and calculated data were utilized to predict the key properties of each crude and their blend. The results of the crude characterization are integrated in the HYSYS model.

In the end a full HYSYS simulation was developed for the Crude Distillation Unit to study different options for desalting of the Maya crude. A full heat and material balance was developed from this simulation and the results are given in Chapter 4.

One of the shortcomings of this piece of work is that it is impossible to mathematically model the behavior of the crude emulsion in the desalter and hence very little can be predicted in this regard without having experimental data. Future research in the field of emulsion, to better understand the properties of emulsion, will definitely help in predicting the behavior of difficult crudes.

The other drawback in this study is that most of the information available on electrostatic desalting, which is THE way for desalting of heavy crudes, is with vendors and unless technology is bought from the vendors, details of the experimental work will not be made available due to confidentiality of the information.

The other area that can be improved in the future is the simulation of the desalting operation, as HSYSY is not a suitable tool to model electrolyte processes, and in order to model the desalting operation in HYSYS, the associated water or formation water with crude was assumed to be pure water. However, this assumption produces inaccuracies in predicting the stream properties of the desalting operation. For future research, it is recommended to either develop a suitable model to better predict the desalting parameters or use a commercially available software that will have better capabilities to model hydrocarbon electrolyte processes.

Appendix A: Process Flow Diagrams (PFDs)

PFD1 – The Cold Preheat Train for Crude Distillation Unit

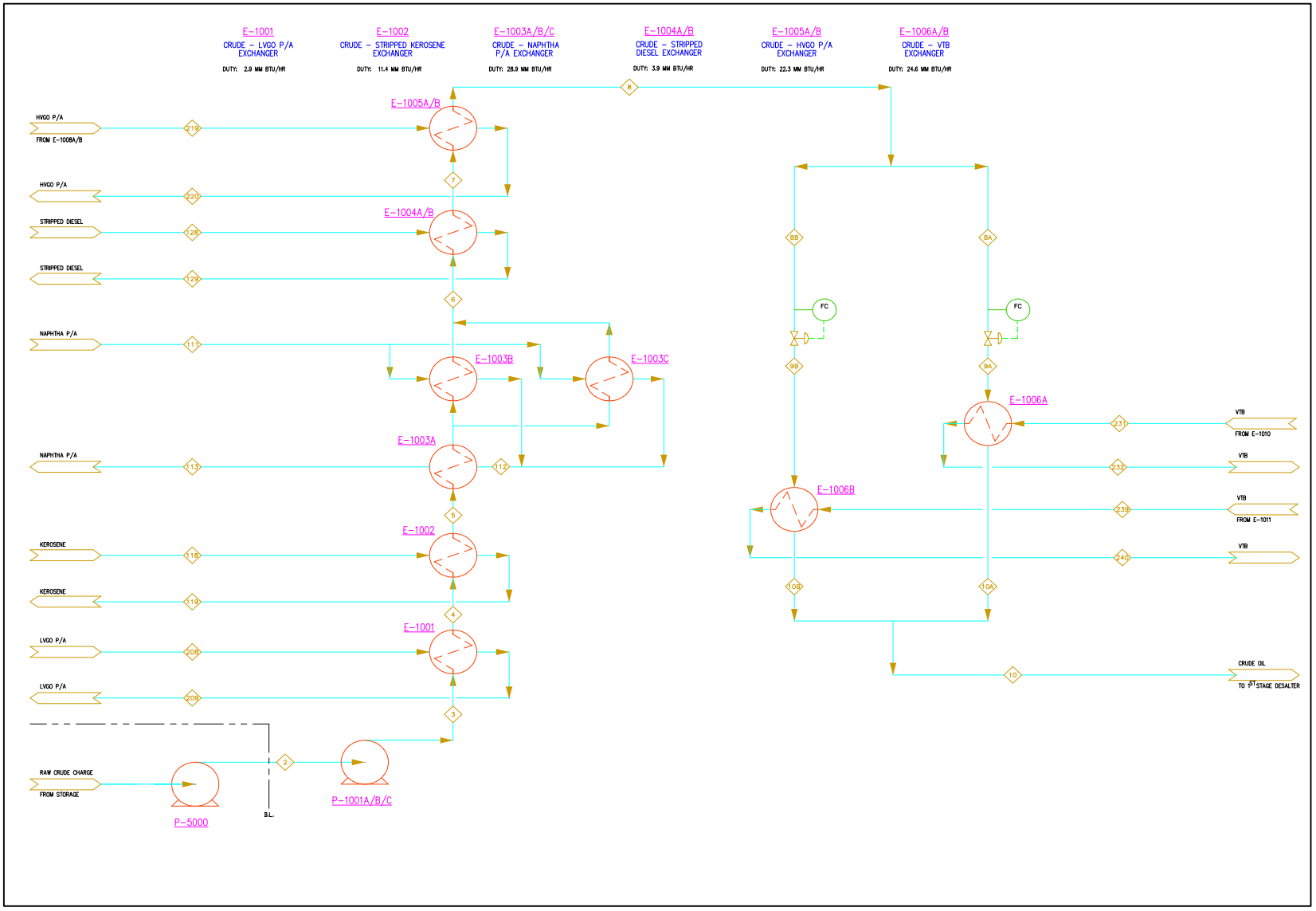

PFD2 – 1st and 2nd Stage Desalters

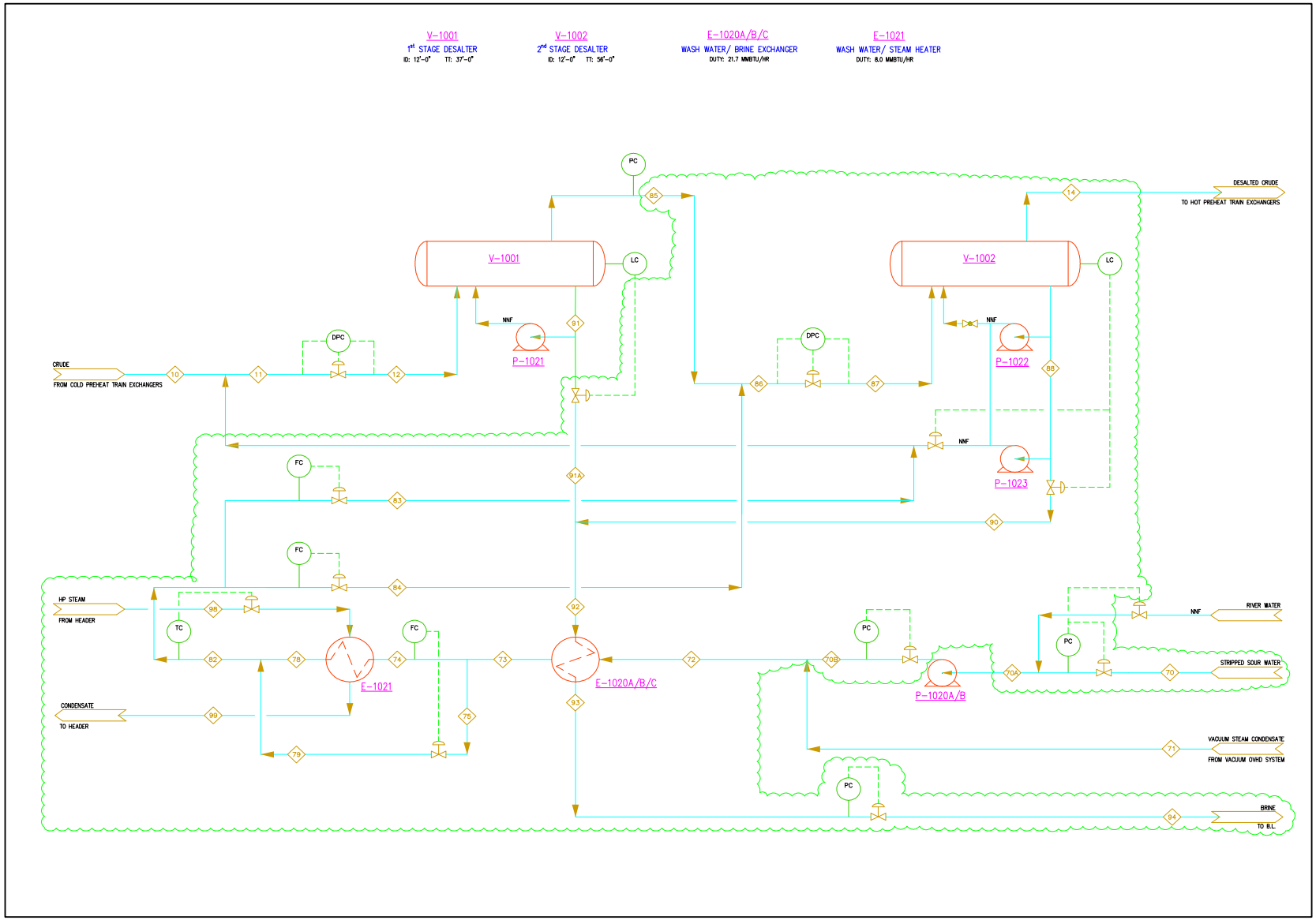

PFD3 – The Hot Preheat Train for Crude Distillation Unit

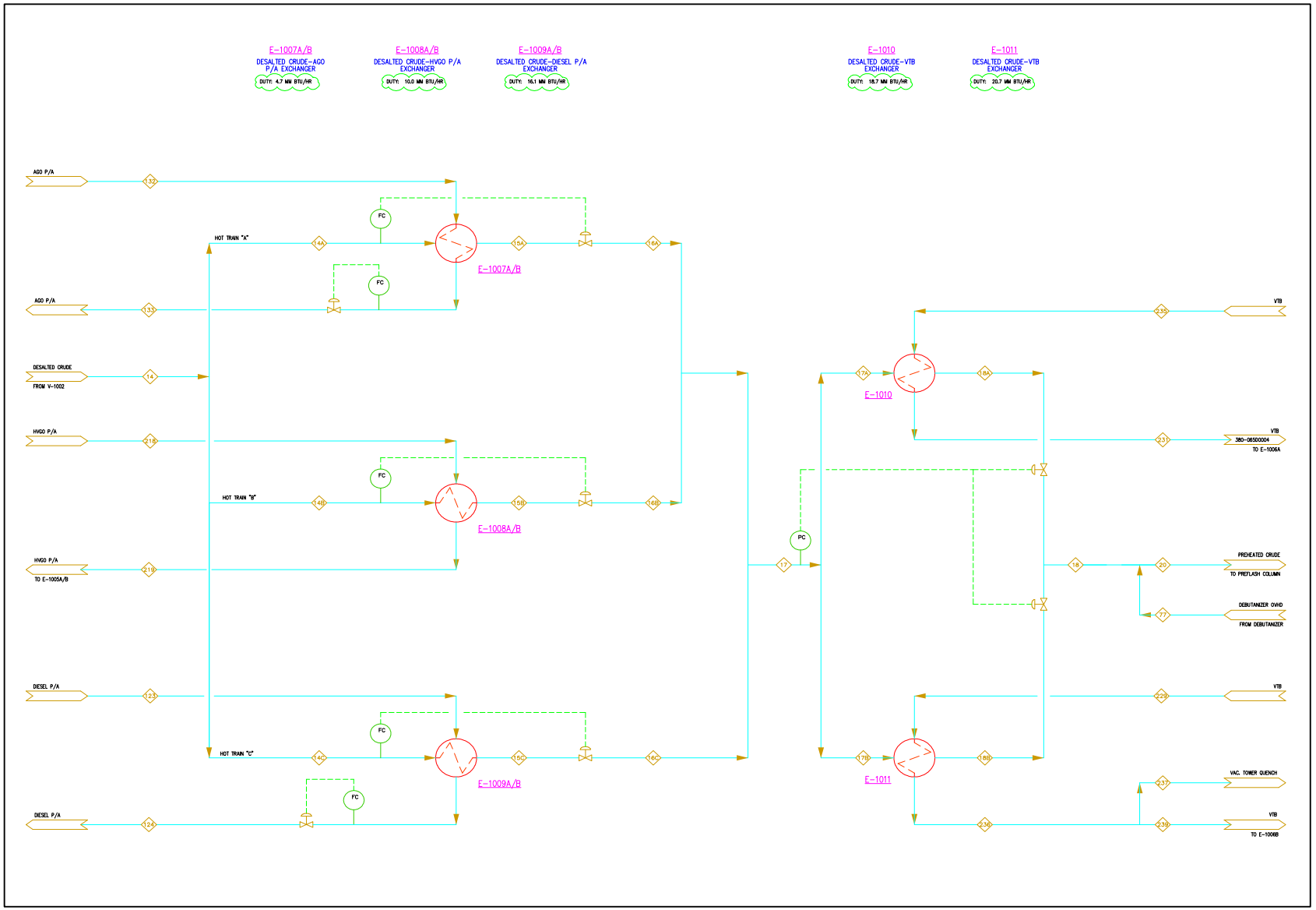

References

1. Noïk C, Chen J, and C Dalmazzone. Electrostatic Demulsification on Crude Oil: A State-of-the-Art Review. *Society of Petroleum Engineers*. SPE 103808. 2006.

2. Johnson, T. Oil Market Volatility. *Council on Foreign Relations*. December 10, 2007. Available online: http://www.cfr.org/publication/15017/ [Accessed February 5, 2008.]

3. Crude Benchmark Analysis. *Energy Economist.* March 7, 2008. Available online: http://www.platts.com/Oil/Resources/News%20Features/crudeanalysis/index.xml [Accessed February 8, 2008]

4. U.S. Refinery Crude Oil Input Qualities. Energy Information Administration. January 29 2008. Available online: http://tonto.eia.doe.gov/dnav/pet/pet_pnp_crq_dcu_nus_m.htm [Accessed February 19, 2008]

5. Sweet and Sour Crudes. *Econbrowser*. August 21, 2005. Available online: http://www.econbrowser.com/archives/2005/08/sweet_and_sour.html [Accessed February 5, 2008]

6. World Crude Oil Prices. Energy Information Administration. February 13, 2008. Available online: http://tonto.eia.doe.gov/dnav/pet/pet_pri_wco_k_w.htm [Accessed February 20, 2008]

7. Annual Energy Outlook 2006 with Projections to 2030. Energy Information Administration. Report #: DOE/EIA-0383(2006). Available online: http://www.eia.doe.gov/oiaf/aeo/otheranalysis/aeo_2006analysispapers/tri.html [Accessed February 5, 2008]

8. R.D. Kane, ASM Handbook

9. P.E. Krystow, Corrosion in Crude and Vacuum Units, Report submitted to NACE Task Group T-8-5 on 2-14-69

10. Smith HV and KE Arnold. Petroleum Engineering Handbook. Chapter 19: Crude Oil Emulsions. Society of Petroleum Engineers. 1987.

11. Khatib ZI, Faucher MS, and El Sellman. Field Evaluation of Disc-Stack Centrifuges for Separating Oil/Water Emulsions on Offshore Platforms. *Society of Petroleum Engineers.* SPE 30674. 1995.

12. Dhuldhoya N, Mileo M, Faucher M, and E Sellman. Dehydration of Heavy Crude Oil Using Disc Stack Centrifuges. *Society of Petroleum Engineers*. SPE 49119. 1990.

13. Meikrantz DH, Macaluso LL, and MM St. George. Advances in Liquid/Liquid Centrifuge Design Provide New Options for Petroleum Production. *Society of Petroleum Engineers*. SPE 56709. 1999.

14. Bai ZS and HL Wang. Crude Oil Desalting Using Hydrocyclones. *Chem Eng Res Design*. 85(A12): 1586-1590. 2007.

15. Egloff G, Nelson EF, Maxutov CD and C Wirth. Desalting Crude Oils. Oklahoma City Meeting. SPE-938048-G. October 1937.

16. Filtration method efficiently desalts crude in commercial test. *J Oil Gas*. 91(20): 59-60. 1993.

17. Chawla, M.L. Field Desalting of Wet Crude in Kuwait. Kuwait Oil Co. *Society of Petroleum Engineers*, SPE 15711.

18. Mandal, K.K. Improve Desalter Control. Hydrocarbon Processing. April 2005.

19. Kokal, S. Crude Oil Emulsions: A State-of-the-Art Review. *Society of Petroleum Engineers*, SPE 77497. 2005.

20. Manning, Dr. F.S., Thompson, Dr. R.E. Oilfield Processing, Volume 2: Crude Oil. Pennwell Books, 1995.

21. Paragon Engineering Services. Desalting. IHRDC Production Facility Bookware Series.

22. Buckley JS and Y Liu. Some mechanisms of crude oil/brine/solid interactions. *J Petro Sci Eng*. 20: 155-160. 1998**.**

23. Shafizadeh A, McAteer G and J Sigmon. High Acid Crudes. New Orleans Meeting Presentation, Crude Oil Quality Group. 2005.

24. Peters, MS, and KD Timmerhaus. Plant Design and Economics for Chemical Engineers, Fourth Edition. McGraw-Hill Inc, 1991.

25. Arnold K, and M Stewart. Surface Production Operations, Volume 1 – Design of Oil Handling Systems and Facilities. Elsevier, 1999.

26. Eddy HC. Discussion on Electrical Dehydration of Crude Oil. *J Indust Eng Chem*. November, 1921.

27. ID-205 Interface Detectors. Agar Corporation. 2001. Available online: http://www.agarcorp.com/detectors.html [Accessed March 2, 2008]

28. Anderson WA. Process Equipment Sizing and Selection. Department of Chemical Engineering, University of Waterloo. 2004.

29. ADMIX. Sizing the *ADMIXER™ Static Mixer and Sanitary Blender*, Tech. Note No.102. Manchester, NH, November 1998. Available online: http://www.admix.com

30. Mukherjee, R. Effectively Design Shell-and-Tube Heat Exchangers. Chemical Engineering Progress. February 1998.

31. World Crude Oil Prices. Energy Information Administration. 2008. Available online: http://tonto.eia.doe.gov/dnav/pet/pet_pri_wco_k_w.htm [Accessed February 14, 2008]

32. Escobedo, E.R.B., Garfias, F.J, Pruneda, E.F. Optimum Temperature in the Electrostatic Desalting of Maya Crude Oil. March 15, 2005. Facultad de Ouimica, Unversidad Nacional Autonoma de Mexico, Ciudad Unversitaria, Mexico.

33. Gibson, D. Oil Industry – Questions and Answers. Gibson Consulting. 2007. Available online: http://www.gravmag.com/oil3.html#barrel [Accessed February 17, 2008]

34. Nelson, W.L. Petroleum Refinery Engineering, Fourth Edition. McGraw-Hill Book Company Inc, 1958.

35. Arnold, K. and Stewart, M.: Surface Production Operations, Vol. 1; Design of Oil Handling Systems and Facilities, Gulf Publishing Co., Houston (1986)

36. Becher, P.: Principles of Emulsion Technology, Reinhold Publishing Corp., New York City (1955)

37. Blair, C.M.: Handling the Emulsion Problem in the Oil Fields, Magna Corp., Santa Fe Springs, CA (1971)

38. Sams, G.W. and Warren, W.: New Methods of Application of Electrostatic Fields, Natco Group, New Orleans, Louisiana (2004)

39. Bailes, Philip J., Freestone, D. and Sams, G.W.: Pulsed DC Fields for Electrostatic Coalescence of Water-in-Oil Emulsions, The Chemical Engineer (1997)

40. Pruneda, E.F., Escobedo, E.R.B., Vazquez, F.J.G.: Optimum Temperature in the Electrostatic Desalting of Maya Crude Oil (2005)

41. Kim, Young H., Wasan, Darsh T.: Effect of Demulsifier Partitioning on the Destabilization of Water-in-Oil Emulsions (1996)

42. Bhardwaj, A., Hartland, S.: Demulsification of Water-in-Oil Emulsions, J. Dispersion Sci. Technol. (1993)

43. Pruneda, E. F., Escobedo E. R. B., Vazquez F. J. G.: Optimum Temperature in the Electrostatic Desalting of Maya Crude Oil, J. Mex. Chem. Society (2005)

44. Lucas, N. Roy: Dehydration of Heavy Crudes by Electrical Means, Petrolite Corp., Petreco Div., Houston, TX (1966)

45. Pearce, C.A.R.: The mechanism of the Resolution of Water-in-Oil Emulsions by Electrical Treatment (1953)

46. AGAR Control, AGAR Corporation, http://www.agarcorp.com

47. Petreco Bilectric Dehydrators and Desalters, Cameron Petreco Process Systems http://www.c-a-m.com/content/products/product_detail.cfm?pid=2630

48. Natco Dual Polarity Dehydrators and Desalters, Natco Oil Treating Technologies, http://www.natcogroup.com/Content.asp?t=ProductPage&ProductID=100